MULTIGRID METHODS FOR MAXWELL'S EQUATIONS

A Dissertation

Submitted to the Graduate Faculty of the
Louisiana State University and
Agricultural and Mechanical College
in partial fulfillment of the
requirements for the degree of
Doctor of Philosophy

in

The Department of Mathematics

by
Jintao Cui
B.S., Dalian University of Technology, 2004
August 2010

Acknowledgments

This dissertation would not have been accomplished without several contributions.

I would like to express my deepest gratitude to my advisor Dr. Susanne C. Brenner, and Dr. Li-yeng Sung for giving directions and suggestions. I would also like to thank Dr. James Madden, Dr. Suresh Rai, Dr. Michael M. Tom, and Dr. Xiaoliang Wan for contributing to my dissertation as readers.

I wish to gratefully acknowledge the Center for Computation and Technology (CCT) at Louisiana State University (LSU) for offering me the Distinguished Graduate Dissertation Fellowship in the last year of my graduate study. My sincere thanks to researchers and friends in CCT and Department of Mathematics at LSU for their help and warm encouragement.

I would like to thank the National Science Foundation for the summer support under Grant No. DMS-03-11790, No. DMS-07-38028 and No. DMS-07-13835.

Special thanks to Dr. Fengyan Li and Dr. Thirupathi Gudi for their help in my research.

Also I would like to thank my wife, Zhengjia Sun for all of her support.

Table of Contents

List of Tables

List of Figures

Abstract

In this work we study finite element methods for two-dimensional Maxwell's equations and their solutions by multigrid algorithms. We begin with a brief survey of finite element methods for Maxwell's equations. Then we review the related fundamentals, such as Sobolev spaces, elliptic regularity results, graded meshes, finite element methods for second order problems, and multigrid algorithms. In Chapter 3, we study two types of nonconforming finite element methods on graded meshes for a two-dimensional curl-curl and grad-div problem that appears in electromagnetics. The first method is based on a discretization using weakly continuous P_1 vector fields. The second method uses discontinuous P_1 vector fields. Optimal convergence rates (up to an arbitrary positive ε) in the energy norm and the L_2 norm are established for both methods on graded meshes. In Chapter 4, we consider a class of symmetric discontinuous Galerkin methods for a model Poisson problem on graded meshes that share many techniques with the nonconforming methods in Chapter 3. Optimal order error estimates are derived in both the energy norm and the L_2 norm. Then we establish the uniform convergence of W-cycle, V-cycle and F-cycle multigrid algorithms for the resulting discrete problems. In Chapter 5, we propose a new numerical approach for two-dimensional Maxwell's equations that is based on the Hodge decomposition for divergence-free vector fields. In this approach, an approximate solution for Maxwell's equations can be obtained by solving standard second order scalar elliptic boundary value problems. We illustrate this new approach by a P_1 finite element method. In Chapter 6, we first report numerical results for multigrid algorithms applied to the discretized curl-curl and grad-div problem using nonconforming finite element methods. Then we present multigrid results for Maxwell's equations based on the approach introduced

in Chapter 5. All the theoretical results obtained in this dissertation are confirmed by numerical experiments.

Chapter 1
Introduction

1.1 Maxwell's Equations

Maxwell's equations consist of two pairs of coupled partial differential equations relating four fields, two of which model the sources of electromagnetism. These equations characterize the fundamental relations between electric field and magnetic field. James Clerk Maxwell (1831–1879) is recognized as the founder of the modern theory of electromagnetism.

There are two fundamental field vectors functions $\mathbf{E}(\mathbf{x}, t)$ and $\mathbf{H}(\mathbf{x}, t)$ in the classical electromagnetic field, with space variable $\mathbf{x} \in \mathbb{R}^3$ and time variable $t \in \mathbb{R}$. The distribution of electric charges is given by a scalar charge density function $\rho(\mathbf{x}, t)$, and the current is described by the current density function $\mathbf{J}(\mathbf{x}, t)$.

Maxwell's equations are stated as the following equations in a region of space in $\mathbb{R}^3$ occupied by the electromagnetic field:

$$\nabla \times \mathbf{E} = -\mu \frac{\partial \mathbf{H}}{\partial t}, \tag{1.1.1a}$$

$$\nabla \cdot \mathbf{E} = \frac{\rho}{\epsilon}, \tag{1.1.1b}$$

$$\nabla \times \mathbf{H} = \epsilon \frac{\partial \mathbf{E}}{\partial t} + \mathbf{J}, \tag{1.1.1c}$$

$$\nabla \cdot \mathbf{H} = 0, \tag{1.1.1d}$$

where ϵ is the electric permittivity, and μ is the magnetic permeability.

Equation (1.1.1a) is called Faraday's law and describes how the changing of magnetic field affects the electric field. The equation (1.1.1c) is referred as Ampère's law. The divergence conditions (1.1.1b) and (1.1.1d) are Gauss' Laws of electric displacement and magnetic induction respectively.

When the radiation has a frequency $\omega > 0$, we want to find solutions of the Maxwell's equations of the form $\mathbf{E}(\mathbf{x},t) = e^{-i\omega t}\hat{\mathbf{E}}(\mathbf{x})$, $\mathbf{H}(\mathbf{x},t) = e^{-i\omega t}\hat{\mathbf{H}}(\mathbf{x})$, $\mathbf{J}(\mathbf{x},t) = e^{-i\omega t}\hat{\mathbf{J}}(\mathbf{x})$, and $\rho(\mathbf{x},t) = e^{-i\omega t}\hat{\rho}(\mathbf{x})$. By substituting these relations into (1.1.1) or using Fourier transforms in the time variable, the time-dependent problem (1.1.1) can be reduced to the time-harmonic Maxwell's equations:

$$\nabla \times \hat{\mathbf{E}} = i\omega\mu\hat{\mathbf{H}}, \tag{1.1.2a}$$

$$\nabla \cdot \hat{\mathbf{E}} = \frac{\hat{\rho}}{\epsilon}, \tag{1.1.2b}$$

$$\nabla \times \hat{\mathbf{H}} = -i\omega\epsilon\hat{\mathbf{E}} + \hat{\mathbf{J}}, \tag{1.1.2c}$$

$$\nabla \cdot \hat{\mathbf{H}} = 0. \tag{1.1.2d}$$

It can be shown that when the charge is conserved, the divergence conditions (1.1.2b) and (1.1.2d) are always satisfied, provided that the equations (1.1.2a) and (1.1.2c) hold. Then by combining the equations (1.1.2a) and (1.1.2c), we have

$$\nabla \times \nabla \times \hat{\mathbf{E}} - \omega^2\mu\epsilon\hat{\mathbf{E}} = i\omega\mu\hat{\mathbf{J}}, \tag{1.1.3a}$$

$$\nabla \times \nabla \times \hat{\mathbf{H}} - \omega^2\mu\epsilon\hat{\mathbf{H}} = \nabla \times \hat{\mathbf{J}}. \tag{1.1.3b}$$

Hence we consider an equation of the following form with perfectly conducting boundary condition for the curl-curl problem (1.1.3):

$$\nabla \times \nabla \times \boldsymbol{u} + \alpha\boldsymbol{u} = \boldsymbol{f} \qquad \text{in } \Omega, \tag{1.1.4a}$$

$$\boldsymbol{n} \times \boldsymbol{u} = 0 \qquad \text{on } \partial\Omega, \tag{1.1.4b}$$

where $\Omega \subset \mathbb{R}^2$ is a bounded polygonal domain, $\alpha \in \mathbb{R}$ is a constant, and $\boldsymbol{f} \in [L_2(\Omega)]^2$.

The curl-curl problem (1.1.4) appears in the semi-discretization of electric fields in the time-dependent (time-domain) Maxwell's equations when $\alpha > 0$ and the time-harmonic (frequency-domain) Maxwell's equations when $\alpha \leq 0$. When $\alpha = 0$, it is also related to electrostatic problems.

1.2 A Brief History of Finite Element Methods for Maxwell's Equations

We consider the following weak form for the curl-curl problem (1.1.4):

Find $\boldsymbol{u} \in H_0(\text{curl}; \Omega)$ such that

$$(\nabla \times \boldsymbol{u}, \nabla \times \boldsymbol{v}) + \alpha(\boldsymbol{u}, \boldsymbol{v}) = (\boldsymbol{f}, \boldsymbol{v}) \tag{1.2.1}$$

for all $\boldsymbol{v} \in H_0(\text{curl}; \Omega)$, where $(\cdot, \cdot)$ denotes the inner product of $[L_2(\Omega)]^2$. Here the space $H_0(\text{curl}; \Omega)$ is defined as follows:

$$H(\text{curl}; \Omega) = \Big\{\boldsymbol{v} = \begin{bmatrix} v_1 \\ v_2 \end{bmatrix} \in [L_2(\Omega)]^2 : \nabla \times \boldsymbol{v} = \frac{\partial v_2}{\partial x_1} - \frac{\partial v_1}{\partial x_2} \in L_2(\Omega)\Big\}, \tag{1.2.2}$$

$$H_0(\text{curl}; \Omega) = \{\boldsymbol{v} \in H(\text{curl}; \Omega) : \boldsymbol{n} \times \boldsymbol{v} = 0 \text{ on } \partial\Omega\}, \tag{1.2.3}$$

where $\boldsymbol{n}$ is the unit outer normal. Note that $\boldsymbol{n} \times \boldsymbol{v} = 0$ on $\partial\Omega$ is equivalent to $\boldsymbol{\tau} \cdot \boldsymbol{v} = 0$ on $\partial\Omega$, where $\boldsymbol{\tau}$ is the unit tangent vector along $\partial\Omega$.

The curl-curl problem (1.2.1) is usually solved directly using $H(\text{curl})$ conforming vector finite elements [83, 84, 75, 80, 62, 24]. However, this problem is non-elliptic when the $H_0(\text{curl})$ formulation is used, and hence the convergence analysis of both the numerical scheme and its fast solvers more complicated.

For any $\boldsymbol{u} \in H_0(\text{curl}; \Omega)$, due to the well-known Helmholtz decomposition [68, 80], we have the following orthogonal decomposition:

$$\boldsymbol{u} = \mathring{\boldsymbol{u}} + \nabla\phi, \tag{1.2.4}$$

where $\mathring{\boldsymbol{u}} \in H_0(\text{curl};\Omega) \cap H(\text{div}^0;\Omega)$ and $\phi \in H_0^1(\Omega)$. Here the space $H(\text{div}^0;\Omega)$ is defined as follows:

$$H(\text{div};\Omega) = \Big\{\boldsymbol{v} \in [L_2(\Omega)]^2 : \nabla \cdot \boldsymbol{v} = \frac{\partial v_1}{\partial x_1} + \frac{\partial v_2}{\partial x_2} \in L_2(\Omega)\Big\}, \tag{1.2.5}$$

$$H(\text{div}^0;\Omega) = \Big\{\boldsymbol{v} \in H(\text{div};\Omega) : \nabla \cdot \boldsymbol{v} = 0\Big\}. \tag{1.2.6}$$

It is easy to show that $\phi \in H_0^1(\Omega)$ satisfies

$$\alpha(\nabla\phi, \nabla\eta) = (\boldsymbol{f}, \nabla\eta) \tag{1.2.7}$$

for all $\eta \in H_0^1(\Omega)$, which is the variational form of the Poisson problem. Many successful schemes have been developed for solving this problem. We can also show that $\mathring{\boldsymbol{u}}$ is the weak solution of the following reduced curl-curl problem (RCCP cf. [39]), on which we are more interested:

Find $\mathring{\boldsymbol{u}} \in H_0(\text{curl};\Omega) \cap H(\text{div}^0;\Omega)$ such that

$$(\nabla \times \mathring{\boldsymbol{u}}, \nabla \times \boldsymbol{v}) + \alpha(\mathring{\boldsymbol{u}}, \boldsymbol{v}) = (\boldsymbol{f}, \boldsymbol{v}) \tag{1.2.8}$$

for all $\boldsymbol{v} \in H_0(\text{curl};\Omega) \cap H(\text{div}^0;\Omega)$.

Unlike the non-elliptic curl-curl problem (1.2.1), the reduced problem (1.2.8) is an elliptic problem. In particular, the solution $\mathring{\boldsymbol{u}}$ has elliptic regularity under the assumption that $\boldsymbol{f} \in [L_2(\Omega)]^2$, which greatly simplifies the analysis. On the other hand, it is difficult to construct finite element subspaces for $H_0(\text{curl};\Omega) \cap H(\text{div}^0;\Omega)$. This difficulty can be overcome by using nonconforming methods [40, 38, 39].

It is known that the zero divergence condition in the reduced problem (1.2.8) leads to a large condition number for the discrete problem, which behaves like a fourth order problem. Hence we consider the following curl-curl and grad-div (CCGD) problem:

Find $\boldsymbol{u} \in H_0(\text{curl};\Omega) \cap H(\text{div};\Omega)$ such that

$$(\nabla \times \boldsymbol{u}, \nabla \times \boldsymbol{v}) + \gamma(\nabla \cdot \boldsymbol{u}, \nabla \cdot \boldsymbol{v}) + \alpha(\boldsymbol{u}, \boldsymbol{v}) = (\boldsymbol{f}, \boldsymbol{v}) \tag{1.2.9}$$

for all $\boldsymbol{v} \in H_0(\text{curl};\Omega) \cap H(\text{div};\Omega)$, where $\alpha \in \mathbb{R}$ and $\gamma > 0$ are constants, $\boldsymbol{f} \in [L_2(\Omega)]^2$. Note that the condition number of the resulting discrete problem behaves like a second order problem.

For $\alpha > 0$, the problem (1.2.9) is uniquely solvable by the Riesz representation theorem applied to the Hilbert space

$$X_N = H_0(\text{curl};\Omega) \cap H(\text{div};\Omega)$$

with the inner product

$$(\boldsymbol{v}, \boldsymbol{w})_{X_N} = (\nabla \times \boldsymbol{v}, \nabla \times \boldsymbol{w}) + (\nabla \cdot \boldsymbol{v}, \nabla \cdot \boldsymbol{w}) + (\boldsymbol{v}, \boldsymbol{w}).$$

Due to the fact that $H_0(\text{curl};\Omega) \cap H(\text{div};\Omega)$ is compactly embedded in $[L_2(\Omega)]^2$ (cf. [77, 93, 54, 97, 80]), there exists a sequence of nonnegative numbers $0 \leq \lambda_{\gamma,1} \leq \lambda_{\gamma,2} \leq \cdots \to \infty$ such that the following eigenproblem has a nontrivial solution $\boldsymbol{w} \in H_0(\text{curl};\Omega) \cap H(\text{div};\Omega)$:

$$(\nabla \times \boldsymbol{w}, \nabla \times \boldsymbol{v}) + \gamma(\nabla \cdot \boldsymbol{w}, \nabla \cdot \boldsymbol{v}) = \lambda_{\gamma,j}(\boldsymbol{w}, \boldsymbol{v}) \tag{1.2.10}$$

for all $\boldsymbol{v} \in H_0(\text{curl};\Omega) \cap H(\text{div};\Omega)$.

For $\alpha \leq 0$, the problem (1.2.9) is well-posed as long as $\alpha \neq -\lambda_{\gamma,j}$ for $j \geq 1$. In particular, when $\alpha = 0$ and Ω is simply connected, the problem (1.2.9) is uniquely solvable due to Friedrichs' inequality [80]:

$$\|\boldsymbol{v}\|_{L_2(\Omega)} \leq C\big(\|\nabla \times \boldsymbol{v}\|_{L_2(\Omega)} + \|\nabla \cdot \boldsymbol{v}\|_{L_2(\Omega)}\big), \quad \forall \boldsymbol{v} \in H_0(\text{curl};\Omega) \cap H(\text{div};\Omega).$$

When $\nabla \cdot \boldsymbol{f} = 0$ and (1.2.9) is well-posed, the solution $\boldsymbol{u}$ of (1.2.9) belongs to the space $H(\text{div}^0;\Omega)$, and the solution of the non-elliptic curl-curl problem (1.2.1) can be obtained by solving the elliptic problem (1.2.9) [85, 53, 87, 94].

The problem (1.2.9) was discretized by H^1 conforming vector nodal finite elements in [53]. However, the space $[H^1(\Omega)]^2 \cap X_N$ turns out to be a closed subspace of X_N [21, 55]. Therefore any H^1 conforming finite element method for (1.2.9) must fail if the solution $\boldsymbol{u}$ does not belong to $[H^1(\Omega)]^2$, which happens when Ω is non-convex [10, 21, 57]. Even worse, the solutions obtained by H^1 conforming finite element methods in such situations converge to the wrong solution (the projection of $\boldsymbol{u}$ in $[H^1(\Omega)]^2 \cap X_N$). Consequently the idea of solving (1.2.1) through (1.2.9) was abandoned.

Nevertheless, the elliptic problem (1.2.9) remains an attractive alternative approach and successful schemes have been discovered in recent years that either solve (1.2.9) using nodal H^1 vector finite elements complemented by singular vector fields [23, 8, 74, 9, 7], or solve a regularized version of (1.2.9) using standard nodal H^1 vector finite elements [58, 59, 50].

1.3 Results Obtained in the Dissertation

There are two classes of results obtained in this dissertation. The first is for Maxwell's equations and the other is for discontinuous Galerkin methods [5].

In Chapter 3, we show that the elliptic curl-curl and grad-div problem (1.2.9) can be solved by nonconforming methods. We first solve (1.2.9) by a classical nonconforming method using Crouzeix-Raviart weakly continuous piecewise P_1 vector fields [60] on graded meshes. Optimal convergence rates in both the energy norm and the L_2 norm are achieved on general polygonal domains, provided that two consistency terms involving the jumps of the vector fields are included in the discretization and properly graded meshes are used. We also solve (1.2.9) by using an interior penalty method. Discontinuous piecewise P_1 functions are used and two additional over-penalized terms are added to the scheme. Similar convergence results are established on nonconforming meshes. We present numerical results for both approaches.

In Chapter 5, we propose a new numerical approach for the reduced curl-curl problem (1.2.8) that is based on the Hodge decomposition for divergence-free vector fields. In this approach an approximate solution for the two-dimensional Maxwell's equations can be obtained by solving standard second order scalar elliptic boundary value problems. We illustrate this new approach by a P_1 finite element method.

In Chapter 6, we first introduce the W-cycle multigrid algorithm for the discretized curl-curl and grad-div problem. The discrete problems are obtained by using nonconforming finite element methods, which are developed in Chapter 3. We report the numerical results on the unit square with uniform meshes. Then we study multigrid methods for the P_1 finite element method, which is proposed in Chapter 5 for solving two-dimensional Maxwell's equations. Numerical results on graded meshes are reported.

Since there are many similarities between nonconforming finite element methods for Maxwell's equations on graded meshes and discontinuous Galerkin (DG) methods for the Poisson problem on graded meshes, we also investigate multigrid algorithms for DG methods as a prelude to the study of multigrid algorithms for Maxwell's equations.

In Section 2.4, we study a class of symmetric, stable and consistent DG methods for the Poisson problem on graded meshes. The elliptic regularity results in terms of weighted Sobolev norms are used in the analysis. Optimal order error estimates are derived in both the energy norm and the L_2 norm.

In Chapter 4, we consider multigrid methods for the discrete problems resulting from DG methods in Section 2.4. We present the convergence analysis of W-cycle, V-cycle and F-cycle multigrid algorithms on non-convex domains, where the model problem has singularities. We show that the convergence of the multigrid algorithms on non-convex domains with properly graded meshes is identical to the convergence of multigrid methods on convex domains with quasi-uniform meshes. Theoretical results are illustrated by numerical experiments.

Chapter 2
Fundamentals

2.1 Sobolev Spaces

Let Ω be a domain in $\mathbb{R}^n$. The locally integrable function space is defined by

$$L^1_{\mathrm{loc}}(\Omega) := \left\{ f \,:\, f \in L^1(K) \ \ \forall \text{ compact } K \subset \text{interior } \Omega \right\}.$$

We say that a given function $f \in L^1_{\mathrm{loc}}(\Omega)$ has a weak derivative of order α if there exists a function $g \in L^1_{\mathrm{loc}}(\Omega)$ such that

$$\int_\Omega g(x)\phi(x)dx = (-1)^{|\alpha|} \int_\Omega f(x) D^\alpha \phi(x) dx \quad \forall\, \phi \in C_0^\infty(\Omega), \tag{2.1.1}$$

where the multi-index α is a vector $(\alpha_1, \alpha_2, \ldots \alpha_n)$ with length $|\alpha| := \sum_{i=1}^n \alpha_i$, and $D^\alpha \phi$ denotes the partial derivative $(\frac{\partial}{\partial x_1})^{\alpha_1} \cdots (\frac{\partial}{\partial x_n})^{\alpha_n} \phi$. We then define the weak derivative $D_w^\alpha f = g$.

Let k be a non-negative integer, and let $f \in L^1_{\mathrm{loc}}(\Omega)$. Suppose the weak derivatives $D_w^\alpha f$ exist for all $|\alpha| \le k$. The Sobolev norm [1] of f is defined by

$$\|f\|_{W_p^k(\Omega)} := \left(\sum_{|\alpha| \le k} \|D_w^\alpha f\|^p_{L^p(\Omega)} \right)^{1/p}, \tag{2.1.2}$$

where $1 \le p < \infty$. In the case where $p = \infty$,

$$\|f\|_{W_\infty^k(\Omega)} := \max_{|\alpha| \le k} \|D_w^\alpha f\|_{L^\infty(\Omega)}.$$

In either case, we define the Sobolev space [1] by

$$W_p^k(\Omega) := \left\{ f \in L^1_{\mathrm{loc}} : \|f\|_{W_p^k(\Omega)} < \infty \right\}. \tag{2.1.3}$$

Remark 2.1. *The Sobolev space $W_p^k(\Omega)$ is a Banach space.*

Remark 2.2. *Let Ω be an open set. Then $C^\infty(\Omega) \cap W_p^k(\Omega)$ is dense in $W_p^k(\Omega)$ for $p < \infty$.*

In particular, when $p = 2$, the Sobolev space $W_p^k(\Omega)$ is also denoted by

$$H^k(\Omega) := \left\{ f \in L^2(\Omega) : f \text{ has weak } L_2 \text{ derivatives up to order } k \right\}, \qquad (2.1.4)$$

which is a Hilbert space for each k.

The next theorem, which is also known as the extension theorem, relates Sobolev spaces on a given domain to those on $\mathbb{R}^n$. The proof can be found in [90].

Theorem 2.3. *Let Ω be a bounded open subset of $\mathbb{R}^n$ with a piecewise smooth boundary. Then there is an extension mapping $E : W_p^k(\Omega) \to W_p^k(\mathbb{R}^n)$ defined for all non-negative integers k and $1 \leq p \leq \infty$ such that $Ev|_\Omega = v$ for all $v \in W_p^k(\Omega)$ and*

$$\|Ev\|_{W_p^k(\mathbb{R}^n)} \leq C\|v\|_{W_p^k(\Omega)}$$

where the constant number C is independent of v.

Theorem 2.4. (Gagliardo-Nirenberg-Sobolev [67]) *Suppose $1 \leq p < n$, then*

$$W_p^1(\mathbb{R}^n) \hookrightarrow L_{p_*}(\mathbb{R}^n),$$

where $\frac{1}{p_*} = \frac{1}{p} - \frac{1}{n}$. More precisely,

$$W_p^1(\mathbb{R}^n) \subseteq L_{p_*}(\mathbb{R}^n),$$

and

$$\|v\|_{L_{p_*}(\mathbb{R}^n)} \leq C\|v\|_{W_p^1(\mathbb{R}^n)} \qquad \forall\, v \in W_p^1(\mathbb{R}^n).$$

Combining Theorem 2.3 and Theorem 2.4, we have the following theorem, which is known as Sobolev embedding theorem [67].

Theorem 2.5. *Let Ω be a bounded open subset of $\mathbb{R}^n$ with a piecewise smooth boundary. Suppose $1 \leq p < n$, then*

$$W_p^1(\Omega) \hookrightarrow L_{p_*}(\Omega),$$

where $\frac{1}{p_*} = \frac{1}{p} - \frac{1}{n}$.

Proof. Let $v \in W_p^1(\Omega)$. By Theorem 2.3, there is an extension mapping $E : W_p^1(\Omega) \to W_p^1(\mathbb{R}^n)$ such that $Ev \in W_p^1(\mathbb{R}^n)$. Therefore $Ev \in L_{p_*}(\mathbb{R}^n)$ and hence $v = Ev|_\Omega \in L_{P_*}(\Omega)$. Moreover,

$$\|v\|_{L_{P_*}(\Omega)} \leq \|Ev\|_{L_{p_*}(\mathbb{R}^n)} \leq C\|Ev\|_{W_p^1(\mathbb{R}^n)} \leq C\|v\|_{W_p^1(\Omega)}.$$

□

Theorem 2.6. (Trace Theorem [67]) *Let Ω be a bounded open subset of $\mathbb{R}^n$ with a piecewise smooth boundary. There exists a unique linear map*

$$Tr : H^1(\Omega) \to L_2(\partial\Omega)$$

such that for all $u \in H^1(\Omega)$,

$$\| Tr(v)\|_{L_2(\partial\Omega)} \leq C\|v\|_{H^1(\Omega)}.$$

We will use the notation $H_0^1(\Omega)$ to denote the subset of $H^1(\Omega)$ that consists of functions whose trace on $\partial\Omega$ is zero, i.e.,

$$H_0^1(\Omega) := \left\{v \in H^1(\Omega) : Tr(v) = 0 \text{ on } L_2(\partial\Omega)\right\}.$$

Details of the next theorem, which is sometimes called Poincaré-Friedrichs inequality, can be found in [67].

Theorem 2.7. *Let Ω be a bounded open subset of $\mathbb{R}^n$. There exist positive constants C_1 and C_2 such that*

$$\|v\|_{L_2(\Omega)} \leq C_1\Big(\Big|\int_\Omega v dx\Big| + |v|_{H^1(\Omega)}\Big) \qquad \forall\, v \in H^1(\Omega), \tag{2.1.5a}$$

$$\|v\|_{L_2(\Omega)} \leq C_2\Big(\Big|\int_{\partial\Omega} v ds\Big| + |v|_{H^1(\Omega)}\Big) \qquad \forall\, v \in H^1(\Omega). \tag{2.1.5b}$$

Corollary 2.8. *Under the conditions of Theorem 2.7, suppose $v \in H^1_0(\Omega)$, then*

$$\|v\|_{L_2(\Omega)} \leq C|v|_{H^1(\Omega)}.$$

2.2 Elliptic Regularity

In this section, we study the elliptic regularity results for both the Poisson problem and the curl-curl and grad-div (CCGD) problem.

2.2.1 Regularity of the Poisson Problem

We first consider the Poisson problem with homogeneous Dirichlet boundary condition:

$$-\Delta u + \alpha u = f \qquad \text{in } \Omega, \tag{2.2.1a}$$

$$u = 0 \qquad \text{on } \partial\Omega, \tag{2.2.1b}$$

where $\Omega \subset \mathbb{R}^2$ is a bounded polygonal domain, $\alpha \in \mathbb{R}$ and $f \in L_2(\Omega)$ (or $H^1(\Omega)$).

The variational problem for (2.2.1) (cf. [43]) is to find $u \in H^1_0(\Omega)$ such that

$$a(u, v) = F(v) \qquad \forall\, v \in H^1_0(\Omega), \tag{2.2.2}$$

where

$$a(w, v) = \int_\Omega \nabla w \cdot \nabla v \, dx + \alpha \int_\Omega wv \, dx,$$
$$F(v) = \int_\Omega fv \, dx.$$

We will briefly state the standard elliptic regularity results for the Poisson problem in the rest of this section. More details can be found in [70, 61, 81].

Let $\omega_1, \ldots, \omega_L$ be the interior angles at the corners $c_1, \ldots, c_L$ of the bounded polygonal domain Ω. Let $\delta > 0$ be small enough so that the neighborhoods $\mathcal{N}_{\ell,\delta} = \{x \in \Omega : |x - c_\ell| < \delta\}$ around the corners c_ℓ for $1 \leq \ell \leq L$ are disjoint. We then define the singular function on $\mathcal{N}_{\ell,2\delta}$ by

$$S_\ell(\gamma_\ell, \theta_\ell) = \chi_\ell(\gamma_\ell)\gamma^{(\pi/\omega_\ell)} \sin((\pi/\omega_\ell)\theta_\ell), \tag{2.2.4}$$

where $(\gamma_\ell, \theta_\ell)$ are the polar coordinates at the corner c_ℓ so that the two edges emanating from c_ℓ are defined by $\theta = 0$ and $\theta = \omega_\ell$, $\chi_\ell(t)$ is a C^∞ cut-off function that $\chi_\ell(t) = 1$ for $t < \delta$, and $\chi_\ell(t) = 0$ for $t > 2\delta$. For $1 \leq \ell \leq L$, the singular function S_ℓ has the following properties:

(i) If $\omega_\ell < \pi$, $S_\ell \in H^2(\Omega)$.

(ii) If $\omega_\ell > \pi$, i.e., c_ℓ is a reentrant corner, $S_\ell \in H^s(\mathcal{N}_{\ell,\delta})$ for any $1 \leq s < 1 + \frac{\pi}{\omega_\ell}$.

Theorem 2.9. *Let $u \in H_0^1(\Omega)$ be the weak solution of the Dirichlet problem* (2.2.1) *with $f \in L_2(\Omega)$ on domain Ω, then*

$$u = u_R + u_S, \tag{2.2.5}$$

where the regular part $u_R \in H^2(\Omega) \cap H_0^1(\Omega)$, the singular part $u_S = \sum_{\omega_\ell > \pi} \kappa_\ell S_\ell$, and the constants κ_ℓ are the generalized stress intensity factors. Moreover,

$$\|u_R\|_{H^2(\Omega)} + \sum_{\omega_\ell > \pi} |\kappa_\ell| \leq C\|f\|_{L_2(\Omega)}.$$

Corollary 2.10. *If Ω is convex, $u \in H^2(\Omega) \cap H_0^1(\Omega)$ and*

$$\|u\|_{H^2(\Omega)} \leq C\|f\|_{L_2(\Omega)}.$$

In the case where $f \in H^1(\Omega)$, we define at each corner c_ℓ the singular function

$$S_{\ell,j}(\gamma_\ell, \theta_\ell) = \chi_\ell(\gamma_\ell)\gamma^{j(\pi/\omega_\ell)} \sin(j(\pi/\omega_\ell)\theta_\ell), \ j = 1, 2, \cdots. \tag{2.2.6}$$

Moreover, the singular function $S_{\ell,j}$ has the following properties:

(i) If $j\frac{\pi}{\omega_\ell} \in \mathbb{N}$, $S_{\ell,j} \in C^\infty(\bar{\Omega})$.

(ii) If $j\frac{\pi}{\omega_\ell} \notin \mathbb{N}$, $S_{\ell,j} \in H^s(\mathcal{N}_{\ell,\delta})$ for any $1 \le s < 1 + j\frac{\pi}{\omega_\ell}$.

Theorem 2.11. *Let $u \in H_0^1(\Omega)$ be the weak solution of Dirichlet problem* (2.2.1) *with $f \in H^1(\Omega)$ on domain Ω, and $\Omega_\delta := \{x \in \Omega : |x - c_\ell| > \delta\}$. Then*

$$u = u_R + u_S, \tag{2.2.7}$$

where $u_R \in H^3(\Omega_\delta)$, $u_R \in H^{3-\varepsilon}(\mathcal{N}_{\ell,2\delta})$ *for any* $\varepsilon > 0$, *and*

$$u_S = \sum_{\ell=1}^{L} \sum_{\substack{j \in \mathbb{N} \\ j(\pi/\omega_\ell) \in (0,2)\setminus\{1\}}} \kappa_{\ell,j} S_{\ell,j}.$$

Moreover,

$$\|u_R\|_{H^3(\Omega_\delta)} + \sum_{\ell=1}^{L} \|u_R\|_{H^{3-\varepsilon}(\mathcal{N}_{\ell,2\delta})} + \sum_{\ell=1}^{L} \sum_{\substack{j \in \mathbb{N} \\ j(\pi/\omega_\ell) \in (0,2)\setminus\{1\}}} |\kappa_{\ell,j}| \le C_{\Omega,\varepsilon} \|f\|_{H^1(\Omega)}.$$

Next we consider the Poisson problem with homogeneous Neumann boundary condition:

$$-\Delta u + \alpha u = f \qquad \text{in } \Omega, \tag{2.2.8a}$$

$$\frac{\partial u}{\partial n} = 0 \qquad \text{on } \partial\Omega, \tag{2.2.8b}$$

where $\alpha \in \mathbb{R}$, $f \in L_2(\Omega)$ (or $H^1(\Omega)$) and $\int_\Omega f dx = \alpha \int_\Omega u dx$. When $\alpha = 0$, there exists a solution u such that $\int_\Omega u \, dx = 0$.

The variational problem for (2.2.8) is to find $u \in H^1(\Omega)$ such that

$$\int_\Omega \nabla u \cdot \nabla v \, dx + \alpha \int_\Omega uv \, dx = \int_\Omega fv \, dx \qquad \forall\, v \in H^1(\Omega). \tag{2.2.9}$$

Theorem 2.12. *The regularity results stated in Theorem 2.9 and Theorem 2.11 are still valid for problem* (2.2.8) *provided that the singular functions* (2.2.4) *and* (2.2.6) *are replaced by*

$$S_\ell(\gamma_\ell, \theta_\ell) = \chi_\ell(\gamma_\ell)\gamma^{(\pi/\omega_\ell)} \cos((\pi/\omega_\ell)\theta_\ell),$$

$$S_{\ell,j}(\gamma_\ell, \theta_\ell) = \chi_\ell(\gamma_\ell)\gamma^{j(\pi/\omega_\ell)} \cos(j(\pi/\omega_\ell)\theta_\ell), \; j = 1, 2, \cdots .$$

2.2.2 Regularity of the Curl-Curl and Grad-Div Problem

Now we turn to the regularity of the solution $\boldsymbol{u}$ of the curl-curl and grad-div problem (1.2.9), which is closely related to the regularity of the Laplace operator with homogeneous Dirichlet and Neumann boundary conditions. Main results can be found in [40, 37].

Since $\boldsymbol{u} \in H_0(\text{curl};\Omega) \cap H(\text{div};\Omega)$, by the Helmholtz decomposition (1.2.4), we have $\boldsymbol{u} = \mathring{\boldsymbol{u}} + \nabla\phi$, where $\mathring{\boldsymbol{u}} \in H_0(\text{curl};\Omega) \cap H(\text{div}^0;\Omega)$ and $\phi \in H_0^1(\Omega)$.

For simplicity, we first assume that Ω is simply connected. Hence there exists $\psi \in H^1(\Omega)$ (cf. [68]) such that

$$\nabla \times \psi = \mathring{\boldsymbol{u}} \text{ and } \int_\Omega \psi\, dx = 0,$$

and we can rewrite (1.2.4) as

$$\boldsymbol{u} = \nabla \times \psi + \nabla\phi. \tag{2.2.10}$$

It is easy to check that the function $\phi \in H_0^1(\Omega)$ in (2.2.10) is the variational solution of the following Dirichlet boundary value problem:

$$\Delta\phi = \nabla \cdot \boldsymbol{u} \quad \text{in } \Omega, \tag{2.2.11a}$$

$$\phi = 0 \quad \text{on } \partial\Omega, \tag{2.2.11b}$$

and the function ψ is the unique variational solution with zero mean of the following Neumann boundary value problem:

$$\Delta\psi = -\nabla \times \boldsymbol{u} \quad \text{in } \Omega, \tag{2.2.12a}$$

$$\frac{\partial\psi}{\partial n} = 0 \quad \text{on } \partial\Omega. \tag{2.2.12b}$$

We first discuss the case where $\alpha > 0$ in (1.2.9). It is clear that

$$\|\boldsymbol{u}\|_{L_2(\Omega)} \le \alpha^{-1}\|\boldsymbol{f}\|_{L_2(\Omega)}, \tag{2.2.13}$$

$$\|\nabla \times \boldsymbol{u}\|^2_{L_2(\Omega)} + \gamma\|\nabla \cdot \boldsymbol{u}\|^2_{L_2(\Omega)} \le \alpha^{-1}\|\boldsymbol{f}\|^2_{L_2(\Omega)}. \tag{2.2.14}$$

In view of (1.2.9), the divergence free part $\mathring{\boldsymbol{u}}$ in the Helmholtz decomposition (1.2.4) satisfies

$$(\nabla \times \mathring{\boldsymbol{u}}, \nabla \times \boldsymbol{v}) + \alpha(\mathring{\boldsymbol{u}}, \boldsymbol{v}) = (\boldsymbol{f}, \boldsymbol{v}) \tag{2.2.15}$$

for all $\boldsymbol{v} \in H_0(\text{curl}; \Omega) \cap H(\text{div}^0; \Omega)$, which implies

$$\nabla \times (\nabla \times \mathring{\boldsymbol{u}}) + \alpha \mathring{\boldsymbol{u}} = Q\boldsymbol{f}, \tag{2.2.16}$$

where Q is the orthogonal projection from $[L_2(\Omega)]^2$ onto $H(\text{div}^0; \Omega)$. Indeed, let $\boldsymbol{\zeta} \in [C_0^\infty(\Omega)]^2$ be a test vector field. Then $\boldsymbol{\zeta} \in H_0(\text{curl}; \Omega)$ and $(\boldsymbol{\zeta} - Q\boldsymbol{\zeta}) \in \nabla H_0^1(\Omega) \subset H_0(\text{curl}; \Omega)$, which imply that $Q\boldsymbol{\zeta} \in H_0(\text{curl}; \Omega) \cap H(\text{div}^0; \Omega)$. Hence it follows from (2.2.15) that

$$\begin{aligned}(\nabla \times \mathring{\boldsymbol{u}}, &\nabla \times \boldsymbol{\zeta}) + \alpha(\mathring{\boldsymbol{u}}, \boldsymbol{\zeta}) = (\nabla \times \mathring{\boldsymbol{u}}, \nabla \times [Q\boldsymbol{\zeta} + (\boldsymbol{\zeta} - Q\boldsymbol{\zeta})]) + \alpha(\mathring{\boldsymbol{u}}, Q\boldsymbol{\zeta} + (\boldsymbol{\zeta} - Q\boldsymbol{\zeta}))\\ &= (\nabla \times \mathring{\boldsymbol{u}}, \nabla \times Q\boldsymbol{\zeta}) + \alpha(\mathring{\boldsymbol{u}}, Q\boldsymbol{\zeta}) = (\boldsymbol{f}, Q\boldsymbol{\zeta}) = (Q\boldsymbol{f}, \boldsymbol{\zeta}),\end{aligned}$$

which yields (2.2.16).

It follows from (2.2.16) that $\nabla \times (\nabla \times \mathring{\boldsymbol{u}}) = Q\boldsymbol{f} - \alpha\mathring{\boldsymbol{u}} \in [L_2(\Omega)]^2$, hence $\nabla \times \mathring{\boldsymbol{u}} \in H^1(\Omega)$. Then we deduce from (1.2.4) and (2.2.13) that $\nabla \times \boldsymbol{u} = \nabla \times \mathring{\boldsymbol{u}} \in H^1(\Omega)$, and

$$|\nabla \times \boldsymbol{u}|_{H^1(\Omega)} = |\nabla \times \mathring{\boldsymbol{u}}|_{H^1(\Omega)} = \|Q\boldsymbol{f} - \alpha\boldsymbol{u}\|_{L_2(\Omega)} \leq 2\|\boldsymbol{f}\|_{L_2(\Omega)}, \tag{2.2.17}$$

which together with (1.2.9) implies that $\nabla \cdot \boldsymbol{u} \in H^1(\Omega)$ and

$$\begin{aligned}|\nabla \cdot \boldsymbol{u}|_{H^1(\Omega)} \leq &\gamma^{-1}\|\boldsymbol{f} - \alpha\boldsymbol{u} - \nabla \times (\nabla \times \boldsymbol{u})\|_{L_2(\Omega)}\\ \leq &4\gamma^{-1}\|\boldsymbol{f}\|_{L_2(\Omega)}.\end{aligned} \tag{2.2.18}$$

In particular, it follows from the regularity of $\nabla \times \boldsymbol{u}$ and $\nabla \cdot \boldsymbol{u}$ and the usual variational argument that the boundary value problem corresponding to (1.2.9) is

$$\nabla \times (\nabla \times \boldsymbol{u}) - \gamma \nabla(\nabla \cdot \boldsymbol{u}) + \alpha \boldsymbol{u} = \boldsymbol{f} \quad \text{in } \Omega, \tag{2.2.19a}$$

$$\boldsymbol{n} \times \boldsymbol{u} = 0 \quad \text{on } \partial\Omega, \tag{2.2.19b}$$

$$\nabla \cdot \boldsymbol{u} = 0 \quad \text{on } \partial\Omega. \tag{2.2.19c}$$

The regularity of $\boldsymbol{u}$ can then be derived through (2.2.10)–(2.2.12), Theorem 2.11 and Theorem 2.12.

Since $\nabla \cdot \boldsymbol{u} \in H^1(\Omega)$, the elliptic regularity theory provides a decomposition

$$\phi = \phi_R + \phi_S, \tag{2.2.20}$$

such that the regular part $\phi_R \in H^3(\Omega_\delta)$, and $\phi_R \in H^{3-\epsilon}(\mathcal{N}_{\ell,2\delta})$ for any $\epsilon > 0$, $1 \le \ell \le L$. The singular part ϕ_S is supported near the corners $c_1, \ldots, c_L$ of Ω. More precisely, we can write

$$\phi_S = \sum_{\ell=1}^{L} \bar{\chi}_\ell(r_\ell) \sum_{\substack{j \in \mathbb{N} \\ j(\pi/\omega_\ell) \in (0,2)\setminus\{1\}}} \kappa_{\ell,j} r_\ell^{j(\pi/\omega_\ell)} \sin\big(j(\pi/\omega_\ell)\theta_\ell\big), \tag{2.2.21}$$

where $\bar{\chi}_\ell(t)$ is a smooth cut-off function that equals 1 for $t < \delta$ and vanishes for $t > 3\delta/2$, and $\kappa_{\ell,j}$ are constants.

Furthermore, it follows from estimates (2.2.14) and (2.2.18) that

$$\|\phi_R\|_{H^3(\Omega_\delta)} \le C\|\nabla \cdot \boldsymbol{u}\|_{H^1(\Omega)} \le C\gamma^{-1/2}(\gamma^{-1/2} + \alpha^{-1/2})\|\boldsymbol{f}\|_{L_2(\Omega)}, \tag{2.2.22a}$$

$$\|\phi_R\|_{H^{3-\epsilon}(\mathcal{N}_{\ell,2\delta})} \le C_\epsilon\|\nabla \cdot \boldsymbol{u}\|_{H^1(\Omega)} \le C_\epsilon\gamma^{-1/2}(\gamma^{-1/2} + \alpha^{-1/2})\|\boldsymbol{f}\|_{L_2(\Omega)}, \tag{2.2.22b}$$

$$\sum_{\ell=1}^{L} \sum_{\substack{j \in \mathbb{N} \\ j(\pi/\omega_\ell) \in (0,2)\setminus\{1\}}} |\kappa_{\ell,j}| \le C\|\nabla \cdot \boldsymbol{u}\|_{H^1(\Omega)} \le C\gamma^{-1/2}(\gamma^{-1/2} + \alpha^{-1/2})\|\boldsymbol{f}\|_{L_2(\Omega)}. \tag{2.2.22c}$$

Similarly, the function ψ in (2.2.10) has the following decomposition:

$$\psi = \psi_R + \psi_S, \tag{2.2.23}$$

where the regular part ψ_R belongs to $H^3(\Omega_\delta)$, and $\psi_R \in H^{3-\epsilon}(\mathcal{N}_{\ell,2\delta})$ for any $\epsilon > 0$, $1 \le \ell \le L$. The singular part ψ_S is given by

$$\psi_S = \sum_{\ell=1}^{L} \bar{\chi}_\ell(r_\ell) \sum_{\substack{j\in\mathbb{N} \\ j(\pi/\omega_\ell)\in(0,2)\setminus\{1\}}} \varrho_{\ell,j} r_\ell^{j(\pi/\omega_\ell)} \cos\big(j(\pi/\omega_\ell)\theta_\ell\big). \tag{2.2.24}$$

Furthermore, the following analog of (2.2.22) holds:

$$\|\psi_R\|_{H^3(\Omega_\delta)} \le C\|\nabla\times\boldsymbol{u}\|_{H^1(\Omega)} \le C(1+\alpha^{-1/2})\|\boldsymbol{f}\|_{L_2(\Omega)}, \tag{2.2.25a}$$

$$\|\psi_R\|_{H^{3-\epsilon}(\mathcal{N}_{\ell,2\delta})} \le C_\epsilon\|\nabla\times\boldsymbol{u}\|_{H^1(\Omega)} \le C_\epsilon(1+\alpha^{-1/2})\|\boldsymbol{f}\|_{L_2(\Omega)}, \tag{2.2.25b}$$

$$\sum_{\ell=1}^{L} \sum_{\substack{j\in\mathbb{N} \\ j(\pi/\omega_\ell)\in(0,2)\setminus\{1\}}} |\varrho_{\ell,j}| \le C\|\nabla\times\boldsymbol{u}\|_{H^1(\Omega)} \le C(1+\alpha^{-1/2})\|\boldsymbol{f}\|_{L_2(\Omega)}, \tag{2.2.25c}$$

where we have used the estimates (2.2.14) and (2.2.17).

Combining (2.2.10), (2.2.20)–(2.2.25), we can describe the regularity of the solution $\boldsymbol{u}$ of (1.2.9) as follows. We have $\boldsymbol{u} \in [H^2(\Omega_\delta)]^2$ and the following estimate is valid:

$$\|\boldsymbol{u}\|_{H^2(\Omega_\delta)} \le C(1+\gamma^{-1}+\alpha^{-1/2}(1+\gamma^{-1/2}))\|\boldsymbol{f}\|_{L_2(\Omega)}. \tag{2.2.26}$$

In the neighborhood $\mathcal{N}_{\ell,3\delta/2}$ of the corner c_ℓ, we have

$$\boldsymbol{u} = \boldsymbol{u}_R + \boldsymbol{u}_S, \tag{2.2.27}$$

such that the regular part $\boldsymbol{u}_R \in [H^{2-\epsilon}(\mathcal{N}_{\ell,3\delta/2})]^2$ for any $\epsilon > 0$, and the singular part

$$\boldsymbol{u}_S = \sum_{\substack{j\in\mathbb{N} \\ j(\pi/\omega_\ell)\in(0,2)\setminus\{1\}}} \nu_{\ell,j}\boldsymbol{\psi}_{\ell,j}, \tag{2.2.28}$$

where

$$\boldsymbol{\psi}_{\ell,j} = r_\ell^{j(\pi/\omega_\ell)-1} \begin{bmatrix} \sin\big(j(\pi/\omega_\ell)-1\big)\theta_\ell \\ \cos\big(j(\pi/\omega_\ell)-1\big)\theta_\ell \end{bmatrix}, \tag{2.2.29a}$$

$$\nu_{\ell,j} = j(\pi/\omega_\ell)(\kappa_{\ell,j}-\varrho_{\ell,j}). \tag{2.2.29b}$$

Moreover, the following corner regularity estimates hold:

$$\sum_{\ell=1}^{L} \|\boldsymbol{u}_R\|_{H^{2-\epsilon}(\mathcal{N}_{\ell,3\delta/2})} \leq C_\epsilon(1+\gamma^{-1}+\alpha^{-1/2}(1+\gamma^{-1/2}))\|\boldsymbol{f}\|_{L_2(\Omega)}, \tag{2.2.30a}$$

$$\sum_{\ell=1}^{L} \sum_{\substack{j\in\mathbb{N} \\ j(\pi/\omega_\ell)\in(0,2)\setminus\{1\}}} |\nu_{\ell,j}| \leq C(1+\gamma^{-1}+\alpha^{-1/2}(1+\gamma^{-1/2}))\|\boldsymbol{f}\|_{L_2(\Omega)}. \tag{2.2.30b}$$

Remark 2.13. *Theorem 2.11 and the singular vector field representation* (2.2.27) *imply that* $\boldsymbol{u} \in [H^s(\mathcal{N}_{\ell,\delta})]^2$ *for any* $s < \frac{\pi}{\omega_\ell}$. *Therefore* $\boldsymbol{u} \in [H^s(\Omega)]^2$ *for any* $s < \min_{1\leq\ell\leq L} \frac{\pi}{\omega_\ell}$. *In particular, we can choose* s *to be strictly greater than* $\frac{1}{2}$.

So far the regularity results for $\boldsymbol{u}$ are derived under the assumption that Ω is simply connected. A standard partition of unity argument yields the same results for general polygonal domains.

For $\alpha \leq 0$, by replacing (2.2.13) and (2.2.14) with

$$\|\nabla \times \boldsymbol{u}\|_{L_2(\Omega)} + \gamma\|\nabla \cdot \boldsymbol{u}\|_{L_2(\Omega)} + \|\boldsymbol{u}\|_{L_2(\Omega)} \leq C_\alpha\|\boldsymbol{f}\|_{L_2(\Omega)}, \tag{2.2.31}$$

we can show that results for $\alpha > 0$ remain valid provided $\alpha \neq -\lambda_{\gamma,j}$ for $j \geq 1$, where $0 \leq \lambda_{\gamma,1} \leq \lambda_{\gamma,2} \leq \cdots \to \infty$ are the eigenvalues defined by (1.2.10).

2.2.3 Regularity Results in Terms of Weighted Sobolev Spaces

In the remaining part of this section we briefly introduce the elliptic regularity results in terms of weighted Sobolev spaces for the Poisson problem. More details can be found in [76, 61, 81].

Let $\omega_1, \ldots, \omega_L$ be the interior angles at the corners $c_1, \ldots, c_L$ of the bounded polygonal domain Ω. Let the parameters $\mu_1, \ldots, \mu_\ell$ be chosen according to

$$\begin{aligned} \mu_\ell &= 1 && \text{if} \quad \omega_\ell \leq \pi, \\ \mu_\ell &< \frac{\pi}{\omega_\ell} && \text{if} \quad \omega_\ell > \pi, \end{aligned} \tag{2.2.32}$$

and the weight function ϕ_μ be defined by

$$\phi_\mu(x) = \prod_{\ell=1}^{L} |x - c_\ell|^{1-\mu_\ell}. \qquad (2.2.33)$$

The weighted Sobolev space $L_{2,\mu}(\Omega)$ is defined by

$$L_{2,\mu}(\Omega) = \{f \in L^2_{\text{loc}}(\Omega) :\ \|f\|^2_{L_{2,\mu}(\Omega)} = \int_\Omega \phi^2_\mu(x) f^2(x)\, dx < \infty\}. \qquad (2.2.34)$$

Note that $L_2(\Omega) \subset L_{2,\mu}(\Omega)$ and

$$\|f\|_{L_{2,\mu}(\Omega)} \le C_\Omega \|f\|_{L_2(\Omega)} \qquad \forall\, f \in L_2(\Omega). \qquad (2.2.35)$$

Lemma 2.14.

$$\int_\Omega |fv|\, dx \le C_\Omega \|f\|_{L_{2,\mu}(\Omega)} \|v\|_{H^1(\Omega)} \qquad \forall\, v \in H^1(\Omega). \qquad (2.2.36)$$

Proof. Note that $\phi^{-2}_\mu(x) \in L^2(\Omega)$. It follows from the Hölder inequality [67] and the Sobolev embedding theorem (cf. Theorem 2.5) that

$$\begin{aligned}
\int_\Omega |fv|\, dx =& \int_\Omega |\phi_\mu f||\phi^{-1}_\mu v|\, dx \\
\le& (\int_\Omega \phi^2_\mu f^2 dx)^{1/2} (\int_\Omega \phi^{-2}_\mu v^2\, dx)^{1/2} \\
\le& \|f\|_{L_{2,\mu}(\Omega)} \|\phi^{-2}_\mu\|^{1/2}_{L^2(\Omega)} \|v^2\|^{1/2}_{L_2(\Omega)} \\
\le& C_\Omega \|f\|_{L_{2,\mu}(\Omega)} \|v\|_{L_4(\Omega)} \\
\le& C_\Omega \|f\|_{L_{2,\mu}(\Omega)} \|v\|_{H^1(\Omega)}.
\end{aligned}$$

□

It follows from Lemma 2.14 that the model problem (2.2.2) has a unique solution u for any $f \in L_{2,\mu}(\Omega)$. Moreover u has the following properties:

(i) The solution u belongs to the weighted Sobolev space $H^2_\mu(\Omega)$, i.e.,

$$\gamma^{|\alpha|-2}(\partial^\alpha u / \partial x^\alpha) \in L_{2,\mu}(\Omega) \qquad \text{for} \quad |\alpha| \le 2,$$

and the following regularity estimate holds:

$$\|u\|_{H^2_\mu(\Omega)} = \Big(\sum_{|\alpha|\le 2} \|\gamma^{|\alpha|-2}(\partial^\alpha u/\partial x^\alpha)\|^2_{L_{2,\mu}(\Omega)} \Big)^{1/2} \le C_\Omega \|f\|_{L_{2,\mu}(\Omega)}, \qquad (2.2.37)$$

where the function $\gamma(x)$ is defined by $\gamma(x) = \prod_{\ell=1}^{L} |x - c_\ell|$.

(ii) At a reentrant corner c_ℓ where $\omega_\ell > \pi$, we have $u \in H^{1+\mu_\ell}(\mathcal{N}_{\ell,\delta})$ and

$$\|u\|_{H^{1+\mu_\ell}(\mathcal{N}_{\ell,\delta})} \le C_\Omega \|f\|_{L_{2,\mu}(\Omega)}. \qquad (2.2.38)$$

(iii) u is continuous on $\bar{\Omega}$.

The regularity of u away from the corners follows from the standard elliptic regularity theory. The elliptic regularity of u near a corner c_ℓ can be obtained by the change of coordinates $(x_1, x_2) = e^t(\cos\theta, \sin\theta)$ and the elliptic regularity theory on the infinite strip $\mathbb{R} \times (0, \omega_\ell)$, where the two edges emanating from c_ℓ are represented by $\theta = 0$ and $\theta = \omega_\ell$ (cf. [61, 81]). The continuity of u away from the reentrant corners follows from the usual Sobolev inequality, while the continuity of u at a reentrant corner c_ℓ follows from the Sobolev inequality on the infinite strip $\mathbb{R} \times (0, \omega_\ell)$ and a change of coordinates.

Remark 2.15. *For the curl-curl and grad-div problem* (1.2.9), *the parameters* $\mu_1, \ldots, \mu_\ell$ *are chosen according to*

$$\begin{aligned} \mu_\ell &= 1 && \textit{if} \quad \omega_\ell \le \frac{\pi}{2}, \\ \mu_\ell &< \frac{\pi}{2\omega_\ell} && \textit{if} \quad \omega_\ell > \frac{\pi}{2}. \end{aligned} \qquad (2.2.39)$$

In the case where $\omega_\ell > \frac{\pi}{2}$, *it follows from Remark 2.13 that the curl-curl and grad-div problem* (1.2.9) *has a solution* $\boldsymbol{u} \in [H^{2\mu_\ell}(\mathcal{N}_{\ell,\delta})]^2$, *and in view of* (2.2.27)–(2.2.30), *the following regularity estimate* [40] *is valid:*

$$\|\boldsymbol{u}\|_{H^{2\mu_\ell}(\mathcal{N}_{\ell,\delta})} \le C\|\boldsymbol{f}\|_{L_2(\Omega)}. \qquad (2.2.40)$$

2.3 Graded Meshes

In Section 2.2, we showed that the exact solution of the model problem (2.2.2) (resp. (1.2.9)) has singularities when the bounded polygonal domain Ω is non-convex (resp. Ω has corners with interior angle larger than $\pi/2$). To compensate for the lack of full elliptic regularity, the meshes need to be graded properly. The graded meshes also play a crucial role to recover optimal *a priori* error estimates for nonconforming finite element methods and to prove uniform convergence of multigrid methods.

We first consider a family of simplicial triangulations $\mathcal{T}_h$ of Ω with mesh-parameter $h = \max_{T\in\mathcal{T}_h} h_T$, where h_T is the diameter of the triangle T. The triangulation $\mathcal{T}_h$ is graded around the corners $c_1, \ldots, c_L$ of Ω with the property that

$$h_T \approx h\Phi_\mu(T), \tag{2.3.1}$$

where

$$\Phi_\mu(T) = \prod_{\ell=1}^{L} |c_\ell - c_T|^{1-\mu_\ell}, \tag{2.3.2}$$

and c_T is the center of T. It can be observed that

$$\Phi_\mu(T) \lesssim 1. \tag{2.3.3}$$

Remark 2.16. *From here on we will use the notation $\alpha \lesssim \beta$ to represent the inequality $\alpha \le C \times \beta$, where the positive constant C is independent of h that can take different values at different occurrences. The relation* (2.3.1) *means $h_T \lesssim h\Phi_\mu(T)$ and $h\Phi_\mu(T) \lesssim h_T$.*

The construction of graded meshes $\mathcal{T}_h$ is described for example in [2, 3, 32, 14, 28]. Note that $\mathcal{T}_h$ satisfies the minimum angle condition for any given grading parameters.

For the Poisson problem (2.2.2), the grading parameters $\mu_1, \ldots, \mu_L$ are chosen according to (2.2.32). In other words, grading is needed around reentrant corners.

However, the grading parameters for the curl-curl and grad-div problem (1.2.9) are chosen according to (2.2.39). Grading is needed around corners with any interior angle larger than $\pi/2$, which is different from the grading strategy for the Laplace operator. This is due to the fact that the singularity of (1.2.9) is one order more severe than the singularity of the Laplace operator.

We note that (2.3.1)–(2.3.3) imply

$$h_T \lesssim h \qquad \forall\, T \in \mathcal{T}_h, \tag{2.3.4}$$

$$h_T \approx h^{1/\mu_\ell} \qquad \text{if } c_\ell \in \partial T. \tag{2.3.5}$$

An example of the construction of graded meshes for (2.2.2) is described as follows (cf. [36]), where the refinement procedure is identical with the one in [28].

Let $\mathcal{T}_0$ be an initial triangulation of Ω. Given triangulation $\mathcal{T}_k$ ($k \geq 1$), we divide each triangle $T \in \mathcal{T}_k$ into four triangles according to the following rules to obtain $\mathcal{T}_{k+1}$.

(i) If none of vertices of T is a reentrant corner, we divide T uniformly by connecting the three midpoints of the edges of T.

(ii) If a reentrant corner c_ℓ is a vertex of T and the other two vertices are denoted by v_1 and v_2, then we divide T by connecting the points m, m_1 and m_2 (cf. Figure 2.1). Here m is the midpoint of the edge v_1v_2 and m_1 (resp. m_2) is the point on the edge $c_\ell v_1$ (resp. $c_\ell v_2$) such that

$$\frac{|c_\ell - m_i|}{|c_\ell - v_i|} = 2^{-(1/\mu_\ell)} \qquad \text{for} \quad i = 1, 2, \tag{2.3.6}$$

where μ_ℓ is the grading factor chosen according to (2.2.32).

The triangulations $\mathcal{T}_0$, $\mathcal{T}_1$ and $\mathcal{T}_2$ for an L-shaped domain are depicted in Figure 2.2, where the grading factor at the reentrant corner is taken to be 2/3.

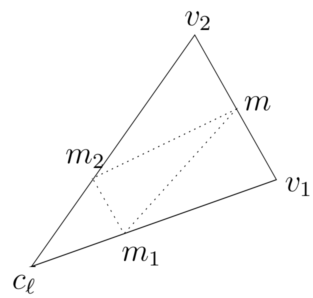

FIGURE 2.1. Refinement of a triangle at a reentrant corner

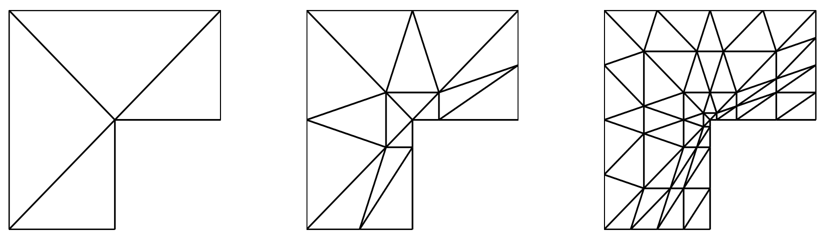

FIGURE 2.2. The triangulations $\mathcal{T}_0$, $\mathcal{T}_1$ and $\mathcal{T}_2$ on the L-shaped domain

It is easy to check that the nested triangulations $\mathcal{T}_k$ constructed as above satisfy (2.3.1), and

$$h_{k-1} \approx h_k \qquad \text{for } k \geq 1, \tag{2.3.7}$$

where $h_k = \max_{T \in \mathcal{T}_k} h_T$.

2.4 Finite Element Methods for the Poisson Problem

We will consider the finite element methods for the Poisson problem in this section.

2.4.1 Conforming Finite Element Methods

Suppose $\mathcal{T}_h$ is a family of uniform triangulations of Ω. Let V_h be the space of continuous P_1 finite element functions defined by

$$V_h = \{v \in C(\bar{\Omega}) : v = 0 \text{ on } \partial\Omega,\ v_T = v\big|_T \in P_1(T) \quad \forall\, T \in \mathcal{T}_h\}.$$

Remark 2.17. *The finite element space V_h is a subspace of $H_0^1(\Omega)$, on which the continuous problem* (2.2.2) *is posed.*

The discrete problem for model problem (2.2.2) is described as follows.

Find $u_h \in V_h$ such that

$$a(u_h, v) = F(v) \qquad \forall\, v \in V_h, \tag{2.4.1}$$

where $a(\cdot,\cdot)$ and $F(\cdot)$ are taken as in (2.2.2) with $f \in L_2(\Omega)$.

It is easy to show that F is a bounded linear functional on $H_0^1(\Omega)$. Moreover, the bilinear form $a(\cdot,\cdot)$ is bounded on $H_0^1(\Omega)$, i.e.,

$$a(v, w) \leq \|v\|_a \|w\|_a \qquad \forall\, v, w \in H_0^1(\Omega), \tag{2.4.2}$$

where

$$\|v\|_a = \sqrt{a(v, v)}. \tag{2.4.3}$$

It follows from Corollary 2.8 that

$$\|v\|_a \approx \|v\|_{H^1(\Omega)} \quad \forall\, v \in H_0^1(\Omega). \tag{2.4.4}$$

Therefore $a(\cdot,\cdot)$ is coercive, i.e., there exists a positive constant C_c such that

$$|a(v, v)| \geq C_c \|v\|^2_{H^1(\Omega)} \qquad \forall\, v \in H_0^1(\Omega). \tag{2.4.5}$$

Hence the discrete problem (2.4.1) has a unique solution (cf. [43, Theorem 2.5.8]).

Let u be the solution of (2.2.2) and u_h solve the discrete problem (2.4.1). By subtracting (2.4.1) from (2.2.2), we arrive at the fundamental Galerkin orthogonality:

$$a(u - u_h, v) = 0 \qquad \forall\, v \in V_h. \tag{2.4.6}$$

Hence the following lemma (cf. [43, Theorem 2.8.1]) stating the abstract error estimate is valid.

Lemma 2.18. (Céa) *Let u solve* (2.2.2) *and u_h solve the discrete problem* (2.4.1)*. Then we have*

$$\|u - u_h\|_{H^1(\Omega)} \lesssim \min_{v \in V_h} \|u - v\|_{H^1(\Omega)}. \tag{2.4.7}$$

To turn the abstract error estimate (2.4.7) into a concrete estimate, we need an interpolation operator. Let $\Pi_h : C(\bar{\Omega}) \longrightarrow V_h$ be the nodal interpolation operator for the conforming P_1 finite element. The following lemma provides a standard interpolation error estimate (cf. [51, 43]).

Lemma 2.19. *Let $\omega_1, \ldots, \omega_L$ be the interior angles at corners $c_1, \ldots, c_L$ of the bounded polygonal domain Ω, $f \in L_2(\Omega)$, and $u = u_R + u_S$ solve* (2.2.2)*, where u_R and u_S are the regular part and singular part of u (cf.* (2.2.5)*). Then we have*

$$\|u_R - \Pi_h u_R\|_{L_2(\Omega)} + h|u_R - \Pi_h u_R|_{H^1(\Omega)} \leq Ch^2 |u_R|_{H^2(\Omega)}. \tag{2.4.8}$$

$$\|u_S - \Pi_h u_S\|_{L_2(\Omega)} + h|u_S - \Pi_h u_S|_{H^1(\Omega)} \leq Ch \sum_{\omega_\ell > \pi} \big(|\kappa_\ell| h^{\pi/\omega_\ell}\big). \tag{2.4.9}$$

The next theorem, which directly follows from Theorem 2.9, Lemma 2.18, Lemma 2.19 and a standard duality argument [43], provides the discrete error estimates for scheme (2.4.1).

Theorem 2.20. *Let Ω be a bounded polygonal domain, u solve* (2.2.2) *and u_h solve the discrete problem* (2.4.1)*. Then under the assumptions of Lemma 2.19, we have*

$$\|u - u_h\|_{L_2(\Omega)} + h|u - u_h|_{H^1(\Omega)} \leq Ch^{1+\beta} \|f\|_{L_2(\Omega)}, \tag{2.4.10}$$

where the index $\beta > \frac{1}{2}$ is defined by

$$\beta = \min\Big(1, \min_{1 \leq \ell \leq L} \frac{\pi}{\omega_\ell}\Big). \tag{2.4.11}$$

Note that $\beta = 1$ if Ω is convex.

Remark 2.21. *The preceding discussion also holds for the conforming P_1 finite element method* (2.4.1) *for the Neumann problem* (2.2.9)*. In this case the P_1 finite element space is defined by $V_h = \{v \in C(\bar{\Omega}) : v_T = v\big|_T \in P_1(T) \quad \forall\, T \in \mathcal{T}_h\}$, which belongs to $H^1(\Omega)$. The discrete error estimate* (2.4.10) *can be obtained.*

2.4.2 Nonconforming Finite Element Methods

In Section 2.4.1, we have considered the error estimates for conforming finite elements for (2.2.2) based on the fact that

$$V_h \subset H_0^1(\Omega). \tag{2.4.12}$$

In the other case, the condition (2.4.12) is violated because of the use of nonconforming finite elements, where $V_h \not\subseteq H_0^1(\Omega)$, i.e., the finite element functions are not sufficiently smooth.

Suppose Ω is a convex polygonal domain and let $\mathcal{T}_h$ be a family of uniform triangulations on Ω. The nonconforming P_1 finite element space is defined to be

$$\begin{aligned} V_h := \{v : v\big|_T \text{ is linear for all } T \text{ in } \mathcal{T}_h,\ v \text{ is continuous} \\ \text{at the midpoints of the edges of } \mathcal{T}_h, \text{ and } v = 0 \\ \text{at the midpoints of the edges on } \partial\Omega\}. \end{aligned}$$

Note that $V_h \not\subseteq H_0^1(\Omega)$ since functions in V_h are no longer continuous. Hence we must use $a_h(\cdot,\cdot)$, which is a modification of $a(\cdot,\cdot)$ in the discrete problem for (2.2.2).

A typical nonconforming method for model problem (2.2.2) with $\alpha = 0$ and $f \in L_2(\Omega)$ is defined as follows:
Find $u_h \in V_h$ such that

$$a_h(u_h, v) = F(v) \qquad \forall\, v \in V_h, \tag{2.4.13}$$

where

$$a_h(v, w) = \sum_{T\in\mathcal{T}_h} \int_T \nabla v \cdot \nabla w dx \qquad \forall\, v, w \in V_h.$$

The following lemma (cf. [43, Theorem 10.1.9]) gives the abstract error estimate for scheme (2.4.13).

Lemma 2.22. *Let* $u \in H_0^1(\Omega)$ *solve* (2.2.2) ($\alpha = 0$) *and* $u_h \in V_h$ *solve* (2.4.13). *Then*

$$\|u - u_h\|_{a_h} \leq \inf_{w \in V_h} \|u - w\|_{a_h} + \sup_{w \in V_h/\{0\}} \frac{|a_h(u - u_h, w)|}{\|w\|_{a_h}}, \tag{2.4.14}$$

where $\|v\|_{a_h} = \sqrt{a_h(v,v)} \quad \forall\, v \in V_h$.

Proof. Let $\tilde{u}_h \in V_h$ satisfy

$$a_h(\tilde{u}_h, v) = a_h(u, v) \quad v \in V_h. \tag{2.4.15}$$

In view of the triangle inequality,

$$\|u - u_h\|_{a_h} \leq \|u - \tilde{u}_h\|_{a_h} + \|\tilde{u}_h - u_h\|_{a_h}. \tag{2.4.16}$$

For any $v \in V_h$, it follows from (2.4.15) that

$$\begin{aligned}
\|u - v\|_{a_h}^2 =& a_h(u - v, u - v) \\
=& a_h(u - \tilde{u}_h + \tilde{u}_h - v, u - \tilde{u}_h + \tilde{u}_h - v) \\
=& a_h(u - \tilde{u}_h, u - \tilde{u}_h) + a_h(\tilde{u}_h - v, \tilde{u}_h - v) \\
\geq& a_h(u - \tilde{u}_h, u - \tilde{u}_h) \\
=& \|u - \tilde{u}_h\|_{a_h}^2.
\end{aligned} \tag{2.4.17}$$

Hence the first term on the right-hand side of (2.4.16) can be estimated by

$$\|u - \tilde{u}_h\|_{a_h} \leq \inf_{v \in V_h} \|u - v\|_{a_h}. \tag{2.4.18}$$

It remains to estimate the second term on the right-hand side of (2.4.16). Combining (2.4.15) and a duality formula, we arrive at

$$\begin{aligned}
\|\tilde{u}_h - u_h\|_{a_h} &= \sup_{w \in V_h/\{0\}} \frac{|a_h(\tilde{u}_h - u_h, w)|}{\|w\|_{a_h}} \\
&= \sup_{w \in V_h/\{0\}} \frac{|a_h(u - u_h, w)|}{\|w\|_{a_h}}.
\end{aligned} \tag{2.4.19}$$

The estimate (2.4.14) the follows from (2.4.16), (2.4.18) and (2.4.19). □

Remark 2.23. *The first term on the right-hand side of* (2.4.14) *describes the approximation property of the space V_h, while the second term measures the non-conforming consistency error.*

Let $\Pi_h u \in V_h$ be the nodal interpolant of u, i.e., $\Pi_h u$ agrees with u at the midpoints of the edges of $\mathcal{T}_h$. Since $u \in H^2(\Omega) \cap H_0^1(\Omega)$ when Ω is convex, a standard interpolation error estimate (cf. [51, 43]) yields:

$$\inf_{v \in V_h} \|u - v\|_{a_h} \leq \|u - \Pi_h u\|_{a_h} \leq Ch|u|_{H^2(\Omega)}. \tag{2.4.20}$$

For the second term on the right-hand side of (2.4.14), we have

$$|a_h(u - u_u, w)| \leq Ch|u|_{H^2(\Omega)}\|w\|_{a_h}. \tag{2.4.21}$$

The next theorem provides the discrete error estimate for scheme (2.4.13) in the energy norm, whose proof uses Corollary 2.10, Lemma 2.22, (2.4.20) and (2.4.21).

Theorem 2.24. *Let Ω be a convex polygonal domain, u solve* (2.2.2) *and u_h solve the discrete problem* (2.4.13)*. Then*

$$\|u - u_h\|_{a_h} \leq Ch\|f\|_{L_2(\Omega)}. \tag{2.4.22}$$

Details of (2.4.21), (2.4.22) and the L_2 error estimate can be found in [43, Section 10.3].

2.4.3 A Class of Symmetric, Stable and Consistent Discontinuous Galerkin Methods

The discontinuous Galerkin (DG) methods are nonconforming finite element methods. In this section, we will carry out the analysis of a class of symmetric, stable and consistent DG methods for (2.2.2) with $\alpha = 0$ and $f \in L_{2,\mu}(\Omega)$ on a general polygonal domain Ω with graded meshes. The results reported in this section, including the numerical experiments, are presented in [36, 34].

Let the family of triangulations $\mathcal{T}_h$ be chosen to satisfy (2.3.1)–(2.3.3). Let V_h be the space of discontinuous P_1 functions defined by

$$V_h = \{v : v_T = v\big|_T \in P_1(T) \quad \forall\, T \in \mathcal{T}_h\}.$$

We first recall the concepts of the jumps and means over the edges of $\mathcal{T}_h$.

Let $H^\theta(\Omega, \mathcal{T}_h)$ $(\theta \geq 1)$ be the space of piecewise Sobolev functions defined by

$$H^\theta(\Omega, \mathcal{T}_h) = \{v \in L_2(T) : v_T = v\big|_T \in H^\theta(T) \quad \forall T \in \mathcal{T}_h\}. \tag{2.4.23}$$

Let e be an interior edge of $\mathcal{T}_h$ shared by two triangles T_1, T_2. We define on e

$$[\![v]\!] = v_1 \boldsymbol{n}_1 + v_2 \boldsymbol{n}_2 \qquad \forall\, v \in H^1(\Omega, \mathcal{T}_h), \tag{2.4.24}$$

where $v_1 = v\big|_{T_1}$, $v_2 = v\big|_{T_2}$ and $\boldsymbol{n}_1$ (resp. $\boldsymbol{n}_2$) is the unit normal of e pointing outside of T_1 (resp. T_2), and

$$\{\!\{\nabla v\}\!\} = \frac{1}{2}(\nabla v_1 + \nabla v_2) \qquad \forall\, v \in H^\theta(\Omega, \mathcal{T}_h),\ \theta > 3/2,$$
$$\{\!\{\boldsymbol{w}\}\!\} = \frac{1}{2}(\boldsymbol{w}_1 + \boldsymbol{w}_2) \qquad \forall\, \boldsymbol{w} \in H^1(\Omega, \mathcal{T}_h) \times H^1(\Omega, \mathcal{T}_h),$$

where $\boldsymbol{w}_1 = \boldsymbol{w}\big|_{T_1}$, $\boldsymbol{w}_2 = \boldsymbol{w}\big|_{T_2}$.

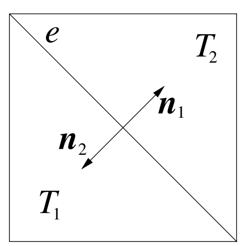

FIGURE 2.3. Triangles and normals in the definitions of $[\![v]\!]$ and $\{\!\{\nabla v\}\!\}$

Let e be a boundary edge of $\mathcal{T}_h$. Then $e \subset \partial T$ for some $T \in \mathcal{T}_h$. We define on e

$$[\![v]\!] = v_T \boldsymbol{n} \qquad \forall\, v \in H^1(\Omega, \mathcal{T}_h),$$

$$\{\!\{\boldsymbol{w}\}\!\} = \boldsymbol{w}_T \qquad \forall\, \boldsymbol{w} \in H^1(\Omega, \mathcal{T}_h) \times H^1(\Omega, \mathcal{T}_h),$$

where $\boldsymbol{n}$ is the unit normal of e pointing towards the outside of Ω.

Next we define for any edge e of $\mathcal{T}_h$ the lifting operator $\ell_e : L_2(e) \times L_2(e) \longrightarrow V_h \times V_h$ by

$$\int_\Omega \ell_e(\boldsymbol{v}) \cdot \boldsymbol{w} \, dx = -\int_e \boldsymbol{v} \cdot \{\{\boldsymbol{w}\}\} \, ds \qquad \forall\, \boldsymbol{w} \in V_h \times V_h. \tag{2.4.25}$$

Let $\mathcal{E}_h$ be the set of the edges of $\mathcal{T}_h$. The global lifting $\ell_h : L_2(\mathcal{E}_h) \times L_2(\mathcal{E}_h) \longrightarrow V_h \times V_h$ is defined by

$$\ell_h(\boldsymbol{v}) = \sum_{e \in \mathcal{E}_h} \ell_e(\boldsymbol{v}). \tag{2.4.26}$$

We can now introduce the DG methods to be studied in this section:

Find $u_h \in V_h$ such that

$$a_h(u_h, v) = \int_\Omega f v \, dx \qquad \forall\, v \in V_h, \tag{2.4.27}$$

where

$$a_h(v, w) = \sum_{T \in \mathcal{T}_h} \int_T \nabla v \cdot \nabla w \, dx - \sum_{e \in \mathcal{E}_h} \int_e \{\{\nabla v\}\} \cdot [[w]] \, ds - \sum_{e \in \mathcal{E}_h} \int_e \{\{\nabla w\}\} \cdot [[v]] \, ds \tag{2.4.28}$$

$$+ \delta \int_\Omega \ell_h\big([[v]]\big) \cdot \ell_h\big([[w]]\big) \, dx + R_h(v, w) \qquad \forall\, v, w \in V_h,$$

$\delta = 1$ or 0, and $R_h = R^j$ or R^r. The jump terms R^j and R^r are defined by

$$R^j(v, w) = \eta \sum_{e \in \mathcal{E}_h} \frac{1}{|e|} \int_e [[v]] \cdot [[w]] \, ds \qquad \forall\, v, w \in V_h, \tag{2.4.29}$$

$$R^r(v, w) = \eta \sum_{e \in \mathcal{E}_h} \int_\Omega \ell_e\big([[v]]\big) \cdot \ell_e\big([[w]]\big) \, ds \qquad \forall\, v, w \in V_h, \tag{2.4.30}$$

where $|e|$ is the length of the edge e and $\eta > 0$ is a penalty parameter.

The different choices for δ and R_h lead to four different DG methods (cf. Table 2.1), where η_* is a sufficiently large positive number that depends only on the shape regularity of $\mathcal{T}_h$.

TABLE 2.1. Discontinuous Galerkin methods

Method [Ref.]	δ	R_h	η
Brezzi et al. [48]	1	R^r	$\eta > 0$
LDG [52, 49]	1	R^j	$\eta > 0$
Bassi et al. [18]	0	R^r	$\eta > 3$
SIP [64, 95, 4]	0	R^j	$\eta > \eta^*$

Note that the weighted Sobolev space $H^2_\mu(\Omega)$ (cf. (2.2.37)) is embedded in the Sobolev space $H^s(\Omega)$, where

$$s = \min_{\omega_\ell > \pi}(1 + \mu_\ell) > 3/2.$$

Hence the bilinear form $a_h(\cdot,\cdot)$ in (2.4.27) is well defined on $H^2_\mu(\Omega)+V_h$ by the trace theorem (cf. Theorem 2.6). These four DG methods are symmetric and consistent in the sense that the solution u of (2.2.2) satisfies

$$a_h(u,v) = \int_\Omega fv\,dx \qquad \forall\, v \in V_h. \tag{2.4.31}$$

Let the mesh-dependent energy norm $\|\cdot\|_h$ on $H^2_\mu(\Omega) + V_h$ be defined by

$$\|v\|_h^2 = \sum_{T\in\mathcal{T}_h} \|\nabla v\|^2_{L_2(T)} + \eta^{-1}\sum_{e\in\mathcal{E}_h} |e|\,\|\{\!\{\nabla v\}\!\}\|^2_{L_2(e)} + \eta\sum_{e\in\mathcal{E}_h} |e|^{-1}\|[\![v]\!]\|^2_{L_2(e)}. \tag{2.4.32}$$

The next lemma states the boundedness of DG methods.

Lemma 2.25. *The bilinear form $a_h(\cdot,\cdot)$ for all four DG methods is bounded by the $\|\cdot\|_h$ norm:*

$$a_h(w,v) \le C_b\|w\|_h\|v\|_h \qquad \forall\, v,w \in H^2_\mu(\Omega) + V_h, \tag{2.4.33}$$

where the positive constant C_b is independent of the penalty parameter η as long as η is bounded away from 0.

Proof. It follows from the Cauchy-Schwarz inequality that

$$\begin{aligned}
&\Big|\sum_{e\in\mathcal{E}_h}\int_e \{\!\{\nabla v\}\!\}\cdot[\![w]\!]\,ds\Big| + \Big|\sum_{e\in\mathcal{E}_h}\int_e \{\!\{\nabla w\}\!\}\cdot[\![v]\!]\,ds\Big| \\
&\qquad \le \Big(\eta^{-1}\sum_{e\in\mathcal{E}_h}|e|\|\{\!\{\nabla v\}\!\}\|^2_{L_2(e)} + \eta\sum_{e\in\mathcal{E}_h}|e|^{-1}\|[\![v]\!]\|^2_{L_2(e)}\Big)^{1/2} \qquad (2.4.34)\\
&\qquad\qquad \times \Big(\eta^{-1}\sum_{e\in\mathcal{E}_h}|e|\|\{\!\{\nabla w\}\!\}\|^2_{L_2(e)} + \eta\sum_{e\in\mathcal{E}_h}|e|^{-1}\|[\![w]\!]\|^2_{L_2(e)}\Big)^{1/2}
\end{aligned}$$

for all $v, w \in H^2_\mu(\Omega) + V_h$, which immediately implies (2.4.33) for the SIP method.

The boundedness estimates for the other three DG methods follow from (2.4.34) and the two estimates below [48, 5]:

$$\|\ell_e([\![v]\!])\|^2_{L_2(\Omega)} \lesssim |e|^{-1}\|[\![v]\!]\|^2_{L_2(e)} \qquad \forall\, v \in H^2_\mu(\Omega) + V_h, \qquad (2.4.35)$$

$$\|\ell_h([\![v]\!])\|^2_{L_2(\Omega)} \lesssim \sum_{e\in\mathcal{E}_h}|e|^{-1}\|[\![v]\!]\|^2_{L_2(e)} \qquad \forall\, v \in H^2_\mu(\Omega) + V_h, \qquad (2.4.36)$$

where the positive constant C depends only on the shape regularity of $\mathcal{T}_h$. □

Lemma 2.26. *The bilinear form $a_h(\cdot,\cdot)$ is coercive for all four DG methods*:

$$a_h(v,v) \ge C\|v\|_h^2 \qquad \forall\, v \in V_h, \qquad (2.4.37)$$

where the positive constant C is independent of the penalty parameter η as long as η is bounded away from 0.

Proof. Let $|\!|\!|\cdot|\!|\!|_h$ be defined by

$$|\!|\!|v|\!|\!|_h^2 = \sum_{T\in\mathcal{T}_h}\|\nabla v\|^2_{L_2(T)} + \eta\sum_{e\in\mathcal{E}_h}|e|^{-1}\|[\![v]\!]\|^2_{L_2(e)}.$$

Since the two norms $\|\cdot\|_h$ and $|\!|\!|\cdot|\!|\!|_h$ are equivalent on V_h (cf. for example [43, Section 10.5]), it suffices to establish the coercivity of $a_h(\cdot,\cdot)$ with respect to $|\!|\!|\cdot|\!|\!|_h$.

From [5] we have the estimate

$$a_h(v,v) \ge C\Big(\sum_{T\in\mathcal{T}_h}\|\nabla v\|^2_{L_2(T)} + \eta\sum_{e\in\mathcal{E}_h}\|r_e([\![v]\!]\|^2_{L_2(e)}\Big) \qquad \forall\, v \in V_h, \qquad (2.4.38)$$

for all four DG methods under the restrictions on η as stated in Table 2.1, where the positive constant C is independent of η as long as it is bounded away from 0. The coercivity with respect to $\|\!|\cdot|\!\|_h$ then follows from the estimate [48, 5]

$$|e|^{-1}\|[[v]]\|_{L_2(e)}^2 \leq C\|r_e([[v]])\|_{L_2(e)}^2 \qquad \forall\, v \in V_h.$$

□

Combining (2.4.31), (2.4.33) and (2.4.37), we have a quasi-optimal error estimate for all four DG methods:

$$\|u - u_h\|_h \leq C \inf_{v \in V_h} \|u - v\|_h, \tag{2.4.39}$$

where the positive constant C is independent of the penalty parameter η as long as η is bounded away from 0. Refer to [43, Section 10.5] for more details.

Note that Lemma 2.25 and Lemma 2.26 imply

$$a_h(v, v) \approx \|v\|_h^2 \qquad \forall\, v \in V_h, \tag{2.4.40}$$

and $a_h(\cdot,\cdot)$ is an inner product on V_h.

Let $\Pi_h : C(\bar{\Omega}) \longrightarrow V_h$ be the nodal interpolation operator for the conforming P_1 finite element, which is the same one used in Section 2.4.1. The following lemma provides an interpolation error estimate.

Lemma 2.27. *Let $f \in L_{2,\mu}(\Omega)$ and $u \in H_0^1(\Omega)$ satisfy* (2.2.2) $(\alpha = 0)$*. Then*

$$\|u - \Pi_h u\|_h \leq Ch\|f\|_{L_{2,\mu}(\Omega)}. \tag{2.4.41}$$

Proof. It follows from (2.4.24) and (2.4.32) that

$$\begin{aligned}\|u - \Pi_h u\|_h^2 &= \sum_{T \in \mathcal{T}_h} |u - \Pi_h u|_{H^1(T)}^2 + \eta^{-1} \sum_{e \in \mathcal{E}_h} |e|\, \|\{\{\nabla(u - \Pi_h u)\}\}\|_{L_2(e)}^2 \\ &\leq C \sum_{T \in \mathcal{T}_h} \Big(|u - \Pi_h u|_{H^1(T)}^2 + |\partial T|\, \|\nabla(u - \Pi_h u)\|_{L_2(\partial T)}^2\Big).\end{aligned} \tag{2.4.42}$$

Let $\mathcal{T}_{h,\ell}$ be the collection of triangles in $\mathcal{T}_h$ that touch a corner c_ℓ of Ω. We assume that $h \ll \delta$ and hence $T \subset \mathcal{N}_{\ell,\delta}$ for all $T \in \mathcal{T}_{h,\ell}$, where $\mathcal{N}_{\ell,\delta} = \{x \in \Omega : \ |x - c_\ell| < \delta\}$ are the neighborhoods of the corners c_ℓ for $1 \le \ell \le L$. We can divide the triangles in $\mathcal{T}_h$ into two disjoint families $\mathcal{T}_h'$ and $\mathcal{T}_h''$ where

$$\mathcal{T}_h' = \bigcup_{\omega_\ell > \pi} \mathcal{T}_{h,\ell} \quad \text{and} \quad \mathcal{T}_h'' = \mathcal{T}_h \setminus \mathcal{T}_h'.$$

For the triangles away from the reentrant corners, we derive from (2.2.33), (2.2.37), (2.3.1), (2.3.2), a standard interpolation error estimate [51, 43] and the trace theorem with scaling that

$$\begin{aligned}\sum_{T \in \mathcal{T}_h''} \Big(|u - \Pi_h u|^2_{H^1(T)} + |\partial T| \, \|\nabla(u - \Pi_h u)\|^2_{L_2(\partial T)} \Big) &\le C \sum_{T \in \mathcal{T}_h''} h_T^2 |u|^2_{H^2(T)} \\ &\le C \sum_{T \in \mathcal{T}_h''} h^2 [\Phi_\mu(T)]^2 \sum_{|\alpha|=2} \|\partial^\alpha u / \partial x^\alpha\|^2_{L_2(T)} \\ &\le C h^2 \sum_{|\alpha|=2} \sum_{T \in \mathcal{T}_h''} \|\phi_\mu^2 (\partial^\alpha u / \partial x^\alpha)\|^2_{L_2(T)} \le C h^2 \|f\|^2_{L_{2,\mu}(\Omega)}.\end{aligned} \tag{2.4.43}$$

For the triangles touching a reentrant corner, we apply an interpolation error estimate for fractional order Sobolev spaces [65] together with (2.2.38), (2.3.5) and the trace theorem with scaling to obtain

$$\begin{aligned}&\sum_{T \in \mathcal{T}_h'} \Big(|u - \Pi_h u|^2_{H^1(T)} + |\partial T| \, \|\nabla(u - \Pi_h u)\|^2_{L_2(\partial T)} \Big) \\ &\qquad \le C \sum_{\omega_\ell > \pi} \sum_{T \in \mathcal{T}_{h,\ell}} h_T^{2\mu_\ell} |u|^2_{H^{1+\mu_\ell}(T)} \\ &\qquad \le C h^2 \sum_{\omega_\ell > \pi} |u|^2_{H^{1+\mu_\ell}(\mathcal{N}_{\ell,\delta})} \le C h^2 \|f\|^2_{L_{2,\mu}(\Omega)}.\end{aligned} \tag{2.4.44}$$

The estimate (2.4.41) follows from (2.4.42)–(2.4.44). □

By using (2.4.39) and (2.4.41), we can immediately establish the error estimate for all four DG methods.

Theorem 2.28. *Let* $f \in L_{2,\mu}(\Omega)$, *u be the solution of* (2.2.2) ($\alpha = 0$), *and u_h be the solution of one of the four DG methods associated with a triangulation $\mathcal{T}_h$ that satisfies* (2.3.1). *We have the following error estimate*:

$$\|u - u_h\|_h \le Ch\|f\|_{L_{2,\mu}(\Omega)}, \tag{2.4.45}$$

where the positive constant C is independent of the penalty parameter η as long as η is bounded away from 0.

We can also establish an error estimate for the DG methods in the norm

$$\|\xi\|^2_{L_{2,-\mu}(\Omega)} = \int_\Omega \phi_\mu^{-2}(x)\xi^2(x)\,dx, \tag{2.4.46}$$

which is the norm for $L_{2,-\mu}(\Omega)$, the dual space of $L_{2,\mu}(\Omega)$.

Theorem 2.29. *Under the assumptions of Theorem* 2.28, *we have*

$$\|u - u_h\|_{L_{2,-\mu}(\Omega)} \le Ch^2\|f\|_{L_{2,\mu}(\Omega)}, \tag{2.4.47}$$

where the positive constant C is independent of the penalty parameter η as long as η is bounded away from 0.

Proof. Observe that (2.4.27) and (2.4.31) imply the following Galerkin orthogonality:

$$a_h(u - u_h, v) = 0 \qquad \forall\, v \in V_h. \tag{2.4.48}$$

Let $\chi = \phi_\mu^{-2}(u - u_h)$. Then $\chi \in L_{2,\mu}(\Omega)$ and

$$\|\chi\|_{L_{2,\mu}(\Omega)} = \|u - u_h\|_{L_{2,-\mu}(\Omega)}. \tag{2.4.49}$$

Let $\zeta \in H_0^1(\Omega)$ satisfy

$$\int_\Omega \nabla v \cdot \nabla \zeta\,dx = \int_\Omega v\chi\,dx \qquad \forall\, v \in H_0^1(\Omega). \tag{2.4.50}$$

It follows from (2.4.49) and Lemma 2.27 (applied to ζ) that

$$\|\zeta - \Pi_h\zeta\|_h \leq Ch\|u - u_h\|_{L_{2,-\mu}(\Omega)}. \tag{2.4.51}$$

Note that we can rewrite (2.4.50) as

$$a_h(v, \zeta) = \int_\Omega v\chi\, dx \qquad \forall\, v \in H_0^1(\Omega), \tag{2.4.52}$$

and the consistency of the DG methods implies

$$a_h(v, \zeta) = \int_\Omega v\chi\, dx \qquad \forall\, v \in V_h. \tag{2.4.53}$$

Hence we have, by (2.4.33), (2.4.45), (2.4.51) and (2.4.53).

$$\begin{aligned}
\|u - u_h\|^2_{L_{2,-\mu}(\Omega)} &= \int_\Omega (u - u_h)\chi\, dx \\
&= a_h(u - u_h, \zeta) \\
&= a_h(u - u_h, \zeta - \Pi_h\zeta) \\
&\leq \|u - u_h\|_h\|\zeta - \Pi_h\zeta\|_h \leq Ch^2\|f\|_{L_{2,\mu}(\Omega)}\|u - u_h\|_{L_{2,-\mu}(\Omega)},
\end{aligned}$$

which implies (2.4.47). □

The following corollary is immediate.

Corollary 2.30. *Under the assumptions of Theorem* 2.28*, we have*

$$\|u - u_h\|_{L_2(\Omega)} \leq Ch^2\|f\|_{L_{2,\mu}(\Omega)}.$$

Next, we report results of several numerical experiments for model problem (2.2.2) on the L-shaped domain $(-1, 1)^2 \setminus ([0, 1] \times [-1, 0])$ (cf. Figure 2.2). The triangulations $\mathcal{T}_0, \mathcal{T}_1, \ldots$ are created by the refinement procedure described in Section 2.3. The grading parameter at the reentrant corner is taken to be $2/3$ and the mesh parameter of $\mathcal{T}_k$ is $h_k = 2^{-k}$.

We take the exact solution to be

$$u(x,y) = (1-x^2)(1-y^2)r^{2/3}\sin\big(2\theta/3\big),$$

where (r,θ) are the polar coordinates at the origin. We computed the energy error and L_2 error for the solution u_k of the method of Brezzi et al. (resp. the LDG method, the method of Bassi et al. and the SIPG method) with $\eta = 1$ (resp. $\eta = 1$, $\eta = 4$ and $\eta = 10$) for $0 \le k \le 7$. The results are plotted against the mesh size in log-log scale and presented in Figure 2.4 and Figure 2.5.

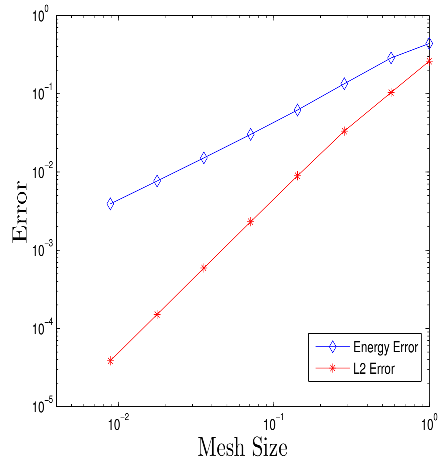

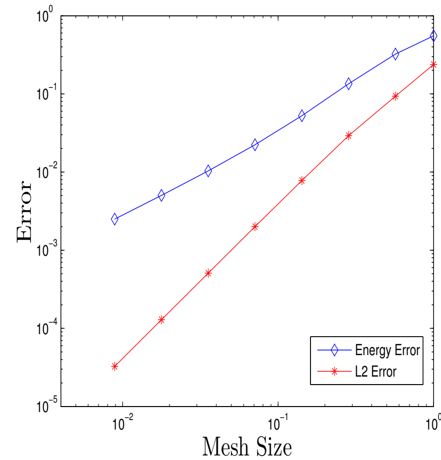

FIGURE 2.4. Energy errors and L_2 errors for the method of Brezzi et al. (left, $\eta = 1$) and for the LDG method (right, $\eta = 1$)

2.5 Multigrid Algorithms

Let $\mathcal{T}_0, \mathcal{T}_1, \ldots$ be a sequence of triangulations generated by the refinement procedure that was described in Section 2.3, h_k be the mesh size of $\mathcal{T}_k$, V_k be the corresponding discontinuous P_1 finite element space associated with $\mathcal{T}_k$ and $a_k(\cdot,\cdot)$ be the analog of $a_h(\cdot,\cdot)$ that is defined by (2.4.27). The k-th level discrete problem for (2.2.2) ($\alpha = 0$) is (cf. [34]):

Find $u_k \in V_k$ such that

$$a_k(u_k, v) = \int_\Omega f v\,dx \qquad \forall\, v \in V_k. \tag{2.5.1}$$

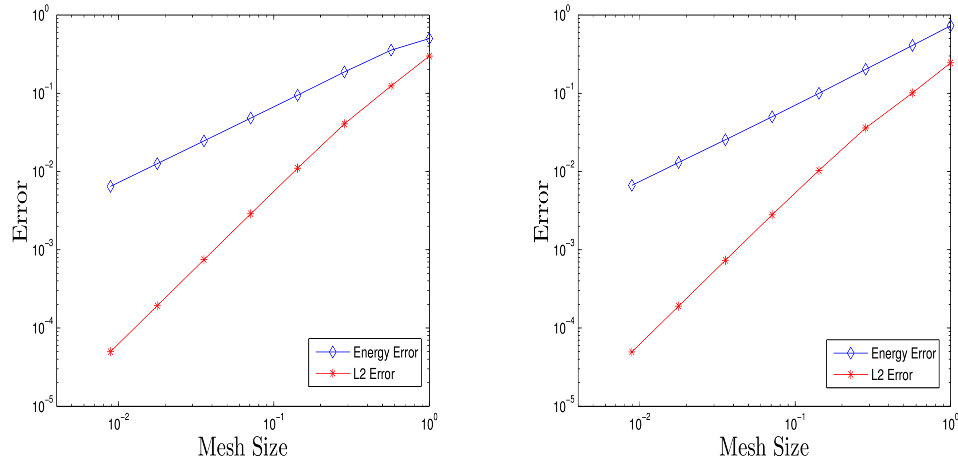

FIGURE 2.5. Energy errors and L_2 errors for the method of Bassi et al. (left, $\eta = 4$) and for the SIPG method (right, $\eta = 10$)

The analog of $\|\cdot\|_h$ is denoted by $\|\cdot\|_k$, i.e.,

$$\|v\|_k^2 = \sum_{T\in\mathcal{T}_k} |v|^2_{H^1(T)} + \eta^{-1}\sum_{e\in\mathcal{E}_k} |e|\, \|\{\{\nabla v\}\}\|^2_{L_2(e)} + \eta \sum_{e\in\mathcal{E}_k} |e|^{-1} \|[[v]]\|^2_{L_2(e)}. \qquad (2.5.2)$$

Note that (2.4.40) becomes

$$a_k(v,v) \approx \|v\|_k^2 \qquad \forall\, v \in V_k, \qquad (2.5.3)$$

and (2.4.41) is translated into

$$\|u - \Pi_k u\|_k \le C h_k \|f\|_{L_{2,\mu}(\Omega)}, \qquad (2.5.4)$$

where $\Pi_k : C(\bar{\Omega}) \longrightarrow V_k$ is the nodal interpolation operator for the conforming P_1 element. Furthermore, the norms $\|\cdot\|_k$ and $\|\cdot\|_{k-1}$ are equivalent for functions that are piecewise smooth on $\mathcal{T}_{k-1}$, i.e.,

$$\|w\|_k \approx \|w\|_{k-1} \qquad \forall\, w \in H^s(\Omega) \cap V_{k-1}, \qquad (2.5.5)$$

where $s > 3/2$.

We can rewrite (2.5.1) as

$$A_k u_k = f_k, \qquad (2.5.6)$$

where $A_k : V_k \longrightarrow V_k'$ and $f_k \in V_k'$ are defined by

$$\langle A_k w, v\rangle = a_k(w,v) \qquad \forall\, v, w \in V_k, \tag{2.5.7}$$

$$\langle f_k, v\rangle = \int_\Omega f v\, dx \qquad \forall\, v \in V_k. \tag{2.5.8}$$

Here $\langle \cdot, \cdot \rangle$ is the canonical bilinear form on $V_k' \times V_k$.

Let the operator $B_k : V_k \longrightarrow V_k'$ be defined by

$$\langle B_k w, v\rangle = h_k^2 \sum_{T\in\mathcal{T}_k} \sum_{m\in\mathcal{M}_T} w(m)v(m) \qquad \forall\, v, w \in V_k, \tag{2.5.9}$$

where $\mathcal{M}_T$ is the set of the midpoints of the three edges of T. The operator B_k will be used later to define a smoother for multigrid algorithms.

Remark 2.31. *The weighted norm $\|\cdot\|_{L_{2,-\mu}(\Omega)}$ is connected to the operator B_k through the relation*

$$\langle B_k v, v\rangle = h_k^2 \sum_{T\in\mathcal{T}_k} \sum_{m\in\mathcal{M}_T} [v(m)]^2 \approx \|v\|^2_{L_{2,-\mu}(\Omega)} \qquad \forall\, v \in V_k, \tag{2.5.10}$$

which follows from (2.3.1)*,* (2.3.2) *and* (2.4.46)*.*

In order to define W-cycle, V-cycle and F-cycle multigrid algorithms [71, 79, 27, 91, 43] for equation (2.5.6), we need intergrid transfer operators that move functions between grids. Since the finite element spaces are nested, we can take the coarse-to-fine intergrid transfer operator $I_{k-1}^k : V_{k-1} \longrightarrow V_k$ to be the natural injection and define the fine-to-coarse intergrid transfer operator $I_k^{k-1} : V_k' \longrightarrow V_{k-1}'$ to be the transpose of I_{k-1}^k with respect to the canonical bilinear forms, i.e.,

$$\langle I_k^{k-1}\alpha, v\rangle = \langle \alpha, I_{k-1}^k v\rangle \qquad \forall\, \alpha \in V_k',\ v \in V_{k-1}. \tag{2.5.11}$$

We are now ready to define the W-cycle algorithm for the equation

$$A_k z = g, \tag{2.5.12}$$

where $g \in V_k'$.

Algorithm 2.32. *W-cycle Algorithm for* (2.5.12)

The output of the algorithm is denoted by $MG_W(k, g, z_0, m_1, m_2)$*, where* $z_0 \in V_k$ *is the initial guess and* m_1 *(resp.* m_2*) is the number of pre-smoothing (resp. post-smoothing) steps.*

For $k = 0$*, we take the output to be the exact solution, i.e.,* $MG_W(0, g, z_0, m_1, m_2) = A_0^{-1} g$*.*

For $k > 0$*, we proceed in three steps.*

Pre-Smoothing. *Compute* $z_l \in V_k$ *for* $1 \le l \le m_1$ *recursively by*

$$z_l = z_{l-1} + (\lambda h_k^2) B_k^{-1}(g - A_k z_{l-1}), \tag{2.5.13}$$

where λ *is a (constant) damping factor such that the spectral radius* $\rho(\lambda h_k^2 B_k^{-1} A_k)$ *satisfies*

$$\rho(\lambda h_k^2 B_k^{-1} A_k) < 1 \qquad \text{for} \;\; k \ge 0. \tag{2.5.14}$$

Coarse-Grid Correction. *Compute* $q \in V_{k-1}$ *by*

$$\begin{aligned} \bar{g} =& I_k^{k-1}(g - A_k z_{m_1}), \\ q_* =& MG_W(k-1, \bar{g}, 0, m_1, m_2), \qquad (2.5.15) \\ q =& MG_W(k-1, \bar{g}, q_*, m_1, m_2), \qquad (2.5.16) \end{aligned}$$

and take

$$z_{m_1+1} = z_{m_1} + I_{k-1}^k q. \tag{2.5.17}$$

Post-Smoothing. *Compute* $z_l \in V_k$ *for* $m_1 + 2 \le l \le m_1 + m_2 + 1$ *recursively by*

$$z_l = z_{l-1} + (\lambda h_k^2) B_k^{-1}(g - A_k z_{l-1}). \tag{2.5.18}$$

The final output is

$$MG_W(k, g, z_0, m_1, m_2) = z_{m_1+m_2+1}.$$

We need the following operators for the analysis of Algorithm 2.32. The operator $R_k : V_k \longrightarrow V_k$ which measures the effect of one smoothing step is defined by

$$R_k = Id_k - (\lambda h_k^2) B_k^{-1} A_k, \tag{2.5.19}$$

where Id_k is the identity operator on V_k. Clearly we have

$$a_k(R_k v, w) = a_k(v, R_k w) \qquad \forall\ v, w \in V_k. \tag{2.5.20}$$

The operator $P_k^{k-1} : V_k \longrightarrow V_{k-1}$ is the transpose of I_{k-1}^k with respect to the variational forms, i.e.,

$$a_{k-1}(P_k^{k-1} w, v) = a_k(w, I_{k-1}^k v) \qquad \forall\, v \in V_{k-1},\ w \in V_k. \tag{2.5.21}$$

We denote the k-th level error propagation operator for Algorithm 2.32 by $E_k : V_k \longrightarrow V_k$, i.e.,

$$E_k(z - z_0) = z - MG_W(k, g, z_0, m_1, m_2). \tag{2.5.22}$$

The next lemma states the well-known recursive relation among operators E_k [71, 43].

Lemma 2.33. *The following recursive relation is valid*

$$E_k = R_k^{m_2}[(Id_k - I_{k-1}^k P_k^{k-1}) + I_{k-1}^k E_{k-1}^2 P_k^{k-1}] R_k^{m_1} \qquad \textit{for } k \geq 1. \tag{2.5.23}$$

Proof. Observe that

$$\begin{aligned} e_{m_1} =& z - z_{m_1} \\ =& z - (z_{m_1-1} + \lambda B_k^{-1}(g - A_k z_{m_1-1})) \\ =& e_{m_1-1} - \lambda B_k^{-1} A_k e_{m_1-1} = R_k^{m_1} e_0. \end{aligned} \tag{2.5.24}$$

Similarly, we have

$$e_{m_1+m_2+1} = R_k^{m_2} e_{m_1+1}. \tag{2.5.25}$$

We proceed by induction on k. Since $MG_W(0, g, z_0, m_1, m_2) = A_0^{-1}z = g$, it is clear that $E_0 = 0$. We assume (2.5.23) holds for $k-1$. Let ρ satisfy $A_{k-1}\rho = \bar{g}$. Then the induction hypothesis implies that

$$\begin{aligned} \rho - q =& E_{k-1}(\rho - q_*) \\ =& E_{k-1}(\rho - (\rho - E_{k-1}\rho)) = E_{k-1}^2\rho, \end{aligned} \tag{2.5.26}$$

where q and q_* are defined by (2.5.15) and (2.5.16). Also for any $w \in V_{k-1}$, we have

$$\begin{aligned} a_{k-1}(\rho, w) =& \langle A_{k-1}\rho, w\rangle \\ =& \langle \bar{g}, w\rangle \\ =& \langle I_k^{k-1}(g - A_k z_{m_1}), w\rangle \\ =& \langle A_k(z - z_{m_1}), I_{k-1}^k w\rangle = a_k(z - z_{m_1}, I_{k-1}^k w), \end{aligned}$$

which together with (2.5.21) implies

$$\rho = P_k^{k-1} e_{m_1}. \tag{2.5.27}$$

From (2.5.24)-(2.5.27), we obtain (2.5.23) in the following way:

$$\begin{aligned} E_k(z - z_0) =& z - MG_W(k, g, z_0, m_1, m_2) \\ =& R_k^{m_2}(z - z_{m_1} - I_{k-1}^k q) \\ =& R_k^{m_2}(e_{m_1} - I_{k-1}^k(\rho - E_{k-1}^2\rho)) \\ =& R_k^{m_2}(e_{m_1} - I_{k-1}^k(P_k^{k-1}e_{m_1} - E_{k-1}^2 P_k^{k-1} e_{m_1})) \\ =& R_k^{m_2}(Id_k - I_{k-1}^k P_k^{k-1} + I_{k-1}^k E_{k-1}^2 P_k^{k-1}) R_k^{m_1} e_0. \end{aligned}$$

□

Corollary 2.34. *The error propagation operator $\tilde{E}_k$ for the two-grid algorithm is given by*

$$\tilde{E}_k = R_k^{m_2}(Id_k - I_{k-1}^k P_k^{k-1}) R_k^{m_1}. \tag{2.5.28}$$

Next, we introduce the V-cycle and F-cycle algorithms.

Algorithm 2.35. *V-cycle Algorithm for* (2.5.12)

The output of the algorithm is denoted by $MG_V(k, g, z_0, m_1, m_2)$, where $z_0 \in V_k$ is the initial guess and m_1 (resp. m_2) is the number of pre-smoothing (resp. post-smoothing) steps.

For $k = 0$, we take the output to be the exact solution, i.e., $MG_V(0, g, z_0, m_1, m_2) = A_0^{-1} g$.

For $k > 0$, we proceed in three steps.

Pre-Smoothing *Compute $z_l \in V_k$ for $1 \leq l \leq m_1$ recursively by*

$$z_l = z_{l-1} + (\lambda h_k^2) B_k^{-1}(g - A_k z_{l-1}), \tag{2.5.29}$$

where λ is a (constant) damping factor chosen to satisfy (2.5.14).

Coarse-Grid Correction *Compute $q \in V_{k-1}$ by*

$$\begin{aligned} \bar{g} =& I_k^{k-1}(g - A_k z_{m_1}), \\ q =& MG_V(k-1, \bar{g}, 0, m_1, m_2), \end{aligned} \tag{2.5.30}$$

and take

$$z_{m_1+1} = z_{m_1} + I_{k-1}^k q. \tag{2.5.31}$$

Post-Smoothing *Compute $z_l \in V_k$ for $m_1 + 2 \leq l \leq m_1 + m_2 + 1$ recursively by*

$$z_l = z_{l-1} + (\lambda h_k^2) B_k^{-1}(g - A_k z_{l-1}). \tag{2.5.32}$$

The final output is

$$MG_V(k, g, z_0, m_1, m_2) = z_{m_1+m_2+1}.$$

Let $\mathbb{E}_k : V_k \longrightarrow V_k$ be the k-th level error propagation operator for Algorithm 2.35, i.e.,

$$\mathbb{E}_k(z - z_0) = z - MG_V(k, g, z_0, m_1, m_2). \tag{2.5.33}$$

The following recursive relation is well known [71, 43]:

$$\mathbb{E}_k = R_k^{m_2}[(Id_k - I_{k-1}^k P_k^{k-1}) + I_{k-1}^k \mathbb{E}_{k-1} P_k^{k-1}] R_k^{m_1} \quad \text{for } k \geq 1. \tag{2.5.34}$$

Algorithm 2.36. *F-cycle Algorithm for* (2.5.12)

The output of the algorithm is denoted by $MG_F(k, g, z_0, m_1, m_2)$*, where* $z_0 \in V_k$ *is the initial guess and* m_1 *(resp.* m_2*) is the number of pre-smoothing (resp. post-smoothing) steps.*

For $k = 0$*, we take the output to be the exact solution, i.e.,* $MG_F(0, g, z_0, m_1, m_2) = A_0^{-1} g$.

For $k > 0$*, we proceed in three steps.*

Pre-Smoothing *Compute* $z_l \in V_k$ *for* $1 \leq l \leq m_1$ *recursively by*

$$z_l = z_{l-1} + (\lambda h_k^2) B_k^{-1}(g - A_k z_{l-1}), \tag{2.5.35}$$

where λ *is a (constant) damping factor to be chosen in* (2.5.14).

Coarse-Grid Correction *Compute* $q \in V_{k-1}$ *by*

$$\begin{aligned} \bar{g} =& I_k^{k-1}(g - A_k z_{m_1}) \\ q_* =& MF_F(k-1, \bar{g}, 0, m_1, m_2) \\ q =& MG_V(k-1, \bar{g}, q_*, m_1, m_2) \end{aligned} \tag{2.5.36}$$

and take

$$z_{m_1+1} = z_{m_1} + I_{k-1}^k q. \tag{2.5.37}$$

Post-Smoothing *Compute* $z_l \in V_k$ *for* $m_1 + 2 \leq k \leq m_1 + m_2 + 1$ *recursively by*

$$z_l = z_{l-1} + (\lambda h_k^2) B_k^{-1}(g - A_k z_{l-1}). \tag{2.5.38}$$

The final output is

$$MG_F(k, g, z_0, m_1, m_2) = z_{m_1+m_2+1}.$$

Let $\tilde{\mathbb{E}}_k : V_k \longrightarrow V_k$ be the operator relating the initial error and the final error of Algorithm 2.36 applied to the equation (2.5.12), i.e.,

$$\tilde{\mathbb{E}}_k(z - z_0) = z - MG_F(k, g, z_0, m_1, m_2). \tag{2.5.39}$$

The following recursive relation is well known [91]:

$$\tilde{\mathbb{E}}_k = R_k^{m_2}[(Id_k - I_{k-1}^k P_k^{k-1}) + I_{k-1}^k \mathbb{E}_{k-1} \tilde{\mathbb{E}}_{k-1} P_k^{k-1}] R_k^{m_1} \quad \text{for } k \geq 1. \tag{2.5.40}$$

Remark 2.37. *Note that the only differences between the W-cycle, V-cycle and F-cycle algorithms are at the coarse-grid correction step. The W-cycle algorithm corrects error on coarser grid twice and both with another W-cycle algorithm, while there is only one error correction in the V-cycle algorithm. On the other hand, the F-cycle algorithm corrects error first with another F-cycle algorithm and then with a V-cycle algorithm. We can observe that the W-cycle algorithm is the most expensive in terms of computation, followed by the F-cycle algorithm, then the V-cycle algorithm.*

The convergence analysis of W-cycle, V-cycle and F-cycle multigrid algorithms for the discrete problem (2.5.6) obtained from DG methods on graded meshes will be presented in Chapter 4.

Chapter 3

Nonconforming Finite Element Methods for the Curl-Curl and Grad-Div Problem

3.1 The Curl-Curl and Grad-Div Problem

In Chapter 1 we showed that the Maxwell's equations (1.1.1) and (1.1.2) can be reduced to the equation of the following form with perfectly conducting boundary condition:

$$\nabla \times \nabla \times \boldsymbol{u} + \alpha \boldsymbol{u} = \boldsymbol{f} \qquad \text{in } \Omega, \tag{3.1.1a}$$

$$\boldsymbol{n} \times \boldsymbol{u} = 0 \qquad \text{on } \partial\Omega, \tag{3.1.1b}$$

where $\Omega \subset \mathbb{R}^2$ is a bounded polygonal domain, $\alpha \in \mathbb{R}$ is a constant, and $\boldsymbol{f} \in [L_2(\Omega)]^2$.

We can derive the non-elliptic weak form for (3.1.1) as follows:

Find $\boldsymbol{u} \in H_0(\text{curl};\Omega)$ such that

$$(\nabla \times \boldsymbol{u}, \nabla \times \boldsymbol{v}) + \alpha(\boldsymbol{u}, \boldsymbol{v}) = (\boldsymbol{f}, \boldsymbol{v}) \tag{3.1.2}$$

for all $\boldsymbol{v} \in H_0(\text{curl};\Omega)$, where the space $H_0(\text{curl};\Omega)$ is defined by (1.2.3).

For any $\boldsymbol{u} \in H_0(\text{curl};\Omega)$, from the Helmholtz decomposition [68, 80], we have

$$\boldsymbol{u} = \mathring{\boldsymbol{u}} + \nabla\phi, \tag{3.1.3}$$

where $\mathring{\boldsymbol{u}} \in H_0(\text{curl};\Omega) \cap H(\text{div}^0;\Omega)$, $\phi \in H_0^1(\Omega)$, and the space $H(\text{div}^0;\Omega)$ is defined by (1.2.6).

Let $\eta \in H_0^1(\Omega)$, by taking $\boldsymbol{v} = \nabla\eta \in H_0(\text{curl};\Omega)$ and $\boldsymbol{u} = \mathring{\boldsymbol{u}} + \nabla\phi$ in (3.1.2) we have,

$$(\nabla \times \boldsymbol{u}, \nabla \times (\nabla\eta)) + \alpha(\mathring{\boldsymbol{u}} + \nabla\phi, \nabla\eta) = (\boldsymbol{f}, \nabla\eta). \tag{3.1.4}$$

Note that $\nabla \times (\nabla \eta) = 0$, the integration by parts formula implies

$$\alpha(\nabla \cdot \mathring{\boldsymbol{u}}, \eta) + \alpha(\nabla \phi, \nabla \eta) = (\boldsymbol{f}, \nabla \eta). \tag{3.1.5}$$

Since $\mathring{\boldsymbol{u}} \in H(\mathrm{div}^0; \Omega)$, then $\phi \in H_0^1(\Omega)$ satisfies

$$\alpha(\nabla \phi, \nabla \eta) = (\boldsymbol{f}, \nabla \eta) \tag{3.1.6}$$

for all $\eta \in H_0^1(\Omega)$, which is the variational form of the Poisson problem.

Since the Poisson problem (3.1.6) (when $\alpha \neq 0$) can be solved by many standard methods under the assumption that $\boldsymbol{f} \in H(\mathrm{div}; \Omega)$, we will focus on the divergence free part $\mathring{\boldsymbol{u}}$. We take $\boldsymbol{v} \in H_0(\mathrm{curl}; \Omega) \cap H(\mathrm{div}^0; \Omega)$ and $\boldsymbol{u} = \mathring{\boldsymbol{u}} + \nabla \phi$ in (3.1.2), then

$$(\nabla \times (\mathring{\boldsymbol{u}} + \nabla \phi), \nabla \times \boldsymbol{v}) + \alpha(\mathring{\boldsymbol{u}} + \nabla \phi, \boldsymbol{v}) = (\boldsymbol{f}, \boldsymbol{v}). \tag{3.1.7}$$

Note that $\nabla \times (\nabla \phi) = 0$, it follows from the integration by parts formula that $\mathring{\boldsymbol{u}}$ is the weak solution of the following reduced curl-curl problem (cf. (1.2.8)):

Find $\mathring{\boldsymbol{u}} \in H_0(\mathrm{curl}; \Omega) \cap H(\mathrm{div}^0; \Omega)$ such that

$$(\nabla \times \mathring{\boldsymbol{u}}, \nabla \times \boldsymbol{v}) + \alpha(\mathring{\boldsymbol{u}}, \boldsymbol{v}) = (\boldsymbol{f}, \boldsymbol{v}) \tag{3.1.8}$$

for all $\boldsymbol{v} \in H_0(\mathrm{curl}; \Omega) \cap H(\mathrm{div}^0; \Omega)$.

Since the condition number for the discrete problem of (3.1.8) behaves like a fourth order problem, we turn to consider the following curl-curl and grad-div problem (cf. (1.2.9)):

Find $\boldsymbol{u} \in H_0(\mathrm{curl}; \Omega) \cap H(\mathrm{div}; \Omega)$ such that

$$(\nabla \times \boldsymbol{u}, \nabla \times \boldsymbol{v}) + \gamma(\nabla \cdot \boldsymbol{u}, \nabla \cdot \boldsymbol{v}) + \alpha(\boldsymbol{u}, \boldsymbol{v}) = (\boldsymbol{f}, \boldsymbol{v}) \tag{3.1.9}$$

for all $\boldsymbol{v} \in H_0(\mathrm{curl}; \Omega) \cap H(\mathrm{div}; \Omega)$, where $\alpha \in \mathbb{R}$ and $\gamma > 0$ are constants, $\boldsymbol{f} \in [L_2(\Omega)]^2$.

3.2 A Nonconforming Finite Element Method for the Curl-Curl and Grad-Div Problem

In this section we solve (1.2.9) by using a classical nonconforming finite element method on graded meshes. The numerical scheme can also be found in [37].

3.2.1 Discretization

Let $\mathcal{T}_h$ be a family of triangulations of Ω that satisfies the property (2.3.1), where the grading parameters μ are chosen according to (2.2.39). Let V_h be the space of weakly continuous P_1 vector fields associated with $\mathcal{T}_h$ whose tangential components vanish at the midpoints of the boundary edges in $\mathcal{T}_h$. More precisely, let $\mathcal{E}_h$ (resp. $\mathcal{E}_h^b$ and $\mathcal{E}_h^i$) be the set of the edges (resp. boundary edges and interior edges) of $\mathcal{T}_h$. Then

$$\begin{aligned} V_h = \{\boldsymbol{v} \in [L_2(\Omega)]^2 : \boldsymbol{v}_T = \boldsymbol{v}\big|_T \in [P_1(T)]^2 \quad \forall T \in \mathcal{T}_h, \\ \boldsymbol{v} \text{ is continuous at the midpoint of any } e \in \mathcal{E}_h, \\ \boldsymbol{n} \times \boldsymbol{v} \text{ vanishes at the midpoint of any } e \in \mathcal{E}_h^b\}. \end{aligned}$$

For any $s > 1/2$, we define a weak interpolation operator $\Pi_T : [H^s(T)]^2 \longrightarrow [P_1(T)]^2$ by

$$(\Pi_T \boldsymbol{v})(m_{e_j}) = \frac{1}{|e_j|} \int_{e_j} \boldsymbol{v}\, ds \quad \text{for } 1 \le j \le 3, \tag{3.2.1}$$

where e_1, e_2 and e_3 are the edges of T, m_e and $|e|$ denote the midpoint and length of the edge e respectively. The operator Π_T satisfies a standard error estimate [60]:

$$\|\boldsymbol{\zeta} - \Pi_T\boldsymbol{\zeta}\|_{L_2(T)} + h_T^{\min(s,1)}|\boldsymbol{\zeta} - \Pi_T\boldsymbol{\zeta}|_{H^{\min(s,1)}(T)} \le C_T h_T^s |\boldsymbol{\zeta}|_{H^s(T)} \tag{3.2.2}$$

for all $\boldsymbol{\zeta} \in [H^s(T)]^2$ and $s \in (1/2, 2]$, where the positive constant C_T depends on the minimum angle of T.

Lemma 3.1. *The operator* Π_T *has the following properties* [40, 37]*:*

$$\int_T \nabla \times (\Pi_T \boldsymbol{u}) dx = \int_T \nabla \times \boldsymbol{u}\, dx, \tag{3.2.3}$$
$$\int_T \nabla \cdot (\Pi_T \boldsymbol{u}) dx = \int_T \nabla \cdot \boldsymbol{u}\, dx. \tag{3.2.4}$$

Proof. It follows from (3.2.1), Green's Theorem and midpoint rule that

$$\begin{aligned} \int_T \nabla \times (\Pi_T \boldsymbol{u}) dx &= \sum_{e \subset \partial T} \int_e \boldsymbol{n} \times (\Pi_T \boldsymbol{u}) dx \\ &= \sum_{e \subset \partial T} [\boldsymbol{n} \times (\Pi_T \boldsymbol{u})](m_e)|e| \\ &= \sum_{e \subset \partial T} \boldsymbol{n} \times \int_e \boldsymbol{u}\, dx \\ &= \int_T \nabla \times \boldsymbol{u}\, dx. \end{aligned} \tag{3.2.5}$$

Similarly, we can also prove (3.2.4). □

Since $H_0(\text{curl};\Omega) \cap H(\text{div};\Omega) \subset [H^s(\Omega)]^2$ for some $s > 1/2$ (cf. [37]), we can define a global interpolation operator $\Pi_h : H_0(\text{curl};\Omega) \cap H(\text{div};\Omega) \longrightarrow V_h$ by piecing together the local interpolation operators:

$$(\Pi_h \boldsymbol{v})_T = \Pi_T \boldsymbol{v}_T \qquad \forall\, T \in \mathcal{T}_h. \tag{3.2.6}$$

Let $\nabla_h \times$ and $\nabla_h \cdot$ be defined by

$$(\nabla_h \times \boldsymbol{v})_T = \nabla \times (\boldsymbol{v}_T) \qquad \forall T \in \mathcal{T}_h,\ \boldsymbol{v} \in V_h, \tag{3.2.7}$$
$$(\nabla_h \cdot \boldsymbol{v})_T = \nabla \cdot (\boldsymbol{v}_T) \qquad \forall T \in \mathcal{T}_h,\ \boldsymbol{v} \in V_h. \tag{3.2.8}$$

In view of (3.2.3) and (3.2.6)–(3.2.8), we can show that for any piecewise constant function P,

$$
\begin{aligned}
\int_\Omega [\nabla_h \times (\Pi_h \boldsymbol{v})]\, P\, dx &= \sum_{T\in\mathcal{T}_h} \int_T [\nabla \times (\Pi_T \boldsymbol{v})]\, P_T\, dx \\
&= \sum_{T\in\mathcal{T}_h} P_T \int_T \nabla \times (\Pi_T \boldsymbol{v})\, dx \\
&= \sum_{T\in\mathcal{T}_h} P_T \int_T \nabla \times \boldsymbol{v}\, dx \\
&= \int_\Omega (\nabla \times \boldsymbol{v})\, P\, dx,
\end{aligned}
\tag{3.2.9}
$$

which implies

$$
\nabla_h \times (\Pi_h \boldsymbol{v}) = \Pi_0^h (\nabla \times \boldsymbol{v}) \qquad \forall\, \boldsymbol{v} \in H_0(\mathrm{curl};\Omega) \cap H(\mathrm{div};\Omega), \tag{3.2.10}
$$

where Π_0^h is the orthogonal projection from $L_2(\Omega)$ onto the space of piecewise constant functions associated with $\mathcal{T}_h$. Similarly

$$
\nabla_h \cdot (\Pi_h \boldsymbol{v}) = \Pi_0^h (\nabla \cdot \boldsymbol{v}) \qquad \forall\, \boldsymbol{v} \in H_0(\mathrm{curl};\Omega) \cap H(\mathrm{div};\Omega). \tag{3.2.11}
$$

The commutative relations (3.2.10) and (3.2.11) indicate that we have good control over $\nabla_h \times (\Pi_h \boldsymbol{u})$ and $\nabla_h \cdot (\Pi_h \boldsymbol{u})$ simultaneously, which explains why weakly continuous P_1 vector fields can be used to solve problems involving the space $H(\mathrm{curl};\Omega) \cap H(\mathrm{div};\Omega)$.

Let $e \in \mathcal{E}_h^i$ be shared by the two triangles $T_1, T_2 \in \mathcal{T}_h$ (cf. Figure 2.3) and $\boldsymbol{n}_1$ (resp. $\boldsymbol{n}_2$) be the unit normal of e pointing towards the outside of T_1 (resp. T_2). We define, on e,

$$
[\![\boldsymbol{n} \times \boldsymbol{v}]\!] = \boldsymbol{n}_1 \times \boldsymbol{v}_{T_1}\big|_e + \boldsymbol{n}_2 \times \boldsymbol{v}_{T_2}\big|_e, \tag{3.2.12a}
$$

$$
[\![\boldsymbol{n} \cdot \boldsymbol{v}]\!] = \boldsymbol{n}_1 \cdot \boldsymbol{v}_{T_1}\big|_e + \boldsymbol{n}_2 \cdot \boldsymbol{v}_{T_2}\big|_e. \tag{3.2.12b}
$$

For an edge $e \in \mathcal{E}_h^b$, we take $\boldsymbol{n}_e$ to be the unit normal of e pointing towards the outside of Ω and define

$$[\![\boldsymbol{n} \times \boldsymbol{v}]\!] = \boldsymbol{n}_e \times \boldsymbol{v}\big|_e. \tag{3.2.13}$$

A nonconforming finite element method for (1.2.9) is:

Find $\boldsymbol{u}_h \in V_h$ such that

$$a_h(\boldsymbol{u}_h, \boldsymbol{v}) = (\boldsymbol{f}, \boldsymbol{v}) \qquad \forall \boldsymbol{v} \in V_h, \tag{3.2.14}$$

where

$$\begin{aligned} a_h(\boldsymbol{w}, \boldsymbol{v}) = (\nabla_h \times \boldsymbol{w}, \nabla_h \times \boldsymbol{v}) + \gamma(\nabla_h \cdot \boldsymbol{w}, \nabla_h \cdot \boldsymbol{v}) + \alpha(\boldsymbol{w}, \boldsymbol{v}) \\ + \sum_{e \in \mathcal{E}_h} \frac{[\Phi_\mu(e)]^2}{|e|} \int_e [\![\boldsymbol{n} \times \boldsymbol{w}]\!]\, [\![\boldsymbol{n} \times \boldsymbol{v}]\!]\, ds \\ + \sum_{e \in \mathcal{E}_h^i} \frac{[\Phi_\mu(e)]^2}{|e|} \int_e [\![\boldsymbol{n} \cdot \boldsymbol{w}]\!][\![\boldsymbol{n} \cdot \boldsymbol{v}]\!] ds, \end{aligned} \tag{3.2.15}$$

and the edge weight $\Phi_\mu(e)$ is defined by

$$\Phi_\mu(e) = \Pi_{\ell=1}^L |c_\ell - m_e|^{1-\mu_\ell}. \tag{3.2.16}$$

Here the grading parameters μ are chosen according to (2.2.39).

By comparing (2.3.2) and (3.2.16), we have

$$\Phi_\mu(e) \approx \Phi_\mu(T) \quad \text{if} \quad e \subset \partial T. \tag{3.2.17}$$

Remark 3.2. *The last two terms on the right-hand side of* (3.2.15) *involving the tangential and normal jumps of the weakly continuous P_1 vector fields are crucial for the convergence of the scheme. A naive discretization of* (1.2.9) *with only the first three terms does not converge. The crucial difference is that the piecewise* $H(\text{curl};\Omega) \cap H(\text{div};\Omega)$ *semi-norm, unlike the piecewise H^1 semi-norm, is too weak to control the jumps even with the weak continuity of the vector fields in V_h. Hence the last two terms involving the jumps must be included in the discretization to control the consistency error.*

3.2.2 Error Analysis

In this section we first establish the abstract error estimate and some preliminary estimates for the scheme (3.2.14), then the convergence analysis will follow. More details can be found in [37].

We will measure the discretization error in both the L_2 norm and the mesh-dependent energy norm $\|\cdot\|_h$ defined by

$$\begin{aligned}\|\boldsymbol{v}\|_h^2 = \|\nabla_h \times \boldsymbol{v}\|_{L_2(\Omega)}^2 + \gamma\|\nabla_h \cdot \boldsymbol{v}\|_{L_2(\Omega)}^2 + \|\boldsymbol{v}\|_{L_2(\Omega)}^2 \\ + \sum_{e\in\mathcal{E}_h} \frac{[\Phi_\mu(e)]^2}{|e|}\|[[\boldsymbol{n}\times\boldsymbol{v}]]\|_{L_2(\Omega)}^2 \\ + \sum_{e\in\mathcal{E}_h^i} \frac{[\Phi_\mu(e)]^2}{|e|}\|[[\boldsymbol{n}\cdot\boldsymbol{v}]]\|_{L_2(\Omega)}^2.\end{aligned} \tag{3.2.18}$$

Note that

$$\|\boldsymbol{v}\|_{L_2(\Omega)} \le \|\boldsymbol{v}\|_h \qquad \forall\ \boldsymbol{v} \in H_0(\mathrm{curl};\Omega)\cap H(\mathrm{div};\Omega) + V_h. \tag{3.2.19}$$

It is easy to check that $a_h(\cdot,\cdot)$ is bounded with respect to $\|\cdot\|_h$, i.e.,

$$|a_h(\boldsymbol{w},\boldsymbol{v})| \le (|\alpha|+1)\|\boldsymbol{w}\|_h\|\boldsymbol{v}\|_h \tag{3.2.20}$$

for all $\boldsymbol{v},\boldsymbol{w} \in H_0(\mathrm{curl};\Omega)\cap H(\mathrm{div};\Omega) + V_h$.

For $\alpha > 0$, $a_h(\cdot,\cdot)$ is also coercive with respect to $\|\cdot\|_h$, i.e.,

$$a_h(\boldsymbol{v},\boldsymbol{v}) \ge \min(1,\alpha)\|\boldsymbol{v}\|_h^2 \tag{3.2.21}$$

for all $\boldsymbol{v} \in H_0(\mathrm{curl};\Omega)\cap H(\mathrm{div};\Omega) + V_h$. In this case the discrete problem is well-posed and we have following abstract error estimate, whose proof is identical with proof of Lemma 3.5 in [39].

Lemma 3.3. *Let α be positive, $\beta = min(1, \alpha)$, $\boldsymbol{u} \in H_0(\text{curl};\Omega) \cap H(\text{div};\Omega)$ be the solution of* (1.2.9)*, and $\boldsymbol{u}_h$ satisfy discrete problem* (3.2.14)*, it holds that*

$$\|\boldsymbol{u}-\boldsymbol{u}_h\|_h \leq (\frac{1+\alpha+\beta}{\beta}) \inf_{\boldsymbol{v}\in V_h} \|\boldsymbol{u}-\boldsymbol{v}\|_h + \frac{1}{\beta} \sup_{\boldsymbol{w}\in V_h\setminus\{0\}} \frac{a_h(\boldsymbol{u}-\boldsymbol{u}_h, \boldsymbol{w})}{\|\boldsymbol{w}\|_h}. \tag{3.2.22}$$

Proof. Let $\boldsymbol{v} \in V_h$ be arbitrary. It follows from (3.2.20), (3.2.21) and the triangle inequality that

$$\begin{aligned}
\|\boldsymbol{u}-\boldsymbol{u}_h\|_h \leq& \|\boldsymbol{u}-\boldsymbol{v}\|_h + \|\boldsymbol{v}-\boldsymbol{u}_h\|_h \\
\leq& \|\boldsymbol{u}-\boldsymbol{v}\|_h + \frac{1}{\beta} \sup_{\boldsymbol{w}\in V_h\setminus\{0\}} \frac{a_h(\boldsymbol{v}-\boldsymbol{u}_h, \boldsymbol{w})}{\|\boldsymbol{w}\|_h} \\
\leq& (\frac{1+\alpha+\beta}{\beta}) \inf_{\boldsymbol{v}\in V_h} \|\boldsymbol{u}-\boldsymbol{v}\|_h + \frac{1}{\beta} \sup_{\boldsymbol{w}\in V_h\setminus\{0\}} \frac{a_h(\boldsymbol{u}-\boldsymbol{u}_h, \boldsymbol{w})}{\|\boldsymbol{w}\|_h},
\end{aligned}$$

which implies (3.2.22). □

For $\alpha \leq 0$, we have a Gårding (in)equality:

$$a_h(\boldsymbol{v}, \boldsymbol{v}) + (|\alpha|+1)(\boldsymbol{v}, \boldsymbol{v}) = \|\boldsymbol{v}\|_h^2 \tag{3.2.23}$$

for all $\boldsymbol{v} \in H_0(\text{curl};\Omega) \cap H(\text{div};\Omega) + V_h$. In this case the discrete problem is indefinite and the following lemma provides an abstract error estimate for the scheme (3.2.14) under the assumption that it has solution. Details of the proof can be found in [39, Lemma 3.6]

Lemma 3.4. *Let $\boldsymbol{u} \in H_0(\text{curl};\Omega) \cap H(\text{div};\Omega)$ satisfy* (1.2.9) *and $\boldsymbol{u}_h$ be the solution of* (3.2.14)*. It holds that*

$$\|\boldsymbol{u}-\boldsymbol{u}_h\|_h \leq (2|\alpha|+3) \inf_{\boldsymbol{v}\in V_h} \|\boldsymbol{u}-\boldsymbol{v}\|_h + \sup_{\boldsymbol{w}\in V_h\setminus\{0\}} \frac{a_h(\boldsymbol{u}-\boldsymbol{u}_h, \boldsymbol{w})}{\|\boldsymbol{w}\|_h} + (|\alpha|+1)\|\boldsymbol{u}-\boldsymbol{u}_h\|_{L_2(\Omega)}. \tag{3.2.24}$$

Proof. It follows from (3.2.19) and (3.2.23) that for any $\boldsymbol{v} \in V_h \setminus \{0\}$,

$$\begin{aligned} \|\boldsymbol{v}\|_h \leq & \frac{a_h(\boldsymbol{v},\boldsymbol{v})}{\|\boldsymbol{v}\|_h} + (|\alpha|+1)\frac{(\boldsymbol{v},\boldsymbol{v})}{\|\boldsymbol{v}\|_h} \\ \leq & \sup_{\boldsymbol{w}\in V_h\setminus\{0\}} \frac{a_h(\boldsymbol{v},\boldsymbol{w})}{\|\boldsymbol{w}\|_h} + (|\alpha|+1)\|\boldsymbol{v}\|_{L_2(\Omega)}. \end{aligned} \tag{3.2.25}$$

Let $\boldsymbol{v} \in V_h$ be arbitrary. By using (3.2.19), (3.2.20), (3.2.25) and the triangle inequality, we find

$$\begin{aligned} \|\boldsymbol{u}-\boldsymbol{u}_h\|_h \leq & \|\boldsymbol{u}-\boldsymbol{v}\|_h + \|\boldsymbol{v}-\boldsymbol{u}_h\|_h \\ \leq & \|\boldsymbol{u}-\boldsymbol{v}\|_h + \sup_{\boldsymbol{w}\in V_h\setminus\{0\}} \frac{a_h(\boldsymbol{v}-\boldsymbol{u}_h,\boldsymbol{w})}{\|\boldsymbol{w}\|_h} + (|\alpha|+1)\|\boldsymbol{v}-\boldsymbol{u}_h\|_{L_2(\Omega)} \\ \leq & (2|\alpha|+3)\|\boldsymbol{u}-\boldsymbol{v}\|_h + \sup_{\boldsymbol{w}\in V_h\setminus\{0\}} \frac{a_h(\boldsymbol{u}-\boldsymbol{u}_h,\boldsymbol{w})}{\|\boldsymbol{w}\|_h} + (|\alpha|+1)\|\boldsymbol{u}-\boldsymbol{u}_h\|_{L_2(\Omega)}, \end{aligned}$$

which implies (3.2.24). □

From here on we consider α and γ to be fixed and drop the dependence on these constants in our estimates.

Remark 3.5. *The first term on the right-hand side of* (3.2.22) *and* (3.2.24) *measures the approximation property of V_h with respect to the energy norm. The second term measures the consistency error. The third term on the right-hand side of* (3.2.24) *addresses the indefiniteness of the problem when $\alpha < 0$.*

Let $\mathcal{T}_{h,\ell}$ be the set of the triangles in $\mathcal{T}_h$ that share the corner c_l as a common vertex. We assume that $h \ll \delta$ and hence $T \subset \mathcal{N}_{\ell,\delta}$ for all $T \in \mathcal{T}_{h,\ell}$, where $\mathcal{N}_{\ell,\delta} = \{x \in \Omega : |x - c_\ell| < \delta\}$ are the neighborhoods of the corners c_ℓ for $1 \leq \ell \leq L$. We will use the notation $\mathcal{T}_h' = \bigcup_{\ell=1}^{L} \mathcal{T}_{h,\ell}$ and $\mathcal{T}_h'' = \mathcal{T}_h \setminus \mathcal{T}_h'$ in the proof of the following lemma, whose proof is identical to the proof of Lemma 5.1 in [40].

Lemma 3.6. *Let $\boldsymbol{u} \in H_0(\mathrm{curl};\Omega) \cap H(\mathrm{div};\Omega)$ be the solution of* (1.2.9)*. For any $\epsilon > 0$ there exists a positive constant C_ϵ independent of h and $\boldsymbol{f}$ such that*

$$\|\boldsymbol{u} - \Pi_h \boldsymbol{u}\|_{L_2(\Omega)} \leq C_\epsilon h^{2-\epsilon} \|\boldsymbol{f}\|_{L_2(\Omega)}. \tag{3.2.26}$$

Proof. We can write

$$\|\boldsymbol{u}-\Pi_h\boldsymbol{u}\|_{L_2(\Omega)}^2=\sum_{T\in\mathcal{T}_h''}\|\boldsymbol{u}-\Pi_T\boldsymbol{u}\|_{L_2(T)}^2+\sum_{T\in\mathcal{T}_h'}\|\boldsymbol{u}-\Pi_T\boldsymbol{u}\|_{L_2(T)}^2. \tag{3.2.27}$$

Then we have, by (2.2.26), (2.3.4) and (3.2.2) (with $s=2$),

$$\sum_{T\in\mathcal{T}_h'',T\not\subset\bigcup_{\ell=1}^L\mathcal{N}_{\ell,\delta}}\|\boldsymbol{u}-\Pi_T\boldsymbol{u}\|_{L_2(T)}^2\lesssim h^4\|\boldsymbol{f}\|_{L_2(\Omega)}^2. \tag{3.2.28}$$

On the other hand, near a corner c_ℓ of Ω we can use (2.2.27) and (2.2.28) to get

$$\begin{aligned}\sum_{T\in\mathcal{T}_h'',T\subset\bigcup_{\ell=1}^L\mathcal{N}_{\ell,\delta}}\|\boldsymbol{u}-\Pi_T\boldsymbol{u}\|^2{}_{L_2(T)}\lesssim&\sum_{T\in\mathcal{T}_h'',T\subset\bigcup_{\ell=1}^L\mathcal{N}_{\ell,\delta}}[\|\boldsymbol{u}_R-\Pi_T\boldsymbol{u}_R\|_{L_2(T)}^2\\&+\sum_{\substack{j\in\mathbb{N}\\ j(\pi/\omega_\ell)\in(0,2)\setminus\{1\}}}|\nu_{\ell,j}|^2\|\boldsymbol{\psi}_{\ell,j}-\Pi_T\boldsymbol{\psi}_{\ell,j}\|_{L_2(T)}^2].\end{aligned} \tag{3.2.29}$$

where $\boldsymbol{\psi}_{\ell,j}$ and $\nu_{\ell,j}$ are defined by (2.2.29).

The estimates (2.2.30a), (2.3.4) and (3.2.2) (with $s=2-\epsilon$) imply

$$\sum_{T\in\mathcal{T}_h'',T\subset\bigcup_{\ell=1}^L\mathcal{N}_{\ell,\delta}}\|\boldsymbol{u}_R-\Pi_T\boldsymbol{u}_R\|_{L_2(T)}^2\le C_\epsilon h^{4-\epsilon}\|\boldsymbol{f}\|_{L_2(\Omega)}^2 \tag{3.2.30}$$

for any $\epsilon>0$.

Note that (2.3.1) and the regularity of $\mathcal{T}_h$ imply that

$$|c_\ell-c_T|\approx|c_\ell-x|\qquad\forall\,x\in T\in\mathcal{T}_h''\quad\text{and}\quad T\subset\mathcal{N}_{\ell,\delta}, \tag{3.2.31}$$

and hence

$$\Phi_\mu(T)\approx|c_\ell-x|^{1-\mu_\ell}\qquad\forall\,x\in T\in\mathcal{T}_h''\quad\text{and}\quad T\subset\mathcal{N}_{\ell,\delta}. \tag{3.2.32}$$

For $\omega_\ell>\frac{\pi}{2}$, we can show that (2.2.29a) and (2.2.39) imply (cf. [40])

$$\sum_{T\in\mathcal{T}_h,T\subset\mathcal{N}_{\ell,\delta}}\int_T|c_\ell-x|^{4(1-\mu_\ell)}|D^2\boldsymbol{\psi}_{\ell,j}|^2\,dx<\infty, \tag{3.2.33}$$

where $|D^2\boldsymbol{v}|^2=\sum_{i,j,k=1}^2(\frac{\partial^2 v_i}{\partial x_j\partial x_k})^2$, because

$$\int_0^1 r^{4(1-\mu_\ell)}r^{2((\pi/\omega_\ell)-3)}r\,dr<\infty,\quad\text{if }\mu_\ell<\frac{\pi}{2\omega_\ell}.$$

Then by using (2.3.1), (3.2.2) (with $s = 2$), (3.2.32) and (3.2.33) we obtain the following estimate for the term involving the singular vector fields:

$$\begin{aligned}\sum_{T\in\mathcal{T}_h'',T\subset\bigcup_{\ell=1}^{L}\mathcal{N}_{\ell,\delta}} \|\boldsymbol{\psi}_{\ell,j}-\Pi_T\boldsymbol{\psi}_{\ell,j}\|^2_{L_2(T)} &\lesssim \sum_{T\in\mathcal{T}_h'',T\subset\bigcup_{\ell=1}^{L}\mathcal{N}_{\ell,\delta}} h_T^4|\boldsymbol{\psi}_{\ell,j}|^2_{H^2(T)}\\ &\approx h^4 \sum_{T\in\mathcal{T}_h'',T\subset\bigcup_{\ell=1}^{L}\mathcal{N}_{\ell,\delta}} [\Phi_\mu(T)]^4|\boldsymbol{\psi}_{\ell,j}|^2_{H^2(T)} \qquad (3.2.34)\\ &\approx h^4 \sum_{T\in\mathcal{T}_h'',T\subset\bigcup_{\ell=1}^{L}\mathcal{N}_{\ell,\delta}} \int_T |c_\ell - x|^{4(1-\mu_\ell)}|D^2\boldsymbol{\psi}_{\ell,j}|^2dx \lesssim h^4.\end{aligned}$$

Combining (2.2.30), (3.2.28)–(3.2.34), we get

$$\sum_{T\in\mathcal{T}_h''}\|\boldsymbol{u}-\Pi_T\boldsymbol{u}\|^2_{L_2(T)} \le C_\epsilon h^{4-\epsilon}\|\boldsymbol{f}\|^2_{L_2(\Omega)} \qquad \text{for any } \epsilon > 0. \qquad (3.2.35)$$

It remains to estimate the second term on the right-hand side of (3.2.27).

In the case where $\omega_l \le \frac{\pi}{2}$, it follows from (2.2.27)–(2.2.30), (2.3.1) and (3.2.2) (with $s = 2-\epsilon$) that

$$\sum_{T\in\mathcal{T}_{h,\ell}}\|\boldsymbol{u}-\Pi_T\boldsymbol{u}\|^2_{L_2(T)} \le C_\epsilon h^{4-\epsilon}\|\boldsymbol{f}\|^2_{L_2(\Omega)}. \qquad (3.2.36)$$

In the case where $\omega_l > \frac{\pi}{2}$, since $\boldsymbol{u} \in [H^{2\mu_\ell}(\Omega)]^2$ (cf. Remark 2.15), we obtain from (2.2.40), (2.3.5) and (3.2.2) (with $s = 2\mu_\ell$) that

$$\sum_{T\in\mathcal{T}_{h,\ell}}\|\boldsymbol{u}-\Pi_T\boldsymbol{u}\|^2_{L_2(T)} \lesssim h_T^{4\mu_\ell}\|\boldsymbol{f}\|^2_{L_2(\Omega)} \approx h^4\|\boldsymbol{f}\|^2_{L_2(\Omega)}. \qquad (3.2.37)$$

Combining (3.2.36) and (3.2.37), we have

$$\sum_{T\in\mathcal{T}_h'}\|\boldsymbol{u}-\Pi_T\boldsymbol{u}\|^2_{L_2(T)} \le C_\epsilon h^{4-\epsilon}\|\boldsymbol{f}\|^2_{L_2(\Omega)} \qquad \text{for any } \epsilon > 0. \qquad (3.2.38)$$

The estimate (3.2.26) follows from (3.2.27), (3.2.35) and (3.2.38). □

Lemma 3.7. *Let $\boldsymbol{u} \in H_0(\mathrm{curl};\Omega) \cap H(\mathrm{div};\Omega)$ be the solution of (1.2.9). It holds that*

$$\sum_{e\in\mathcal{E}_h}\frac{[\Phi_\mu(e)]^2}{|e|}\|[\![\boldsymbol{u}-\Pi_h\boldsymbol{u}]\!]\|^2_{L_2(e)} \le C_\epsilon h^{2-\varepsilon}\|\boldsymbol{f}\|^2_{L_2(\Omega)} \qquad (3.2.39)$$

for any $\epsilon > 0$.

Proof. The proof is identical with the proof of Lemma 5.2 in [40], which is obtained by using (2.2.26)–(2.2.30), (2.3.1), (2.3.3), (2.3.4) and (3.2.2). □

Lemma 3.8. *Let* $\boldsymbol{u} \in H_0(\mathrm{curl};\Omega) \cap H(\mathrm{div};\Omega)$ *be the solution of* (1.2.9). *It holds that*

$$\inf_{\boldsymbol{v}\in V_h} \|\boldsymbol{u}-\boldsymbol{v}\|_h \le \|\boldsymbol{u}-\Pi_h\boldsymbol{u}\|_h < C_\epsilon h^{1-\epsilon}\|\boldsymbol{f}\|_{L_2(\Omega)} \tag{3.2.40}$$

for any $\epsilon > 0$.

Proof. According to (3.2.18), we have

$$\begin{aligned}\|\boldsymbol{u}-\Pi_h\boldsymbol{u}\|_h^2 = &\|\nabla_h\times(\boldsymbol{u}-\Pi_h\boldsymbol{u})\|_{L_2(\Omega)}^2 \\ &+\gamma\|\nabla_h\cdot(\boldsymbol{u}-\Pi_h\boldsymbol{u})\|_{L_2(\Omega)}^2 + \|\boldsymbol{u}-\Pi_h\boldsymbol{u}\|_{L_2(\Omega)}^2 \\ &+\sum_{e\in\mathcal{E}_h}\frac{[\Phi_\mu(e)]^2}{|e|}\|[\![\boldsymbol{n}\times(\boldsymbol{u}-\Pi_h\boldsymbol{u})]\!]\|_{L_2(\Omega)}^2 \\ &+\sum_{e\in\mathcal{E}_h^i}\frac{[\Phi_\mu(e)]^2}{|e|}\|[\![\boldsymbol{n}\cdot(\boldsymbol{u}-\Pi_h\boldsymbol{u})]\!]\|_{L_2(\Omega)}^2.\end{aligned} \tag{3.2.41}$$

The third term on the right-hand side of (3.2.41) has been estimated in Lemma 3.6, and the last two terms can be estimated by using Lemma 3.7. Therefore it only remains to estimate the first two terms.

It follows from (2.2.17), (2.2.18), (3.2.10), (3.2.11) and a standard interpolation error estimate [51, 43] that

$$\begin{aligned}\|\nabla_h\times(\boldsymbol{u}-\Pi_h\boldsymbol{u})\|_{L_2(\Omega)}^2 =&\|\nabla\times\boldsymbol{u}-\Pi_h^0(\nabla\times\boldsymbol{u})\|_{L_2(\Omega)}^2 \\ \le& Ch^2|\nabla\times\boldsymbol{u}|_{H^1(\Omega)}^2 \le Ch^2\|\boldsymbol{f}\|_{L_2(\Omega)}^2,\end{aligned} \tag{3.2.42}$$

$$\begin{aligned}\gamma\|\nabla_h\cdot(\boldsymbol{u}-\Pi_h\boldsymbol{u})\|_{L_2(\Omega)}^2 =&\gamma\|\nabla\cdot\boldsymbol{u}-\Pi_h^0(\nabla\cdot\boldsymbol{u})\|_{L_2(\Omega)}^2. \\ \le& Ch^2|\nabla\cdot\boldsymbol{u}|_{H^1(\Omega)}^2 \le Ch^2\|\boldsymbol{f}\|_{L_2(\Omega)}^2.\end{aligned} \tag{3.2.43}$$

The estimate (3.2.40) follows from (3.2.41)–(3.2.43), Lemma 3.6 and Lemma 3.7.

□

The next lemma is useful for estimating terms involving the jumps of the weakly continuous P_1 vector fields across edges (cf. [40, Lemma 5.3]).

Lemma 3.9. *It holds that*

$$\sum_{e\in\mathcal{E}_h} |e|\,[\Phi_\mu(e)]^{-2}\|\eta - \hat{\eta}_{T_e}\|^2_{L_2(e)} \leq Ch^2|\eta|^2_{H^1(\Omega)} \qquad \forall\,\eta \in H^1(\Omega),$$

where

$$\hat{\eta}_{T_e} = \frac{1}{|T_e|}\int_{T_e} \eta\,dx \tag{3.2.44}$$

is the mean of η *over* T_e*, one of the triangles in* $\mathcal{T}_h$ *that has* e *as an edge.*

Proof. This is the consequence of (2.3.1), (3.2.17), the trace theorem (with scaling) and a standard interpolation error estimate [51, 43]:

$$\begin{aligned}
&\sum_{e\in\mathcal{E}_h} |e|\,[\Phi_\mu(e)]^{-2}\|\eta - \hat{\eta}_{T_e}\|^2_{L_2(e)} \\
&\qquad \leq C\sum_{e\in\mathcal{E}_h}[\Phi_\mu(T)]^{-2}\big(\|\eta - \hat{\eta}_{T_e}\|^2_{L_2(T_e)} + h_T^2|\eta - \hat{\eta}_{T_e}|^2_{H^1(T_e)}\big) \\
&\qquad \leq C\sum_{e\in\mathcal{E}_h}[\Phi_\mu(T)]^{-2}h_T^2|\eta|^2_{H^1(T_e)} \leq Ch^2|\eta|^2_{H^1(\Omega)}.
\end{aligned}$$

□

The following lemma gives an optimal bound for the consistency error.

Lemma 3.10. *Let* $\boldsymbol{u} \in H_0(\mathrm{curl};\Omega) \cap H(\mathrm{div};\Omega)$ *be the solution of* (1.2.9)*, and* $\boldsymbol{u}_h \in V_h$ *satisfy* (3.2.14)*. Then*

$$\sup_{\boldsymbol{w}\in V_h\setminus\{0\}} \frac{a_h(\boldsymbol{u}-\boldsymbol{u}_h,\boldsymbol{w})}{\|\boldsymbol{w}\|_h} \leq Ch\|\boldsymbol{f}\|_{L_2(\Omega)}. \tag{3.2.45}$$

Proof. Let $\boldsymbol{w} \in V_h$ be arbitrary. Since the strong form of (1.2.9) is given by (2.2.19), from (3.2.12), (3.2.13), (3.2.15) and integration by parts formula, we have

$$\begin{aligned} a_h(\boldsymbol{u},\boldsymbol{w}) &= \sum_{T\in\mathcal{T}_h}\int_T (\nabla\times\boldsymbol{u})(\nabla\times\boldsymbol{w})dx \\ &\qquad + \sum_{T\in\mathcal{T}_h}\gamma\int_T(\nabla\cdot\boldsymbol{u})(\nabla\cdot\boldsymbol{w})dx + \alpha(\boldsymbol{u},\boldsymbol{w}) \\ &= (\boldsymbol{f},\boldsymbol{w}) + \sum_{e\in\mathcal{E}_h}\int_e(\nabla\times\boldsymbol{u})[\![\boldsymbol{n}\times\boldsymbol{w}]\!]ds + \sum_{e\in\mathcal{E}_h^i}\gamma\int_e(\nabla\cdot\boldsymbol{u})[\![\boldsymbol{n}\cdot\boldsymbol{w}]\!]ds. \end{aligned} \tag{3.2.46}$$

Remark 3.11. *Recall from* (2.2.19c) *that* $\nabla\cdot\boldsymbol{u} = 0$ *on* $\partial\Omega$ *if* $\boldsymbol{u}$ *is the solution of* (1.2.9). *Hence the integrals in the last term on the right-hand side of* (3.2.46) *vanish on boundary edges.*

Subtracting (3.2.14) from (3.2.46), we have

$$a_h(\boldsymbol{u}-\boldsymbol{u}_h,\boldsymbol{w}) = \sum_{e\in\mathcal{E}_h}\int_e(\nabla\times\boldsymbol{u})[\![\boldsymbol{n}\times\boldsymbol{w}]\!]ds + \sum_{e\in\mathcal{E}_h^i}\int_e(\nabla\cdot\boldsymbol{u})[\![\boldsymbol{n}\cdot\boldsymbol{w}]\!]ds. \tag{3.2.47}$$

Since $\boldsymbol{w}$ is continuous at the midpoints of interior edges and its tangential components vanish at the midpoints of the boundary edges, we can write, using the midpoint rule,

$$\sum_{e\in\mathcal{E}_h}\int_e(\nabla\times\boldsymbol{u})[\![\boldsymbol{n}\times\boldsymbol{w}]\!]ds = \sum_{e\in\mathcal{E}_h}\int_e(\nabla\times\boldsymbol{u} - (\widehat{\nabla\times\boldsymbol{u}})_{T_e})[\![\boldsymbol{n}\times\boldsymbol{w}]\!]ds, \tag{3.2.48}$$

where $(\widehat{\nabla\times\boldsymbol{u}})_{T_e}$ is the mean of $\nabla\times\boldsymbol{u}$ on T_e, one of the triangles in $\mathcal{T}_h$ that has e as an edge. It then follows from Cauchy-Schwarz inequality, (2.2.17), (3.2.18) and Lemma 3.9 that

$$\begin{aligned} &\sum_{e\in\mathcal{E}_h}\int_e(\nabla\times\boldsymbol{u})[\![\boldsymbol{n}\times\boldsymbol{w}]\!]ds \\ &\qquad \le \Big\{\sum_{e\in\mathcal{E}_h}|e|[\Phi_\mu(e)]^{-2}\|(\nabla\times\boldsymbol{u}-(\widehat{\nabla\times\boldsymbol{u}})_{T_e})\|^2_{L_2(e)}\Big\}^{1/2} \\ &\qquad\qquad \times\Big\{\sum_{e\in\mathcal{E}_h}\frac{[\Phi_\mu(e)]^2}{|e|}\|[\![\boldsymbol{n}\times\boldsymbol{w}]\!]\|^2_{L_2(e)}\Big\}^{1/2} \\ &\qquad \le C(h|\nabla\times\boldsymbol{u}|_{H^1(\Omega)})\|\boldsymbol{w}\|_h \le Ch\|\boldsymbol{f}\|_{L_2(\Omega)}\|\boldsymbol{w}\|_h, \end{aligned} \tag{3.2.49}$$

and similarly

$$\sum_{e\in\mathcal{E}_h^i}\gamma\int_e(\nabla\cdot\boldsymbol{u})[\![\boldsymbol{n}\cdot\boldsymbol{w}]\!]ds \le Ch\|\boldsymbol{f}\|_{L_2(\Omega)}\|\boldsymbol{w}\|_h. \tag{3.2.50}$$

The estimate (3.2.45) follows from (3.2.47), (3.2.49) and (3.2.50).

□

We now derive an L_2 error estimate by a duality argument.

Theorem 3.12. *Let* $\boldsymbol{u}\in H_0(\mathrm{curl};\Omega)\cap H(\mathrm{div};\Omega)$ *be the solution of* (1.2.9)*, and* $\boldsymbol{u}_h\in V_h$ *satisfy* (3.2.14)*. Then*

$$\|\boldsymbol{u}-\boldsymbol{u}_h\|_{L_2(\Omega)} \le C_\varepsilon(h^{2-\varepsilon}\|\boldsymbol{f}\|_{L_2(\Omega)} + h^{1-\varepsilon}\|\boldsymbol{u}-\boldsymbol{u}_h\|_h) \tag{3.2.51}$$

for any $\varepsilon>0$*.*

Proof. Let $\boldsymbol{z}\in H_0(\mathrm{curl};\Omega)\cap H(\mathrm{div};\Omega)$ satisfy

$$(\nabla\times\boldsymbol{v},\nabla\times\boldsymbol{z})+\gamma(\nabla\cdot\boldsymbol{v},\nabla\cdot\boldsymbol{z})+\alpha(\boldsymbol{v},\boldsymbol{z}) = (\boldsymbol{v},(\boldsymbol{u}-\boldsymbol{u}_h)) \tag{3.2.52}$$

for all $\boldsymbol{v}\in H_0(\mathrm{curl};\Omega)\cap H(\mathrm{div};\Omega)$. Note that the strong form of (3.2.52) is

$$\nabla\times(\nabla\times\boldsymbol{z})-\gamma\nabla(\nabla\cdot\boldsymbol{z})+\alpha\boldsymbol{z}=\boldsymbol{u}-\boldsymbol{u}_h, \tag{3.2.53}$$

and we have the following analog of (2.2.17) and (2.2.18):

$$|\nabla\times\boldsymbol{z}|_{H^1(\Omega)}+|\nabla\cdot\boldsymbol{z}|_{H^1(\Omega)} \le C\|\boldsymbol{u}-\boldsymbol{u}_h\|_{L_2(\Omega)}. \tag{3.2.54}$$

Furthermore, we can write (3.2.52) as

$$a_h(\boldsymbol{v},\boldsymbol{z})=(\boldsymbol{v},(\boldsymbol{u}-\boldsymbol{u}_h)) \qquad \forall\,\boldsymbol{v}\in H_0(\mathrm{curl};\Omega)\cap H(\mathrm{div};\Omega). \tag{3.2.55}$$

From (3.2.53), (3.2.55) and integration by parts we have the following analog of (3.2.46):

$$
\begin{aligned}
a_h(\boldsymbol{u}_h, \boldsymbol{z}) = \sum_{T\in\mathcal{T}_h} \int_T (\nabla\times\boldsymbol{u}_h)(\nabla\times\boldsymbol{z})dx \\
+ \sum_{T\in\mathcal{T}_h} \gamma \int_T (\nabla\cdot\boldsymbol{u}_h)(\nabla\cdot\boldsymbol{z})dx + \alpha(\boldsymbol{u}_h, \boldsymbol{z}) \\
= (\boldsymbol{u}_h, (\boldsymbol{u}-\boldsymbol{u}_h)) + \sum_{e\in\mathcal{E}_h} \int_e [\![\boldsymbol{n}\times\boldsymbol{u}_h]\!](\nabla\times\boldsymbol{z})ds \\
+ \sum_{e\in\mathcal{E}_h^i} \gamma \int_e [\![\boldsymbol{n}\cdot\boldsymbol{u}_h]\!](\nabla\cdot\boldsymbol{z})ds.
\end{aligned}
\tag{3.2.56}
$$

Combine (3.2.55) and (3.2.56), we have

$$
\begin{aligned}
\|\boldsymbol{u}-\boldsymbol{u}_h\|_{L_2(\Omega)}^2 = (\boldsymbol{u}, \boldsymbol{u}-\boldsymbol{u}_h) - (\boldsymbol{u}_h, \boldsymbol{u}-\boldsymbol{u}_h) \\
= a_h(\boldsymbol{u}-\boldsymbol{u}_h, \boldsymbol{z}) + \sum_{e\in\mathcal{E}_h} \int_e [\![\boldsymbol{n}\times\boldsymbol{u}_h]\!](\nabla\times\boldsymbol{z})ds \\
+ \sum_{e\in\mathcal{E}_h^i} \gamma \int_e [\![\boldsymbol{n}\cdot\boldsymbol{u}_h]\!](\nabla\cdot\boldsymbol{z})ds,
\end{aligned}
\tag{3.2.57}
$$

and we will estimate the three terms on the right-hand side of (3.2.57) separately.

We can write the first term as

$$
a_h(\boldsymbol{u}-\boldsymbol{u}_h, \boldsymbol{z}) = a_h(\boldsymbol{u}-\boldsymbol{u}_h, \boldsymbol{z}-\Pi_h\boldsymbol{z}) + a_h(\boldsymbol{u}-\boldsymbol{u}_h, \Pi_h\boldsymbol{z}).
\tag{3.2.58}
$$

From (3.2.20) and Lemma 3.8 (applied to $\boldsymbol{z}$) we immediately have the following estimate:

$$
\begin{aligned}
a_h(\boldsymbol{u}-\boldsymbol{u}_h, \boldsymbol{z}-\Pi_h\boldsymbol{z}) \leq & C\|\boldsymbol{u}-\boldsymbol{u}_h\|_h \|\boldsymbol{z}-\Pi_h\boldsymbol{z}\|_h \\
\leq & C_\varepsilon h^{1-\varepsilon} \|\boldsymbol{u}-\boldsymbol{u}_h\|_h \|\boldsymbol{u}-\boldsymbol{u}_h\|_{L_2(\Omega)}.
\end{aligned}
\tag{3.2.59}
$$

By using (3.2.47), we can rewrite the second term on the right-hand side of (3.2.58) as

$$a_h(\boldsymbol{u}-\boldsymbol{u}_h,\Pi_h\boldsymbol{z}) = \sum_{e\in\mathcal{E}_h}\int_e (\nabla\times\boldsymbol{u})[\![\boldsymbol{n}\times(\Pi_h\boldsymbol{z})]\!]ds + \sum_{e\in\mathcal{E}_h^i}\int_e \gamma(\nabla\cdot\boldsymbol{u})[\![\boldsymbol{n}\cdot(\Pi_h\boldsymbol{z})]\!]ds. \tag{3.2.60}$$

Following the notation introduced in (3.2.48), the first term on the right-hand side of (3.2.60) can be written as:

$$\begin{aligned}
&\sum_{e\in\mathcal{E}_h}\int_e (\nabla\times\boldsymbol{u})[\![\boldsymbol{n}\times\Pi_h\boldsymbol{z}]\!]ds\\
&\quad=\sum_{e\in\mathcal{E}_h}\int_e (\nabla\times\boldsymbol{u}-(\widehat{\nabla\times\boldsymbol{u}})_{T_e})[\![\boldsymbol{n}\times(\Pi_h\boldsymbol{z})]\!]ds\\
&\quad=\sum_{e\in\mathcal{E}_h}\int_e (\nabla\times\boldsymbol{u}-(\widehat{\nabla\times\boldsymbol{u}})_{T_e})[\![\boldsymbol{n}\times(\Pi_h\boldsymbol{z}-\boldsymbol{z})]\!]ds.
\end{aligned}$$

Since $\boldsymbol{n}\times(\Pi_h\boldsymbol{z})$ is continuous at the midpoints of interior edges and vanishes at the midpoints of boundary edges, and $[\![\boldsymbol{n}\times\boldsymbol{z}]\!]=0$. It then follows from the Cauchy-Schwarz inequality, (2.2.17), Lemma 3.7 (applied to $\boldsymbol{z}$) and Lemma 3.9 that

$$\begin{aligned}
&\sum_{e\in\mathcal{E}_h}\int_e (\nabla\times\boldsymbol{u})[\![\boldsymbol{n}\times(\Pi_h\boldsymbol{z})]\!]ds\\
&\quad\le\{\sum_{e\in\mathcal{E}_h}|e|[\Phi_\mu(e)]^{-2}\|(\nabla\times\boldsymbol{u}-(\widehat{\nabla\times\boldsymbol{u}})_{T_e})\|^2_{L_2(e)}\}^{1/2}\\
&\qquad\times\{\sum_{e\in\mathcal{E}_h}\frac{[\Phi_\mu(e)]^2}{|e|}\|[\![\mathbf{n}\times(\Pi_h\boldsymbol{z}-\boldsymbol{z})]\!]\|^2_{L_2(e)}\}^{1/2} \qquad (3.2.61)\\
&\quad\le C_\varepsilon(h|\nabla\times\boldsymbol{u}|_{H_1(\Omega)})(h^{1-\varepsilon}\|\boldsymbol{u}-\boldsymbol{u}_h\|_{L_2(\Omega)})\\
&\quad\le C_\varepsilon h^{2-\varepsilon}\|\boldsymbol{f}\|_{L_2(\Omega)}\|\boldsymbol{u}-\boldsymbol{u}_h\|_{L_2(\Omega)}.
\end{aligned}$$

Similarly, the second term on the right-hand side of (3.2.60) satisfies the following estimate:

$$\sum_{e\in\mathcal{E}_h^i}\int_e \gamma(\nabla\cdot\boldsymbol{u})[\![\boldsymbol{n}\cdot\Pi_h\boldsymbol{z}]\!]ds \le C_\varepsilon h^{2-\varepsilon}\|\boldsymbol{f}\|_{L_2(\Omega)}\|\boldsymbol{u}-\boldsymbol{u}_h\|_{L_2(\Omega)}. \tag{3.2.62}$$

Combing (3.2.58)–(3.2.62), we have

$$\begin{aligned}&a_h(\boldsymbol{u}-\boldsymbol{u}_h,\boldsymbol{z}) &(3.2.63)\\ &\qquad\le C_\varepsilon(h^{2-\varepsilon}\|\boldsymbol{f}\|_{L_2(\Omega)}+h^{1-\varepsilon}\|\boldsymbol{u}-\boldsymbol{u}_h\|_h)\|\boldsymbol{u}-\boldsymbol{u}_h\|_{L_2(\Omega)}.\end{aligned}$$

We now consider the second term on the right-hand side of (3.2.57). Since $\boldsymbol{n}\times\boldsymbol{u}_h$ is continuous at the midpoints of interior edges and vanishes at the midpoints of boundary edges, and $[\![\boldsymbol{n}\times\boldsymbol{u}]\!]=0$, we can write, following the notation introduced in (3.2.48),

$$\begin{aligned}&\sum_{e\in\mathcal{E}_h}\int_e[\![\boldsymbol{n}\times\boldsymbol{u}_h]\!](\nabla\times\boldsymbol{z})ds\\ &\quad=\sum_{e\in\mathcal{E}_h}\int_e[\![\boldsymbol{n}\times\boldsymbol{u}_h]\!](\nabla\times\boldsymbol{z}-(\widehat{\nabla\times\boldsymbol{z}})_{T_e})ds\\ &\quad=\sum_{e\in\mathcal{E}_h}\int_e[\![\boldsymbol{n}\times(\boldsymbol{u}_h-\boldsymbol{u})]\!](\nabla\times\boldsymbol{z}-(\widehat{\nabla\times\boldsymbol{z}})_{T_e})ds.\end{aligned}$$

Using the Cauchy-Schwarz inequality, (3.2.18), (3.2.54) and Lemma 3.9, we obtain

$$\begin{aligned}&\sum_{e\in\mathcal{E}_h}\int_e[\![\boldsymbol{n}\times\boldsymbol{u}_h]\!](\nabla\times\boldsymbol{z})ds\\ &\quad\le\Big(\sum_{e\in\mathcal{E}_h}|e|[\Phi_\mu(e)]^{-2}\|\nabla\times\boldsymbol{z}-(\widehat{\nabla\times\boldsymbol{z}})_{T_e}\|^2_{L_2(e)}\Big)^{1/2}\\ &\qquad\quad\times\Big(\sum_{e\in\mathcal{E}_h}\frac{[\Phi_\mu(e)]^2}{|e|}\|[\![\boldsymbol{n}\times(\boldsymbol{u}_h-\boldsymbol{u})]\!]\|^2_{L_2(e)}\Big)^{1/2} &(3.2.64)\\ &\quad\le Ch|\nabla\times\boldsymbol{z}|_{H^1(\Omega)}\|\boldsymbol{u}-\boldsymbol{u}_h\|_h\\ &\quad\le Ch\|\boldsymbol{u}-\boldsymbol{u}_h\|_{L_2(\Omega)}\|\boldsymbol{u}-\boldsymbol{u}_h\|_h.\end{aligned}$$

Similarly, we have the following bound on the third term on the right-hand side of (3.2.57).

$$\sum_{e\in\mathcal{E}_h^i}\int_e \gamma[\![\boldsymbol{n}\cdot\boldsymbol{u}_h]\!](\nabla\cdot\boldsymbol{z})ds \leq Ch\|\boldsymbol{u}-\boldsymbol{u}_h\|_{L_2(\Omega)}\|\boldsymbol{u}-\boldsymbol{u}_h\|_h \tag{3.2.65}$$

The estimate (3.2.51) can be obtained by combining (3.2.57) and (3.2.63)–(3.2.65). □

In the case where $\alpha > 0$, the following theorem is an immediate consequence of Lemma 3.3, Lemma 3.8, Lemma 3.10 and Lemma 3.12.

Theorem 3.13. *Let α be positive. The following discretization error estimates hold for the solution $\boldsymbol{u}_h$ of* (3.2.14)*:*

$$\begin{aligned}\|\boldsymbol{u}-\boldsymbol{u}_h\|_h \leq& C_\epsilon h^{1-\epsilon}\|\boldsymbol{f}\|_{L_2(\Omega)} \quad \textit{for any } \epsilon > 0,\\ \|\boldsymbol{u}-\boldsymbol{u}_h\|_{L_2(\Omega)} \leq& C_\epsilon h^{2-\epsilon}\|\boldsymbol{f}\|_{L_2(\Omega)} \quad \textit{for any } \epsilon > 0.\end{aligned}$$

In the case where $\alpha \leq 0$, we have the following theorem for the scheme (3.2.14). The proof, which is based on the approach of Schatz for indefinite problems [89], is identical with the proof of Theorem 4.5 in [39].

Theorem 3.14. *Assume $-\alpha \geq 0$ is not one of the eigenvalues $\lambda_{\gamma,j}$ defined by* (1.2.10)*. There exists a positive number h_* such that the discrete problem* (3.2.14) *is uniquely solvable for all $h \leq h_*$, in which case the following discretization error estimates are valid:*

$$\|\boldsymbol{u}-\boldsymbol{u}_h\|_h \leq C_\epsilon h^{1-\epsilon}\|\boldsymbol{f}\|_{L_2(\Omega)} \quad \textit{for any } \epsilon > 0, \tag{3.2.66}$$

$$\|\boldsymbol{u}-\boldsymbol{u}_h\|_{L_2(\Omega)} \leq C_\epsilon h^{2-\epsilon}\|\boldsymbol{f}\|_{L_2(\Omega)} \quad \textit{for any } \epsilon > 0. \tag{3.2.67}$$

Proof. Assuming $\boldsymbol{u}_h$ satisfies (3.2.14), it can be obtained from Lemma 3.4, Lemma 3.8, Lemma 3.10 and Lemma 3.12 that

$$\|\boldsymbol{u}-\boldsymbol{u}_h\|_h \leq C_\epsilon h^{1-\epsilon}(\|\boldsymbol{f}\|_{L_2(\Omega)} + \|\boldsymbol{u}-\boldsymbol{u}_h\|_h) \qquad \forall\ \epsilon > 0. \tag{3.2.68}$$

By choosing an $\epsilon_* > 0$, we deduce from (3.2.68) that for

$$h \le h_* = (\frac{1}{2C_{\epsilon_*}})^{1/(1-\epsilon_*)},$$

$$\begin{aligned}\|\boldsymbol{u}-\boldsymbol{u}_h\|_h \le& C_{\epsilon_*} h^{1-\epsilon_*}(\|\boldsymbol{f}\|_{L_2(\Omega)} + \|\boldsymbol{u}-\boldsymbol{u}_h\|_h) \\ \le& C_{\epsilon_*} h^{1-\epsilon_*}\|\boldsymbol{f}\|_{L_2(\Omega)} + C_{\epsilon_*} h_*^{1-\epsilon_*}\|\boldsymbol{u}-\boldsymbol{u}_h\|_h \\ \le& C_{\epsilon_*} h^{1-\epsilon_*}\|\boldsymbol{f}\|_{L_2(\Omega)} + \frac{1}{2}\|\boldsymbol{u}-\boldsymbol{u}_h\|_h,\end{aligned}$$

and hence

$$\|\boldsymbol{u}-\boldsymbol{u}_h\|_h \le 2C_{\epsilon_*} h^{1-\epsilon_*}\|\boldsymbol{f}\|_{L_2(\Omega)}. \tag{3.2.69}$$

Therefore, any solution $\boldsymbol{z}_h \in V_h$ of the homogeneous discrete problem

$$a_h(\boldsymbol{z}_h, \boldsymbol{v}) = 0 \qquad \forall\ \boldsymbol{v} \in V_h, \tag{3.2.70}$$

which corresponds to the special case where $\boldsymbol{f} = 0 = \boldsymbol{z}$, will satisfy the following special case of (3.2.69):

$$\|\boldsymbol{z}_h\|_h = 0.$$

Hence the only solution of (3.2.70) is the trivial solution and the discrete problem (3.2.14) is uniquely solvable for $h \le h_*$.

The energy error estimate (3.2.66) now follows from (3.2.68) and (3.2.69), and the L_2 error estimate (3.2.67) follows from Theorem 3.12 and (3.2.66). □

3.3 An Interior Penalty Method for the Curl-Curl and Grad-Div Problem

In this section we study an interior penalty version of the nonconforming scheme presented in Section 3.2 for the CCGD problem (1.2.9). By removing the weak continuity condition of the vector fields, the interior penalty method can be applied to meshes with hanging nodes. This method belongs to a growing family of finite element methods for problems posed on $H(\text{curl};\Omega) \cap H(\text{div};\Omega)$ [40, 37, 38, 46, 39].

The numerical scheme studied in this section is posed in [35] and the convergence analysis can also be found in that paper.

We take $\tilde{V}_h$ to be the space of (discontinuous) P_1 vector fields, i.e.,

$$\tilde{V}_h = \{\boldsymbol{v} \in [L_2(\Omega)]^2 : \boldsymbol{v}_T = \boldsymbol{v}\big|_T \in [P_1(T)]^2 \quad \forall\, T \in \mathcal{T}_h\}.$$

Since the vector fields in $\tilde{V}_h$ are (in general) discontinuous, their jumps across the edges of $\mathcal{T}_h$, which are defined by (3.2.12)–(3.2.13), play an important role in the interior penalty method.

We now define the discrete problem:

Find $\boldsymbol{u}_h \in \tilde{V}_h$ such that

$$\tilde{a}_h(\boldsymbol{u}_h, \boldsymbol{v}) = (\boldsymbol{f}, \boldsymbol{v}) \qquad \forall\, \boldsymbol{v} \in \tilde{V}_h, \tag{3.3.1}$$

where

$$\begin{aligned}
\tilde{a}_h(\boldsymbol{w}, \boldsymbol{v}) = (\nabla_h \times \boldsymbol{w}, \nabla_h \times \boldsymbol{v}) + \gamma(\nabla_h \cdot \boldsymbol{w}, \nabla_h \cdot \boldsymbol{v}) + \alpha(\boldsymbol{w}, \boldsymbol{v})& \\
+ \sum_{e \in \mathcal{E}_h} \frac{[\Phi_\mu(e)]^2}{|e|} \int_e [\![\boldsymbol{n} \times \boldsymbol{w}]\!]\, [\![\boldsymbol{n} \times \boldsymbol{v}]\!] ds& \\
+ \sum_{e \in \mathcal{E}_h^i} \frac{[\Phi_\mu(e)]^2}{|e|} \int_e [\![\boldsymbol{n} \cdot \boldsymbol{w}]\!][\![\boldsymbol{n} \cdot \boldsymbol{v}]\!] ds& \\
+ h^{-2} \sum_{e \in \mathcal{E}_h} \frac{1}{|e|} \int_e (\Pi_e^0 [\![\boldsymbol{n} \times \boldsymbol{w}]\!])\, (\Pi_e^0 [\![\boldsymbol{n} \times \boldsymbol{v}]\!]) ds& \\
+ h^{-2} \sum_{e \in \mathcal{E}_h^i} \frac{1}{|e|} \int_e (\Pi_e^0 [\![\boldsymbol{n} \cdot \boldsymbol{w}]\!])(\Pi_e^0 [\![\boldsymbol{n} \cdot \boldsymbol{v}]\!]) ds&,
\end{aligned} \tag{3.3.2}$$

$|e|$ denotes the length of the edge e, and Π_e^0 is the orthogonal projection from $L_2(e)$ to $P_0(e)$ (the space of constant functions on e). The edge weight $\Phi_\mu(e)$ in (3.3.2) is defined by (3.2.16).

We also use the Crouzeix-Raviart interpolation operator Π_T defined by (3.2.1) in the analysis of the interior penalty method.

The discretization error will be measured in both the L_2 norm and the mesh-dependent energy norm $\|\!|\cdot|\!\|_h$ defined by

$$
\begin{aligned}
&\|\!|\boldsymbol{v}|\!\|_h^2 \\
&= \|\nabla_h \times \boldsymbol{v}\|_{L_2(\Omega)}^2 + \gamma\|\nabla_h \cdot \boldsymbol{v}\|_{L_2(\Omega)}^2 + \|\boldsymbol{v}\|_{L_2(\Omega)}^2 \\
&\quad + \sum_{e\in\mathcal{E}_h} \frac{[\Phi_\mu(e)]^2}{|e|}\|[\![\boldsymbol{n}\times\boldsymbol{v}]\!]\|_{L_2(e)}^2 + \sum_{e\in\mathcal{E}_h^i} \frac{[\Phi_\mu(e)]^2}{|e|}\|[\![\boldsymbol{n}\cdot\boldsymbol{v}]\!]\|_{L_2(e)}^2 \\
&\quad + h^{-2}\big(\sum_{e\in\mathcal{E}_h}\frac{1}{|e|}\|\Pi_e^0[\![\boldsymbol{n}\times\boldsymbol{v}]\!]\|_{L_2(e)}^2 + \sum_{e\in\mathcal{E}_h^i}\frac{1}{|e|}\|\Pi_e^0[\![\boldsymbol{n}\cdot\boldsymbol{v}]\!]\|_{L_2(e)}^2\big).
\end{aligned}
\tag{3.3.3}
$$

It is easy to show that Lemma 3.3 and Lemma 3.4 hold for interior penalty method in terms of $\tilde{a}_h(\cdot,\cdot)$ and mesh-dependent energy norm $\|\!|\cdot|\!\|_h$. Lemma 3.6, Lemma 3.7 and Lemma 3.9 also hold with identical proofs.

The approximation property of $\tilde{V}_h$ is established by the following lemma.

Lemma 3.15. *Let* $\boldsymbol{u} \in H_0(\text{curl};\Omega)\cap H(\text{div};\Omega)$ *be the solution of* (1.2.9)*. It holds that*

$$
\inf_{\boldsymbol{v}\in\tilde{V}_h} \|\!|\boldsymbol{u}-\boldsymbol{v}|\!\|_h \le \|\!|\boldsymbol{u}-\Pi_h\boldsymbol{u}|\!\|_h < C_\epsilon h^{1-\epsilon}\|\boldsymbol{f}\|_{L_2(\Omega)} \tag{3.3.4}
$$

for any $\epsilon > 0$.

Proof. It follows from (3.2.1) that $\Pi_e^0[\![\boldsymbol{n}\times(\boldsymbol{u}-\Pi_h\boldsymbol{u})]\!] = 0$ for all $e \in \mathcal{E}_h$ and $\Pi_e^0[\![\boldsymbol{n}\cdot(\boldsymbol{u}-\Pi_h\boldsymbol{u})]\!] = 0$ for all $e \in \mathcal{E}_h^i$. Therefore we have

$$
\begin{aligned}
\|\!|\boldsymbol{u}-\Pi_h\boldsymbol{u}|\!\|_h^2 &= \|\nabla_h\times(\boldsymbol{u}-\Pi_h\boldsymbol{u})\|_{L_2(\Omega)}^2 \\
&\quad + \gamma\|\nabla_h\cdot(\boldsymbol{u}-\Pi_h\boldsymbol{u})\|_{L_2(\Omega)}^2 + \|\boldsymbol{u}-\Pi_h\boldsymbol{u}\|_{L_2(\Omega)}^2 \\
&\quad + \sum_{e\in\mathcal{E}_h}\frac{[\Phi_\mu(e)]^2}{|e|}\|[\![\boldsymbol{n}\times(\boldsymbol{u}-\Pi_h\boldsymbol{u})]\!]\|_{L_2(e)}^2 \\
&\quad + \sum_{e\in\mathcal{E}_h^i}\frac{[\Phi_\mu(e)]^2}{|e|}\|[\![\boldsymbol{n}\cdot(\boldsymbol{u}-\Pi_h\boldsymbol{u})]\!]\|_{L_2(e)}^2.
\end{aligned}
\tag{3.3.5}
$$

The rest of the proof is identical with the proof of Lemma 3.8.

□

The next lemma gives an optimal bound for the consistency error.

Lemma 3.16. *Let* $\boldsymbol{u} \in H_0(\text{curl};\Omega) \cap H(\text{div};\Omega)$ *be the solution of* (1.2.9) *and* $\boldsymbol{u}_h \in \tilde{V}_h$ *satisfy* (3.3.1). *We have*

$$\sup_{\boldsymbol{w}\in\tilde{V}_h\setminus\{0\}} \frac{\tilde{a}_h(\boldsymbol{u}-\boldsymbol{u}_h,\boldsymbol{w})}{\|\boldsymbol{w}\|_h} \lesssim h\|\boldsymbol{f}\|_{L_2(\Omega)}. \tag{3.3.6}$$

Proof. Let $\boldsymbol{w} \in \tilde{V}_h$ be arbitrary. The following analog of (3.2.46) holds for $\tilde{a}_h(\cdot,\cdot)$:

$$\begin{aligned}\tilde{a}_h(\boldsymbol{u},\boldsymbol{w}) = (\boldsymbol{f},\boldsymbol{w}) + \sum_{e\in\mathcal{E}_h}\int_e(\nabla\times\boldsymbol{u})[\![\boldsymbol{n}\times\boldsymbol{w}]\!]ds \\ + \sum_{e\in\mathcal{E}_h^i}\gamma\int_e(\nabla\cdot\boldsymbol{u})[\![\boldsymbol{n}\cdot\boldsymbol{w}]\!]ds.\end{aligned} \tag{3.3.7}$$

Subtracting (3.3.1) from (3.3.7), we have

$$\begin{aligned}\tilde{a}_h(\boldsymbol{u}-\boldsymbol{u}_h,\boldsymbol{w}) = \sum_{e\in\mathcal{E}_h}\int_e(\nabla\times\boldsymbol{u})[\![\boldsymbol{n}\times\boldsymbol{w}]\!]ds \\ + \sum_{e\in\mathcal{E}_h^i}\gamma\int_e(\nabla\cdot\boldsymbol{u})[\![\boldsymbol{n}\cdot\boldsymbol{w}]\!]ds.\end{aligned} \tag{3.3.8}$$

Following the notation introduced in (3.2.48), we can rewrite the first term on the right-hand side of (3.3.8) as

$$\begin{aligned}&\sum_{e\in\mathcal{E}_h}\int_e(\nabla\times\boldsymbol{u})[\![\boldsymbol{n}\times\boldsymbol{w}]\!]ds \\ &\quad= \sum_{e\in\mathcal{E}_h}\int_e(\nabla\times\boldsymbol{u}-(\widehat{\nabla\times\boldsymbol{u}})_{T_e})[\![\boldsymbol{n}\times\boldsymbol{w}]\!]ds \\ &\qquad+ \sum_{e\in\mathcal{E}_h}\int_e(\widehat{\nabla\times\boldsymbol{u}})_{T_e}(\Pi_e^0[\![\boldsymbol{n}\times\boldsymbol{w}]\!])ds.\end{aligned} \tag{3.3.9}$$

It follows from (2.2.17), (3.3.3), Lemma 3.9 and the Cauchy-Schwarz inequality that the first term on the right-hand side of (3.3.9) satisfies

$$\begin{aligned}
&\sum_{e\in\mathcal{E}_h}\int_e(\nabla\times\boldsymbol{u}-(\widehat{\nabla\times\boldsymbol{u}})_{T_e})[\![\boldsymbol{n}\times\boldsymbol{w}]\!]ds \\
&\qquad\le\Big(\sum_{e\in\mathcal{E}_h}|e|[\Phi_\mu(e)]^{-2}\|\nabla\times\boldsymbol{u}-(\widehat{\nabla\times\boldsymbol{u}})\|^2_{L_2(e)}\Big)^{1/2} \qquad (3.3.10)\\
&\qquad\qquad\times\Big(\sum_{e\in\mathcal{E}_h}|e|^{-1}[\Phi_\mu(e)]^2\|\boldsymbol{n}\times\boldsymbol{w}\|^2_{L_2(e)}\Big)^{1/2}\\
&\qquad\le Ch\|\boldsymbol{f}\|_{L_2(\Omega)}|\!|\!|\boldsymbol{w}|\!|\!|_h.
\end{aligned}$$

For the second term on the right-hand side of (3.3.9), by using the (2.2.17), (3.3.3) and Cauchy-Schwarz inequality, we find

$$\begin{aligned}
&\sum_{e\in\mathcal{E}_h}\int_e(\widehat{\nabla\times\boldsymbol{u}})_{T_e}(\Pi^0_h[\![\boldsymbol{n}\times\boldsymbol{w}]\!])ds\\
&\qquad\le\sum_{e\in\mathcal{E}_h}\big(|e|^{1/2}\|(\widehat{\nabla\times\boldsymbol{u}})_{T_e}\|_{L_2(e)}\big)\big(|e|^{-1/2}\|\Pi^0_e[\![\boldsymbol{n}\times\boldsymbol{w}]\!]\|_{L_2(e)}\big)\\
&\qquad\le Ch\big(\sum_{e\in\mathcal{E}_h}\|(\widehat{\nabla\times\boldsymbol{u}})_{T_e}\|^2_{L_2(T_e)}\big)^{1/2} \qquad (3.3.11)\\
&\qquad\qquad\times\big(h^{-2}\sum_{e\in\mathcal{E}_h}\frac{1}{|e|}\|\Pi^0_e[\![\boldsymbol{n}\times\boldsymbol{w}]\!]\|^2_{L_2(e)}\big)^{1/2}\\
&\qquad\le Ch\|\nabla\times\boldsymbol{u}\|_{L_2(\Omega)}|\!|\!|\boldsymbol{w}|\!|\!|_h\le Ch\|\boldsymbol{f}\|_{L_2(\Omega)}|\!|\!|\boldsymbol{w}|\!|\!|_h.
\end{aligned}$$

Here we have used the simple fact that, if e is an edge of a triangle T,

$$|e|\|q\|^2_{L_2(e)}\le C\|q\|^2_{L_2(T)}\quad\text{for any constant function } q, \qquad (3.3.12)$$

where the positive constant C depends only on the shape of T.

Combining (3.3.9)–(3.3.11), we have

$$\sum_{e\in\mathcal{E}_h}\int_e(\nabla\times\boldsymbol{u})[\![\boldsymbol{n}\cdot\boldsymbol{w}]\!]ds\le Ch\|\boldsymbol{f}\|_{L_2(\Omega)}|\!|\!|\boldsymbol{w}|\!|\!|_h, \qquad (3.3.13)$$

and similarly,

$$\sum_{e\in\mathcal{E}_h^i}\int_e(\nabla\cdot\boldsymbol{u})[\![\boldsymbol{n}\cdot\boldsymbol{w}]\!]ds \le Ch\|\boldsymbol{f}\|_{L_2(\Omega)}|\!|\!|\boldsymbol{w}|\!|\!|_h. \tag{3.3.14}$$

The estimate (3.3.6) follows from (3.3.8), (3.3.13) and (3.3.14). □

The next lemma gives an L_2 error estimate under the assumption that the discrete problem (3.3.1) has a solution.

Lemma 3.17. *Let* $\boldsymbol{u} \in H_0(\text{curl};\Omega)\cap H(\text{div};\Omega)$ *be the solution of* (1.2.9) *and* $\boldsymbol{u}_h \in \tilde{V}_h$ *satisfy* (3.3.1). *We have*

$$\|\boldsymbol{u}-\boldsymbol{u}_h\|_{L_2(\Omega)} \le C_\epsilon\big(h^{2-\epsilon}\|\boldsymbol{f}\|_{L_2(\Omega)} + h^{1-\epsilon}|\!|\!|\boldsymbol{u}-\boldsymbol{u}_h|\!|\!|_h\big) \tag{3.3.15}$$

for any $\epsilon > 0$.

Proof. The proof is based on a duality argument.

Let $\boldsymbol{z} \in H_0(\text{curl};\Omega)\cap H(\text{div};\Omega)$ satisfy

$$(\nabla\times\boldsymbol{v},\nabla\times\boldsymbol{z}) + \gamma(\nabla\cdot\boldsymbol{v},\nabla\cdot\boldsymbol{z}) + \alpha(\boldsymbol{v},\boldsymbol{z}) = (\boldsymbol{v},(\boldsymbol{u}-\boldsymbol{u}_h)) \tag{3.3.16}$$

for all $\boldsymbol{v} \in H_0(\text{curl};\Omega)\cap H(\text{div};\Omega)$. The following analog of (3.2.57) holds:

$$\begin{aligned}\|\boldsymbol{u}-\boldsymbol{u}_h\|^2_{L_2(\Omega)} &= (\boldsymbol{u},\boldsymbol{u}-\boldsymbol{u}_h) - (\boldsymbol{u}_h,\boldsymbol{u}-\boldsymbol{u}_h)\\ &= \tilde{a}_h(\boldsymbol{u}-\boldsymbol{u}_h,\boldsymbol{z}) + \sum_{e\in\mathcal{E}_h}\int_e[\![\boldsymbol{n}\times\boldsymbol{u}_h]\!](\nabla\times\boldsymbol{z})ds\\ &\quad + \sum_{e\in\mathcal{E}_h^i}\gamma\int_e[\![\boldsymbol{n}\cdot\boldsymbol{u}_h]\!](\nabla\cdot\boldsymbol{z})ds,\end{aligned} \tag{3.3.17}$$

and we will estimate the three terms on the right-hand side of (3.3.17) separately.

Using (3.3.8) and the fact that $\Pi_e^0[\![\boldsymbol{n}\times(\Pi_h\boldsymbol{z})]\!]$ (resp. $\Pi_e^0[\![\boldsymbol{n}\cdot(\Pi_h\boldsymbol{z})]\!]$) vanishes for all $e\in\mathcal{E}_h$ (resp. $e\in\mathcal{E}_h^i$), we can rewrite the first term as

$$\begin{aligned}\tilde{a}_h(\boldsymbol{u}-\boldsymbol{u}_h,\boldsymbol{z}) &= \tilde{a}_h(\boldsymbol{u}-\boldsymbol{u}_h,\boldsymbol{z}-\Pi_h\boldsymbol{z})+\tilde{a}_h(\boldsymbol{u}-\boldsymbol{u}_h,\Pi_h\boldsymbol{z})\\ &= \tilde{a}_h(\boldsymbol{u}-\boldsymbol{u}_h,\boldsymbol{z}-\Pi_h\boldsymbol{z})\\ &\quad+\sum_{e\in\mathcal{E}_h}\int_e(\nabla\times\boldsymbol{u}-(\widehat{\nabla\times\boldsymbol{u}})_{T_e})[\![\boldsymbol{n}\times(\Pi_h\boldsymbol{z})]\!]ds\\ &\quad+\sum_{e\in\mathcal{E}_h^i}\int_e\gamma(\nabla\cdot\boldsymbol{u}-(\widehat{\nabla\cdot\boldsymbol{u}})_{T_e})[\![\boldsymbol{n}\cdot(\Pi_h\boldsymbol{z})]\!]ds.\end{aligned}$$

Then the similar arguments for (3.2.63) yield

$$\begin{aligned}&\tilde{a}_h(\boldsymbol{u}-\boldsymbol{u}_h,\boldsymbol{z})\\ &\quad\le C_\epsilon(h^{2-\epsilon}\|\boldsymbol{f}\|_{L_2(\Omega)}+h^{1-\epsilon}|\!|\!|\boldsymbol{u}-\boldsymbol{u}_h|\!|\!|_h)\|\boldsymbol{u}-\boldsymbol{u}_h\|_{L_2(\Omega)}.\end{aligned}\tag{3.3.18}$$

We now consider the second term on the right-hand side of (3.3.17). First we write

$$\begin{aligned}&\sum_{e\in\mathcal{E}_h}\int_e[\![\boldsymbol{n}\times\boldsymbol{u}_h]\!](\nabla\times\boldsymbol{z})ds\\ &\quad=\sum_{e\in\mathcal{E}_h}\int_e[\![\boldsymbol{n}\times\boldsymbol{u}_h]\!](\nabla\times\boldsymbol{z}-(\widehat{\nabla\times\boldsymbol{z}})_{T_e})ds\\ &\qquad+\sum_{e\in\mathcal{E}_h}\int_e(\Pi_e^0[\![\boldsymbol{n}\times\boldsymbol{u}_h]\!])(\widehat{\nabla\times\boldsymbol{z}})_{T_e}ds.\end{aligned}\tag{3.3.19}$$

The first term on the right-hand side of (3.3.19) satisfies the estimate below, which follows from Lemma 3.9, (3.2.54), (3.3.3), and the Cauchy-Schwarz inequality:

$$\begin{aligned}&\sum_{e\in\mathcal{E}_h}\int_e[\![\boldsymbol{n}\times\boldsymbol{u}_h]\!](\nabla\times\boldsymbol{z}-(\widehat{\nabla\times\boldsymbol{z}})_{T_e})ds\\ &\qquad\le Ch\|\boldsymbol{u}-\boldsymbol{u}_h\|_{L_2(\Omega)}|\!|\!|\boldsymbol{u}-\boldsymbol{u}_h|\!|\!|_h.\end{aligned}\tag{3.3.20}$$

On the other hand, as in the derivation of (3.3.11), we obtain by the Cauchy–Schwarz inequality, (3.2.54), (3.3.3) and (3.3.12),

$$
\begin{aligned}
\sum_{e\in\mathcal{E}_h}\int_e (\Pi_e^0[\![\boldsymbol{n}\times\boldsymbol{u}_h]\!])(\widehat{\nabla\times\boldsymbol{z}})_{T_e}\,ds \\
&= \sum_{e\in\mathcal{E}_h}\int_e (\Pi_e^0[\![\boldsymbol{n}\times(\boldsymbol{u}_h-\boldsymbol{u})]\!])(\widehat{\nabla\times\boldsymbol{z}})_{T_e}\,ds \qquad (3.3.21)\\
&\le Ch|\!|\!|\boldsymbol{u}-\boldsymbol{u}_h|\!|\!|_h\|\nabla\times\boldsymbol{z}\|_{L_2(\Omega)}\\
&\le Ch|\!|\!|\boldsymbol{u}-\boldsymbol{u}_h|\!|\!|_h\|\boldsymbol{u}-\boldsymbol{u}_h\|_{L_2(\Omega)}.
\end{aligned}
$$

Combining (3.3.19)–(3.3.21), we have

$$
\sum_{e\in\mathcal{E}_h}\int_e [\![\boldsymbol{n}\times\boldsymbol{u}_h]\!](\nabla\times\boldsymbol{z})ds \le Ch\|\boldsymbol{u}-\boldsymbol{u}_h\|_{L_2(\Omega)}|\!|\!|\boldsymbol{u}-\boldsymbol{u}_h|\!|\!|_h. \qquad (3.3.22)
$$

Similarly, we have the following bound on the third term on the right-hand side of (3.3.17):

$$
\sum_{e\in\mathcal{E}_h^i}\int_e \gamma[\![\boldsymbol{n}\cdot\boldsymbol{u}_h]\!](\nabla\cdot\boldsymbol{z})ds \le Ch\|\boldsymbol{u}-\boldsymbol{u}_h\|_{L_2(\Omega)}|\!|\!|\boldsymbol{u}-\boldsymbol{u}_h|\!|\!|_h. \qquad (3.3.23)
$$

The estimate (3.3.15) follows from (3.3.17), (3.3.18), (3.3.22) and (3.3.23).

□

The following two theorems provide the discretization error estimates for scheme (3.3.1) in both energy norm and L_2 norm. The arguments are identical to those in the proofs of Theorem 3.13 and Theorem 3.14.

Theorem 3.18. *Let α be positive. The following discretization error estimates hold for the solution $\boldsymbol{u}_h$ of* (3.3.1)*:*

$$
\begin{aligned}
|\!|\!|\boldsymbol{u}-\boldsymbol{u}_h|\!|\!|_h &\le C_\epsilon h^{1-\epsilon}\|\boldsymbol{f}\|_{L_2(\Omega)} \quad \text{for any } \epsilon>0,\\
\|\boldsymbol{u}-\boldsymbol{u}_h\|_{L_2(\Omega)} &\le C_\epsilon h^{2-\epsilon}\|\boldsymbol{f}\|_{L_2(\Omega)} \quad \text{for any } \epsilon>0.
\end{aligned}
$$

Theorem 3.19. *Assume $-\alpha\ge 0$ is not one of the eigenvalues $\lambda_{\gamma,j}$ defined by* (1.2.10). *There exists a positive number h_* such that the discrete problem* (3.3.1) *is uniquely solvable for all $h \leq h_*$, in which case the following discretization error estimates are valid:*

$$\begin{aligned} \|\boldsymbol{u} - \boldsymbol{u}_h\|_h &\leq C_\epsilon h^{1-\epsilon} \|\boldsymbol{f}\|_{L_2(\Omega)} \quad \textit{for any } \epsilon > 0, \\ \|\boldsymbol{u} - \boldsymbol{u}_h\|_{L_2(\Omega)} &\leq C_\epsilon h^{2-\epsilon} \|\boldsymbol{f}\|_{L_2(\Omega)} \quad \textit{for any } \epsilon > 0. \end{aligned}$$

3.4 Numerical Results

In this section we report the results of a series of numerical experiments that confirm the theoretical results obtained in Section 3.2 and Section 3.3. We take γ to be 1 in all the experiments.

In the first experiment we examine the convergence behavior of our numerical scheme (3.2.14) on the square domain $(0, 0.5)^2$ with uniform meshes (Figure 3.1, left), where the exact solution $\boldsymbol{u}$ is given by

$$\boldsymbol{u} = \begin{bmatrix} \left(\frac{x^3}{3} - \frac{x^2}{4}\right)(y^2 - 0.5y)\sin(ky) \\ \left(\frac{y^3}{3} - \frac{y^2}{4}\right)(x^2 - 0.5x)\cos(kx) \end{bmatrix}. \tag{3.4.1}$$

The results are tabulated in Table 3.1 for $\alpha = 1$, 0 and -1 and they agree with the error estimates in Theorem 3.13 and Theorem 3.14. That is, the scheme is second order accurate in the L_2 norm and first order accurate in the energy norm.

In the second experiment we check the behavior of the scheme (3.3.1) on unit square $(0, 1)^2$ using nonconforming meshes with hanging nodes depicted in Figure 3.1 (right), where the exact solution $\boldsymbol{u}$ is given by

$$\boldsymbol{u} = \begin{bmatrix} y(1-y) \\ x(1-x) \end{bmatrix}. \tag{3.4.2}$$

Table 3.2 shows that the scheme (3.3.1) behaves as predicted in Theorem 3.18 and Theorem 3.19.

TABLE 3.1. Convergence of the scheme (3.2.14) on the square domain $(0, 0.5)^2$ with uniform meshes and the exact solution given by (3.4.1)

h	$\frac{\|\boldsymbol{u}-\boldsymbol{u}_h\|_{L_2(\Omega)}}{\|\boldsymbol{u}\|_{L_2(\Omega)}}$	order	$\frac{\|\boldsymbol{u}-\boldsymbol{u}_h\|_h}{\|\boldsymbol{u}\|_h}$	order
		$\alpha = 1$		
1/10	5.49E−02	–	3.23E−01	–
1/20	1.20E−02	2.19	1.59E−01	1.02
1/40	2.83E−03	2.09	7.92E−02	1.01
1/80	6.87E−04	2.04	3.94E−02	1.01
		$\alpha = 0$		
1/10	6.45E−02	–	3.46E−01	–
1/20	1.38E−02	2.23	1.70E−01	1.03
1/40	3.20E−03	2.11	8.37E−02	1.01
1/80	7.73E−04	2.05	4.17E−02	1.01
		$\alpha = -1$		
1/10	5.59E−02	–	3.24E−01	–
1/20	1.21E−02	2.20	1.59E−01	1.02
1/40	2.86E−03	2.09	7.92E−02	1.01
1/80	6.94E−04	2.04	3.94E−02	1.01

TABLE 3.2. Convergence of the scheme (3.3.1) on the square domain $(0, 1)^2$ with nonconforming meshes and the exact solution given by (3.4.2)

h	$\frac{\|\boldsymbol{u}-\boldsymbol{u}_h\|_{L_2(\Omega)}}{\|\boldsymbol{u}\|_{L_2(\Omega)}}$	order	$\frac{\|\!\|\boldsymbol{u}-\boldsymbol{u}_h\|\!\|_h}{\|\!\|\boldsymbol{u}\|\!\|_h}$	order
		$\alpha = 1$		
1/8	8.82E−02	1.80	2.98E−01	0.90
1/16	2.27E−02	1.96	1.51E−01	0.98
1/32	5.69E−03	2.00	7.59E−02	1.00
1/64	1.42E−03	2.00	3.81E−02	0.99
		$\alpha = 0$		
1/8	1.28E−01	1.93	3.59E−01	0.97
1/16	3.21E−02	2.00	1.80E−01	1.00
1/32	8.00E−03	2.00	8.99E−02	1.00
1/64	1.96E−03	2.03	4.03E−02	1.15
		$\alpha = -1$		
1/8	2.36E−01	2.38	4.85E−01	1.20
1/16	5.52E−02	2.10	2.35E−01	1.01
1/32	1.35E−02	2.03	1.16E−01	1.01
1/64	3.31E−03	2.03	5.80E−02	1.00

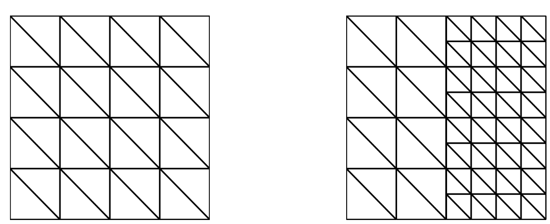

FIGURE 3.1. Conforming uniform meshes (left) and nonconforming meshes (right) on the square domain

The goal of the third experiment is to demonstrate the convergence behavior of scheme (3.2.14) on the L-shaped domain $(-0.5, 0.5)^2 \setminus [0, 0.5]^2$. The exact solution is chosen to be

$$\boldsymbol{u} = \nabla \times \Big(r^{2/3} \cos\Big(\frac{2}{3}\theta - \frac{\pi}{3}\Big)\phi(r/0.5)\Big), \tag{3.4.3}$$

where (r, θ) are the polar coordinates at the origin and the cut-off function is given by

$$\phi(r) = \begin{cases} 1 & r \leq 0.25 \\ -16(r-0.75)^3 & \\ \quad \times\big[5 + 15(r-0.75) + 12(r-0.75)^2\big] & 0.25 \leq r \leq 0.75 \\ 0 & r \geq 0.75 \end{cases}.$$

The meshes are graded around the re-entrant corner (0,0) using the refinement procedure described in Section 2.3 with the grading parameter 1/3. The first three levels of graded meshes are depicted in Figure 3.2. The results are tabulated in Table 3.3 and they agree with the error estimates for our scheme.

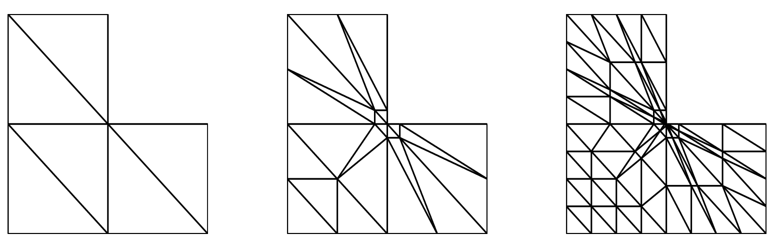

FIGURE 3.2. Graded meshes on the L-shaped domain

In the last set of experiment, we demonstrate the convergence behavior of the scheme (3.3.1) on the L-shaped domain with the graded meshes used in the third experiment. The right-hand side function is chosen to be

$$\boldsymbol{f} = \begin{bmatrix} 1 \\ 1 \end{bmatrix}. \tag{3.4.4}$$

TABLE 3.3. Convergence of the scheme (3.2.14) on the L-shaped domain with graded meshes and the exact solution given by (3.4.3)

h	$\frac{\\|\boldsymbol{u}-\boldsymbol{u}_h\\|_{L_2(\Omega)}}{\\|\boldsymbol{u}\\|_{L_2(\Omega)}}$	order	$\frac{\\|\boldsymbol{u}-\boldsymbol{u}_h\\|_h}{\\|\boldsymbol{u}\\|_h}$	order
$\alpha = 1$				
1/4	7.57E+01	–	1.01E+01	–
1/8	2.82E+01	1.43	6.07E−00	0.74
1/16	3.23E−00	3.13	2.21E−00	1.46
1/32	6.84E−01	2.23	1.10E−00	1.00
1/64	1.67E−01	2.04	5.54E−01	1.00
$\alpha = 0$				
1/4	9.93E+01	–	1.32E+01	–
1/8	3.24E+01	1.62	6.70E−00	0.97
1/16	3.29E−00	3.30	2.24E−00	1.58
1/32	6.91E−01	2.25	1.11E−00	1.01
1/64	1.71E−01	2.01	5.54E−01	1.00
$\alpha = -1$				
1/4	1.46E+02	–	1.90E+01	–
1/8	3.85E+01	1.92	7.58E−00	1.32
1/16	3.37E−00	3.51	2.25E−00	1.75
1/32	6.99E−01	2.27	1.11E−00	1.03
1/64	1.77E−01	1.98	5.54E−01	1.00

The results are tabulated in Table 3.4 and they demonstrate that the scheme is second order accurate in the L_2 norm and first order accurate in the energy norm.

TABLE 3.4. Convergence of the scheme (3.3.1) on the L-shaped domain with graded meshes and right-hand side function given by (3.4.4)

h	$\frac{\\|\boldsymbol{u}-\boldsymbol{u}_h\\|_{L_2(\Omega)}}{\\|\boldsymbol{u}\\|_{L_2(\Omega)}}$	order	$\frac{\\|\\|\boldsymbol{u}-\boldsymbol{u}_h\\|\\|_h}{\\|\\|\boldsymbol{u}\\|\\|_h}$	order
$\alpha = 1$				
1/16	4.77E−01	1.67	1.02E+00	1.13
1/32	1.28E−01	1.89	4.65E−01	1.13
1/64	3.23E−02	1.99	2.20E−01	1.08
1/128	8.03E−03	2.01	1.07E−01	1.04
$\alpha = 0$				
1/16	6.21E−01	2.11	1.14E+00	1.37
1/32	1.52E−01	2.03	5.01E−01	1.19
1/64	3.74E−02	2.02	2.34E−01	1.10
1/128	9.22E−03	2.02	1.13E−01	1.05
$\alpha = -1$				
1/16	9.07E−01	3.45	1.46E+00	1.48
1/32	1.90E−01	2.26	5.47E−01	1.37
1/64	4.49E−02	2.08	2.55E−01	1.15
1/128	1.10E−02	2.04	1.22E−01	1.06

Chapter 4

Multigrid Methods for Symmetric Discontinuous Galerkin Methods on Graded Meshes

In this chapter we study the multigrid methods for a class of symmetric discontinuous Galerkin methods presented in Section 2.4. We establish the uniform convergence of W-cycle, V-cycle and F-cycle multigrid algorithms for the resulting discrete problems on graded meshes. Results of numerical experiments will be reported in Section 4.3.

4.1 Convergence of the W-Cycle Algorithm

In this section we study the convergence of the W-cycle algorithm for the discrete problem $A_k u_k = f_k$ resulting from DG methods (2.5.1) on graded meshes, where $A_k : V_k \longrightarrow V_k'$ and $f_k \in V_k'$ are defined by (2.5.7) and (2.5.8). Recall that the error propagation operator $E_k : V_k \longrightarrow V_k$ for the k-th level W-cycle algorithm has the following recursive relation:

$$E_k = R_k^{m_2}(Id_k - I_{k-1}^k P_k^{k-1} + I_{k-1}^k E_{k-1}^2 P_k^{k-1}) R_k^{m_1},$$

where Id_k is the identity operator on V_k, $R_k : V_k \longrightarrow V_k$, and $P_k^{k-1} : V_{k-1} \longrightarrow V_k$ are defined by (2.5.19) and (2.5.21).

We will follow the approach of [17, 99] in the analysis below. The results are also presented in [36, 34].

The keys to the convergence analysis of the W-cycle algorithm are the estimates for the operators R_k^m (smoothing property) and $Id_k - I_{k-1}^k P_k^{k-1}$ (approximation property) in terms of mesh-dependent norms.

For $j = 0, 1, 2$ and $k \geq 0$, let the mesh-dependent norms $\|\!|v|\!\|_{j,k}$ be defined by

$$\|\!|v|\!\|_{j,k} = \sqrt{\langle B_k (B_k^{-1} A_k)^j v, v \rangle} \qquad \forall\, v \in V_k,\ k \geq 0. \tag{4.1.1}$$

In particular, we have

$$\|v\|_{0,k}^2 = \langle B_k v, v\rangle \qquad \forall\, v \in V_k, \tag{4.1.2}$$

$$\|v\|_{1,k}^2 = \langle A_k v, v\rangle = a_k(v,v) \qquad \forall\, v \in V_k, \tag{4.1.3}$$

where the operator $B_k : V_k \longrightarrow V_k'$ is defined by (2.5.9) in terms of canonical bilinear form $\langle \cdot, \cdot \rangle$ on $V_k' \times V_k$. Also the Cauchy-Schwarz inequality implies that

$$\|v\|_{2,k} = \max_{w \in V_k \setminus \{0\}} \frac{\langle A_k v, w\rangle}{\|w\|_{0,k}} \qquad \forall\, v \in V_k. \tag{4.1.4}$$

It follows from (2.5.14) and (4.1.4) that

$$\|v\|_{2,k} \le C h_k^{-1} \|v\|_{1,k} \qquad \forall\, v \in V_k. \tag{4.1.5}$$

There is an important connection between the mesh-dependent norm $\|\cdot\|_{0,k}$ and the norm $\|\cdot\|_{L_{2,-\mu}(\Omega)}$ defined by (2.4.46). From (2.2.33), (2.3.1), (2.3.2), (2.5.10) and (4.1.2), we have

$$\|v\|_{0,k}^2 \approx \|v\|_{L_{2,-\mu}(\Omega)}^2 \qquad \forall\, v \in V_k, \tag{4.1.6}$$

where the positive constants in the equivalence depend only on the shape regularity of $\mathcal{T}_k$.

The smoothing properties in the following lemma are simple consequences of (2.5.14), (2.5.19) and (4.1.1). Their proofs are standard [71, 43].

Lemma 4.1. *There exists a positive constant C independent of k such that*

$$\|R_k v\|_{j,k} \le \|v\|_{j,k} \qquad \forall\, v \in V_k,\ k \ge 1,\ j = 0,1,2, \tag{4.1.7}$$

$$\|R_k^m v\|_{j+1,k} \le C h_k^{-1}(1+m)^{-1/2} \|v\|_{j,k} \qquad \forall\, v \in V_k,\ k \ge 1,\ j = 0,1. \tag{4.1.8}$$

Note that, for $z \in V_{k-1} \cap H_0^1(\Omega)$, we have

$$a_{k-1}(P_k^{k-1} I_{k-1}^k z, v) = a_k(I_{k-1}^k z, I_{k-1}^k v) = a_{k-1}(z, v) \qquad \forall\, v \in V_{k-1},$$

which implies

$$P_k^{k-1} I_{k-1}^k z = z \qquad \forall\, z \in V_{k-1} \cap H_0^1(\Omega).$$

Hence

$$\begin{aligned} a_k(I_{k-1}^k z, (Id_k - I_{k-1}^k P_k^{k-1})v) &= a_k(I_{k-1}^k z, v) - a_k(P_k^{k-1} I_{k-1}^k z, P_k^{k-1} v) \\ &= a_k(z, P_k^{k-1} v) - a_k(z, P_k^{k-1} v) \qquad (4.1.9) \\ &= 0 \qquad\qquad \forall\, z \in V_{k-1} \cap H_0^1(\Omega),\ v \in V_k. \end{aligned}$$

The following lemma gives a preliminary approximation property.

Lemma 4.2. *There exists a positive constant C independent of k such that*

$$\|(Id_k - I_{k-1}^k P_k^{k-1})v\|_{0,k} \le C h_k \|(Id_k - I_{k-1}^k P_k^{k-1})v\|_{1,k} \qquad \forall\, v \in V_k,\ k \ge 1. \quad (4.1.10)$$

Proof. We will prove (4.1.10) by a duality argument.

Let $v \in V_k$ be arbitrary and $\chi = \phi_\mu^{-2}(Id_k - I_{k-1}^k P_k^{k-1})v$, where the weight function ϕ_μ is defined by (2.2.33). From (2.2.34) and (2.4.46), it is easy to see that

$$\|\chi\|_{L_{2,\mu}(\Omega)} = \|(Id_k - I_{k-1}^k P_k^{k-1})v\|_{L_{2,-\mu}(\Omega)}. \quad (4.1.11)$$

Let $\xi \in H_0^1(\Omega)$ satisfy

$$\int_\Omega \nabla \xi \cdot \nabla v\, dx = \int_\Omega \chi v\, dx \qquad \forall\, v \in H_0^1(\Omega).$$

It follows from the consistency of the DG methods that

$$a_k(\xi, v) = \int_\Omega \chi v\, dx \qquad \forall\, v \in V_k. \quad (4.1.12)$$

Furthermore, by (2.3.7), (2.5.4) (applied to ξ), (2.5.5) and (4.1.11), we have

$$\begin{aligned} \|\xi - I_{k-1}^k \Pi_{k-1} \xi\|_k &\le C \|\xi - \Pi_{k-1}\xi\|_{k-1} \qquad (4.1.13) \\ &\le C h_{k-1} \|\chi\|_{L_{2,\mu}(\Omega)} \le C h_k \|(Id_k - I_{k-1}^k P_k^{k-1})v\|_{L_{2,-\mu}(\Omega)}. \end{aligned}$$

Combining (2.4.33), (2.4.46), (2.5.3), (2.5.10), (4.1.2), (4.1.9), (4.1.12) and (4.1.13), we find

$$\begin{aligned}
\|\!|(Id_k - I_{k-1}^k P_k^{k-1})v\|\!|_{0,k}^2 &= \langle B_k(Id_k - I_{k-1}^k P_k^{k-1})v, (Id_k - I_{k-1}^k P_k^{k-1})v\rangle \\
&\approx \|(Id_k - I_{k-1}^k P_k^{k-1})v\|_{L_{2,-\mu}(\Omega)}^2 \\
&= \int_\Omega \phi_\mu^{-2}[(Id_k - I_{k-1}^k P_k^{k-1})v]^2 dx \\
&= \int_\Omega \chi(Id_k - I_{k-1}^k P_k^{k-1})v\, dx \\
&= a_k(\xi, (Id_k - I_{k-1}^k P_k^{k-1})v) \qquad (4.1.14) \\
&= a_k(\xi - I_{k-1}^k \Pi_{k-1}\xi, (Id_k - I_{k-1}^k P_k^{k-1})v) \\
&\le C\|\xi - I_{k-1}^k \Pi_{k-1}\xi\|_k \|(Id_k - I_{k-1}^k P_k^{k-1})v\|_k \\
&\approx Ch_k \|(Id_k - I_{k-1}^k P_k^{k-1})v\|_{L_{2,-\mu}(\Omega)} \|\!|(Id_k - I_{k-1}^k P_k^{k-1})v\|\!|_{1,k} \\
&\approx Ch_k \|\!|(Id_k - I_{k-1}^k P_k^{k-1})v\|\!|_{0,k} \|\!|(Id_k - I_{k-1}^k P_k^{k-1})v\|\!|_{1,k},
\end{aligned}$$

which implies (4.1.10). □

The approximation property for the convergence analysis is provided by the next lemma.

Lemma 4.3. *There exists a positive constant C independent of k such that*

$$\|\!|(Id_k - I_{k-1}^k P_k^{k-1})v\|\!|_{0,k} \le Ch_k^2 \|\!|v\|\!|_{2,k} \qquad \forall\, v \in V_k,\ k \ge 1. \tag{4.1.15}$$

Proof. From (4.1.3) and duality, we have

$$\|\!|(Id_k - I_{k-1}^k P_k^{k-1})v\|\!|_{1,k} = \sup_{w \in V_k \setminus \{0\}} \frac{a_k((Id_k - I_{k-1}^k P_k^{k-1})v, w)}{\|\!|w\|\!|_{1,k}}. \tag{4.1.16}$$

Combining (2.5.21), (4.1.4) and (4.1.10), we obtain

$$\begin{aligned}
a_k((Id_k - I_{k-1}^k P_k^{k-1})v, w) &= a_k(v, (Id_k - I_{k-1}^k P_k^{k-1})w) \\
&\le \|\!|v\|\!|_{2,k} \|\!|(Id_k - I_{k-1}^k P_k^{k-1})w\|\!|_{0,k} \le Ch_k \|\!|v\|\!|_{2,k} \|\!|w\|\!|_{1,k},
\end{aligned}$$

which together with (4.1.16) implies

$$\|(Id_k - I_{k-1}^k P_k^{k-1})v\|_{1,k} \le Ch_k \|v\|_{2,k} \qquad \forall\, v \in V_k,\ k \ge 1. \tag{4.1.17}$$

The estimate (4.1.15) follows from (4.1.10) and (4.1.17). □

Combining (4.1.8) and (4.1.15), we immediately have the following theorem on the two-grid algorithm.

Theorem 4.4. *Let $\tilde{E}_k$ be the error propagation operator for the two-grid algorithm defined by* (2.5.28)*. There exists a positive constant C_{TG} independent of k such that*

$$\|\tilde{E}_k v\|_{1,k} \le C_{TG}[(1+m_1)(1+m_2)]^{-1/2}\|v\|_{1,k} \quad \forall\, v \in V_k,\ k \ge 1. \tag{4.1.18}$$

Proof.

$$\begin{aligned}
\|\tilde{E}_k v\|_{1,k} &= \|R_k^{m_2}(Id_k - I_{k-1}^k P_k^{k-1})R_k^{m_1} v\|_{1,k} \\
&\le C(1+m_2)^{-1/2} h_k^{-1} \|(Id_k - I_{k-1}^k P_k^{k-1})R_k^{m_1} v\|_{0,k} \\
&\le C(1+m_2)^{-1/2} h_k \|R_k^{m_1} v\|_{2,k} \\
&\le C(1+m_2)^{-1/2}(1+m_1)^{-1/2}\|v\|_{1,k}.
\end{aligned}$$

□

To go from the two-grid estimate (4.1.18) to an estimate for the W-cycle multigrid algorithm, we need the next lemma on the stability of I_{k-1}^k and P_k^{k-1}, which directly follows from (2.5.3), (2.5.5), (4.1.3) and duality.

Lemma 4.5. *There exists a positive constant C_{IT} independent of k such that*

$$\|I_{k-1}^k v\|_{1,k} \le C_{IT}\|v\|_{1,k-1} \qquad \forall\, v \in V_{k-1}, \tag{4.1.19}$$

$$\|P_k^{k-1} v\|_{1,k-1} \le C_{IT}\|v\|_{1,k} \qquad \forall\, v \in V_k. \tag{4.1.20}$$

Theorem 4.6. *Given any $C_* > C_{TG}$, there exists a positive integer m_* independent of k such that the output $MG_W(k, g, z_0, m_1, m_2)$ of the W-cycle algorithm (Algorithm 2.32) applied to* (2.5.12) *satisfies the estimate*

$$\|z - MG_W(k, g, z_0, m_1, m_2)\|_{1,k} \le \frac{C_*}{[(1+m_1)(1+m_2)]^{1/2}} \|z - z_0\|_{1,k}, \qquad (4.1.21)$$

provided $m_1 + m_2 \ge m_*$.

Proof. In view of Lemma 2.33, it suffices to show that

$$\|E_k v\|_{1,k} \le \frac{C_*}{[(1+m_1)(1+m_2)]^{1/2}} \|v\|_{1,k} \qquad \forall\, v \in V_k,\ k \ge 0, \qquad (4.1.22)$$

where E_k is the k-th level error operator for the W-cycle algorithm (Algorithm 2.32) defined by (2.5.23).

We will prove (4.1.22) by mathematical induction. The case $k = 0$ holds for any m_* since $A_0 z = g$ is solved exactly.

Assume $k \ge 1$ and (4.1.22) is valid for $k - 1$. Let $v \in V_k$ be arbitrary. In view of (2.5.23) and (2.5.28), we have

$$\begin{aligned} E_k v &= R_k^{m_2}(Id_k - I_{k-1}^k P_k^{k-1}) R_k^{m_1} v + R_k^{m_2}(I_{k-1}^k E_{k-1}^2 P_k^{k-1}) R_k^{m_1} v \qquad (4.1.23) \\ &= \tilde{E}_k v + R_k^{m_2}(I_{k-1}^k E_{k-1}^2 P_k^{k-1}) R_k^{m_1} v. \end{aligned}$$

For the first term on the right-hand side of (4.1.23), we obtain from (4.1.18) that

$$\|\tilde{E}_k v\|_{1,k} \le C_{TG}[(1+m_1)(1+m_2)]^{-1/2} \|v\|_{1,k}.$$

From (4.1.7), (4.1.19), (4.1.20) and the induction hypothesis, we obtain

$$\|R_k^{m_2} I_{k-1}^k E_{k-1}^2 P_k^{k-1} R_k^{m_1} v\|_{1,k} \le C_{IT}^2 C_*^2 [(1+m_1)(1+m_2)]^{-1} \|v\|_{1,k}.$$

It follows that

$$\|E_k v\|_{1,k} \le (C_{TG}[(1+m_1)(1+m_2)]^{-1/2} + C_{IT}^2 C_*^2 [(1+m_1)(1+m_2)]^{-1}) \|v\|_{1,k}. \qquad (4.1.24)$$

If we choose $m_1 + m_2 \geq m_*$, where

$$m_*^{-1/2} \leq \frac{C_* - C_{TG}}{C_{IT}^2 C_*^2},$$

then

$$\begin{aligned} C_{TG}[(1+m_1)(1+m_2)]^{-1/2} &+ C_{IT}^2 C_*^2 [(1+m_1)(1+m_2)]^{-1} \\ &\leq (C_{TG} + C_{IT}^2 C_*^2 m_*^{-1/2})[(1+m_1)(1+m_2)]^{-1/2} \\ &\leq C_*[(1+m_1)(1+m_2)]^{-1/2}, \end{aligned}$$

which together with (4.1.24) implies (4.1.22). Therefore (4.1.21) is also valid for $k \geq 0$. □

Theorem 4.6 shows that the W-cycle algorithm (Algorithm 2.32) is a contraction with contraction number independent of grid levels provided the number of smoothing steps is sufficiently large. Furthermore, the contraction number decreases at the rate of $1/m$ for the W-cycle algorithm with m pre-smoothing and m post-smoothing steps. Numerical results will be presented in Section 4.3 to illustrate the theoretical results.

4.2 Convergence of the V-Cycle and F-Cycle Algorithms

In this section we study the convergence of the V-cycle and F-cycle algorithms for the discrete problem

$$A_k u_k = f_k,$$

where $A_k : V_k \longrightarrow V_k'$ and $f_k \in V_k'$ are defined by (2.5.7) and (2.5.8). The analysis is based on the additive multigrid theory developed in [30, 31].

By iterating the recursive relation (2.5.34) for the V-cycle error propagation operator $\mathbb{E}_k$ with m pre-smoothing and m post-smoothing steps and taking into account that $\mathbb{E}_0 = 0$, we have

$$
\begin{aligned}
\mathbb{E}_k &= R_k^m (Id_k - I_{k-1}^k P_k^{k-1} + I_{k-1}^k \mathbb{E}_{k-1} P_k^{k-1}) R_k^m \\
&= R_k^m [(Id_k - I_{k-1}^k P_k^{k-1}) R_k^m \\
&\qquad + R_k^m I_{k-1}^k R_{k-1}^m [(Id_{k-1} - I_{k-2}^{k-1} P_{k-1}^{k-2}) \\
&\qquad\qquad + I_{k-2}^{k-1} E_{k-2} P_{k-1}^{k-2}] R_{k-1}^m P_k^{k-1} R_k^m \\
&= \sum_{j=2}^{k} T_{k,j} R_j^m (Id_j - I_{j-1}^j P_j^{j-1}) R_j^m T_{j,k},
\end{aligned} \tag{4.2.1}
$$

where $T_{k,k} = Id_k$, and for $j < k$, $T_{j,k} : V_k \longrightarrow V_j$ and $T_{k,j} : V_j \longrightarrow V_k$ are the multilevel operators defined by

$$
\begin{aligned}
T_{j,k} =& P_{j+1}^j R_{j+1}^m \cdots P_k^{k-1} R_k^m, \\
T_{k,j} =& R_k^m I_{k-1}^k \cdots R_{j+1}^m I_j^{j+1}.
\end{aligned}
$$

Note that (2.5.20) and (2.5.21) imply that

$$
a_j(T_{j,k} v, w) = a_k(v, T_{k,j}, w) \qquad \forall\ v \in V_k,\ w \in V_j.
$$

The additive expression (4.2.1) for $\mathbb{E}_k$ is the starting point of the additive theory. The convergence theory based on (4.2.1) has been applied successfully to classical nonconforming finite elements on quasi-uniform meshes [31, 100, 47, 45]. In this section we extend the theory to DG methods on graded meshes.

The convergence of the V-cycle and F-cycle algorithms (Algorithm 2.35 and Algorithm 2.36) is obtained within the framework of [31]. Therefore, we must verify the assumptions in [31, Section 3]. Moreover, by using weighted Sobolev spaces and graded meshes, we can treat the convergence of the V-cycle and F-cycle algorithms with full elliptic regularity. In other words, we can apply the additive theory in [31] for the case $\alpha = 1$ (α is the index of elliptic regularity), which means that we need to establish the following estimates besides the estimates in Section 4.1:

$$\|I_{k-1}^k v\|_{1,k}^2 \leq (1+\theta^2)\|v\|_{1,k-1}^2 + C\theta^{-2}h_k^2\|v\|_{2,k-1}^2 \quad \forall\, v \in V_{k-1},\ \theta \in (0,1), \quad (4.2.2)$$

$$\|I_{k-1}^k v\|_{0,k}^2 \leq (1+\theta^2)\|v\|_{0,k-1}^2 + C\theta^{-2}h_k^2\|v\|_{1,k-1}^2 \quad \forall\, v \in V_{k-1},\ \theta \in (0,1), \quad (4.2.3)$$

$$\|P_k^{k-1} v\|_{0,k-1}^2 \leq (1+\theta^2)\|v\|_{0,k}^2 + C\theta^{-2}h_k^2\|v\|_{1,k}^2 \quad \forall\, v \in V_k\,,\ \theta \in (0,1)\,, \quad (4.2.4)$$

and

$$\|\big(Id_{k-1} - P_k^{k-1} I_{k-1}^k\big)v\|_{0,k-1} \leq Ch_k\|v\|_{1,k-1} \qquad \forall\, v \in V_{k-1}. \quad (4.2.5)$$

For future reference we state here two simple inequalities:

$$ab \leq (\theta a)^2 + b^2/(4\theta^2) \qquad \forall\, a,b \in \mathbb{R},\ \theta \in (0,1), \quad (4.2.6)$$

$$(a+b)^2 \leq (1+\theta^2)a^2 + (1+\theta^{-2})b^2 \quad \forall\, a,b \in \mathbb{R},\ \theta \in (0,1). \quad (4.2.7)$$

The following result is also useful for the analysis.

Lemma 4.7. *Given any $w \in V_k$, there exists $\phi \in L_{2,\mu}(\Omega)$ such that*

$$a_k(w,v) = \int_\Omega \phi v\, dx \qquad \forall\, v \in V_k, \quad (4.2.8)$$

and

$$\|\phi\|_{L_{2,\mu}(\Omega)} \leq C\|w\|_{2,k}. \quad (4.2.9)$$

Proof. In view of (4.1.4) and (4.1.6), the linear functional $L(v) = a_k(w,v)$ defined on V_k satisfies the estimate

$$|L(v)| \leq \|w\|_{2,k}\|v\|_{0,k} \leq C\|w\|_{2,k}\|v\|_{L_{2,-\mu}(\Omega)} \qquad \forall\, v \in V_k.$$

By the Hahn-Banach Theorem [98], we can extend L to a bounded linear functional on $L_{2,-\mu}(\Omega)$ with the same bound, i.e., there exists $\phi \in L_{2,\mu}(\Omega)$ that satisfies (4.2.8) and (4.2.9). □

The statements of the proof for the following four lemmas, which verify assumptions (4.2.2)–(4.2.5), are carried out in [34]. We state them in below.

Lemma 4.8. *The estimate* (4.2.2) *is valid.*

Proof. It suffices to show that

$$\|\zeta_{k-1}\|_{1,k}^2 \le \|\zeta_{k-1}\|_{1,k-1}^2 + Ch_k^2 \|\zeta_{k-1}\|_{2,k-1}^2 \qquad \forall\, \zeta_{k-1} \in V_{k-1},\ k \ge 1,$$

where C is a positive constant.

Let $\zeta_{k-1} \in V_{k-1}$ be arbitrary. By Lemma 4.7, there exists $\phi \in L_{2,\mu}(\Omega)$ such that

$$a_{k-1}(\zeta_{k-1}, v) = \int_\Omega \phi v\, dx \qquad \forall\, v \in V_{k-1}, \tag{4.2.10}$$

and

$$\|\phi\|_{L_{2,\mu}(\Omega)} \le C\|\zeta_{k-1}\|_{2,k-1}. \tag{4.2.11}$$

Let $\zeta \in H_0^1(\Omega) \cap H_\mu^2(\Omega)$ satisfy

$$\int_\Omega \nabla\zeta \cdot \nabla\, v\, dx = \int_\Omega \phi v\, dx \qquad \forall\, v \in H_0^1(\Omega). \tag{4.2.12}$$

Therefore ζ_{k-1} is the approximation of ζ by DG methods (2.5.1) on the $(k-1)$-st level. From (2.4.28), (2.4.35), (2.4.36), (2.5.2), (2.5.3), (4.1.3), (4.2.12) and Theorem 2.28, we have

$$\begin{aligned}
\|\zeta_{k-1}\|_{1,k}^2 &\le \|\zeta_{k-1}\|_{1,k-1}^2 + C \sum_{e\in\mathcal{E}_{k-1}} \frac{1}{|e|} \|[[\zeta_{k-1}]]\|_{L_2(e)}^2 \\
&= \|\zeta_{k-1}\|_{1,k-1}^2 + C \sum_{e\in\mathcal{E}_{k-1}} \frac{1}{|e|} \|[[\zeta - \zeta_{k-1}]]\|_{L_2(e)}^2 \\
&\le \|\zeta_{k-1}\|_{1,k-1}^2 + C\|\zeta - \zeta_{k-1}\|_k^2 \\
&\le \|\zeta_{k-1}\|_{1,k-1}^2 + Ch_k^2 \|\phi\|_{L_{2,\mu}(\Omega)}^2 \\
&\le \|\zeta_{k-1}\|_{1,k-1}^2 + Ch_k^2 \|\zeta_{k-1}\|_{2,k-1}^2.
\end{aligned}$$

□

Lemma 4.9. *The estimate* (4.2.3) *is valid.*

Proof. Let $v \in V_{k-1}$ be arbitrary. From (2.3.7), (2.5.9) and (4.1.2), we have

$$
\begin{aligned}
|\!|\!| v |\!|\!|_{0,k}^2 &= h_k^2 \sum_{T' \in \mathcal{T}_k} \sum_{m' \in \mathcal{M}_{T'}} v_{T'}^2(m') \\
&= h_k^2 \sum_{T \in \mathcal{T}_{k-1}} \sum_{\substack{T' \subset T \\ T' \in \mathcal{T}_k}} \sum_{m' \in \mathcal{M}_{T'}} v_{T'}^2(m') \\
&= h_{k-1}^2 \sum_{T \in \mathcal{T}_{k-1}} \sum_{m \in \mathcal{M}_T} v_T^2(m) \\
&\quad + h_k^2 \sum_{T \in \mathcal{T}_{k-1}} \Big[\sum_{\substack{T' \subset T \\ T' \in \mathcal{T}_k}} \sum_{m' \in \mathcal{M}_{T'}} v_{T'}^2(m') - 4 \sum_{m \in \mathcal{M}_T} v_T^2(m) \Big] \\
&= |\!|\!| v |\!|\!|_{0,k-1}^2 + h_k^2 \sum_{T \in \mathcal{T}_{k-1}} \Big[\sum_{\substack{T' \subset T \\ T' \in \mathcal{T}_k}} \sum_{m' \in \mathcal{M}_{T'}} v_{T'}^2(m') - 4 \sum_{m \in \mathcal{M}_T} v_T^2(m) \Big].
\end{aligned}
\tag{4.2.13}
$$

Let $T \in \mathcal{T}_{k-1}$, $m \in \mathcal{M}_T$, $T' \in \mathcal{T}_k$, $T' \subset T$, and $m' \in \mathcal{M}_{T'}$. It follows from the mean value theorem that

$$
\begin{aligned}
\big| v_T^2(m) - v_{T'}^2(m') \big| &= \big| v_T(m) - v_{T'}(m') \big| \big| v_T(m) + v_{T'}(m') \big| \\
&\le C \| \nabla v_T \|_{L_2(T)} \| v_T \|_{L_\infty(T)}.
\end{aligned}
\tag{4.2.14}
$$

Hence by combining (2.3.7), (2.5.2), (2.5.3), (2.5.9), (4.1.2), (4.1.3), (4.2.13), (4.2.14) and the Cauchy-Schwarz inequality, we have

$$
\begin{aligned}
\big| |\!|\!| v |\!|\!|_{0,k-1}^2 - |\!|\!| v |\!|\!|_{0,k}^2 \big| \le & h_k^2 \Big| \sum_{\substack{T' \subset T \\ T' \in \mathcal{T}_k}} \sum_{m' \in \mathcal{M}_{T'}} v_{T'}^2(m') - 4 \sum_{m \in \mathcal{M}_T} v_T^2(m) \Big| \\
\le & C h_k^2 \| \nabla v \|_{L_2(T)} \Big[\sum_{m \in \mathcal{M}_T} v_T^2(m) \Big]^{1/2} \\
\le & C h_k \Big[\sum_{T \in \mathcal{T}_{k-1}} \| \nabla v \|_{L_2(T)}^2 \Big]^{1/2} \Big[h_{k-1}^2 \sum_{T \in \mathcal{T}_{k-1}} \sum_{m \in \mathcal{M}_T} v_T^2(m) \Big]^{1/2} \\
\le & C h_k \| v \|_{k-1} |\!|\!| v |\!|\!|_{0,k-1} \\
\le & C h_k |\!|\!| v |\!|\!|_{1,k-1} |\!|\!| v |\!|\!|_{0,k-1}.
\end{aligned}
\tag{4.2.15}
$$

The estimate (4.2.3) then follows from (4.2.6) and (4.2.15). $\square$

Lemma 4.10. *The estimate* (4.2.4) *is valid.*

Proof. Let $\zeta_k \in V_k$ be arbitrary. By Lemma 4.7, there exists $\phi \in L_{2,\mu}(\Omega)$ such that

$$a_k(\zeta_k, v) = \int_\Omega \psi v\, dx \quad \forall\, v \in V_k \quad \text{and} \quad \|\phi\|_{L_{2,\mu}(\Omega)} \le C|\!|\!|\zeta_k|\!|\!|_{2,k}. \tag{4.2.16}$$

Let $\zeta \in H_0^1(\Omega) \cap H_\mu^2(\Omega)$ satisfy (4.2.12) and $\zeta_{k-1} = P_k^{k-1}\zeta_k$. Then (4.2.16) implies that ζ_k is the DG approximation of ζ on the k-th level, and (2.5.21) implies that

$$a_{k-1}(\zeta_{k-1}, v) = a_k(\zeta_k, I_{k-1}^k v) = \int_\Omega \phi v\, dx \qquad \forall\, v \in V_{k-1},$$

i.e., ζ_{k-1} is the DG approximation of ζ on the $(k-1)$-st level.

Let $\theta \in (0,1)$ be arbitrary. From (4.1.20), (4.2.6) and (4.2.15), we have

$$\begin{aligned}
|\!|\!|\zeta_{k-1}|\!|\!|_{0,k-1}^2 \le & |\!|\!|\zeta_{k-1}|\!|\!|_{0,k}^2 + \frac{\theta^2}{2}|\!|\!|\zeta_{k-1}|\!|\!|_{0,k-1}^2 + C\theta^{-2}h_k^2|\!|\!|\zeta_{k-1}|\!|\!|_{1,k-1}^2 \\
\le & |\!|\!|\zeta_{k-1}|\!|\!|_{0,k}^2 + \frac{\theta^2}{2}|\!|\!|\zeta_{k-1}|\!|\!|_{0,k-1}^2 + C\theta^{-2}h_k^2|\!|\!|\zeta_k|\!|\!|_{1,k}^2,
\end{aligned}$$

and hence

$$\begin{aligned}
|\!|\!|\zeta_{k-1}|\!|\!|_{0,k-1}^2 &\le \frac{1}{1-(\theta^2/2)}|\!|\!|\zeta_{k-1}|\!|\!|_{0,k}^2 + C\theta^{-2}h_k^2|\!|\!|\zeta_k|\!|\!|_{1,k}^2 \\
&\le (1+\theta^2)|\!|\!|\zeta_{k-1}|\!|\!|_{0,k}^2 + C\theta^{-2}h_k^2|\!|\!|\zeta_k|\!|\!|_{1,k}^2.
\end{aligned} \tag{4.2.17}$$

On the other hand, we have, by (4.1.6), (4.2.6), (4.2.16) and Theorem 2.29,

$$\begin{aligned}
|\!|\!|\zeta_{k-1}|\!|\!|_{0,k}^2 &\le \left(|\!|\!|\zeta_k|\!|\!|_{0,k} + |\!|\!|\zeta_{k-1} - \zeta_k|\!|\!|_{0,k}\right)^2 \\
&\le (1+\theta^2)|\!|\!|\zeta_k|\!|\!|_{0,k}^2 + (1+\theta^{-2})|\!|\!|\zeta_{k-1} - \zeta_k|\!|\!|_{0,k}^2 \\
&\le (1+\theta^2)|\!|\!|\zeta_k|\!|\!|_{0,k}^2 + C\theta^{-2}\|\zeta_{k-1} - \zeta_k\|_{L_{2,-\mu}(\Omega)}^2 \\
&\le (1+\theta^2)|\!|\!|\zeta_k|\!|\!|_{0,k}^2 + C\theta^{-2}\big(\|\zeta_{k-1} - \zeta\|_{L_{2,-\mu}(\Omega)} + \|\zeta - \zeta_k\|_{L_{2,-\mu}(\Omega)}\big)^2 \\
&\le (1+\theta^2)|\!|\!|\zeta_k|\!|\!|_{0,k}^2 + C\theta^{-2}h_k^4\|\phi\|_{L_{2,\mu}(\Omega)}^2 \\
&\le (1+\theta^2)|\!|\!|\zeta_k|\!|\!|_{0,k}^2 + C\theta^{-2}h_k^4|\!|\!|\zeta_k|\!|\!|_{2,k}^2.
\end{aligned} \tag{4.2.18}$$

Combining (4.1.5), (4.2.17) and (4.2.18), we find

$$\|P_k^{k-1}\zeta_k\|_{0,k-1}^2 \le (1+\theta^2)^2\|\zeta_k\|_{0,k}^2 + C\theta^{-2}h_k^2\|\zeta_k\|_{1,k}^2,$$

which implies that (4.2.4) holds for ζ_k because $\theta \in (0,1)$ is arbitrary. □

Lemma 4.11. *The estimate* (4.2.5) *is valid.*

Proof. Let $\zeta_{k-1} \in V_{k-1}$ be arbitrary. By Lemma 4.7, there exists $\phi \in L_{2,\mu}(\Omega)$ such that

$$a_k(\zeta_{k-1}, v) = \int_\Omega \phi v\,dx \quad \forall\, v \in V_k \quad \text{and} \quad \|\phi\|_{L_{2,\mu}(\Omega)} \le C\|\zeta_{k-1}\|_{2,k}. \tag{4.2.19}$$

Let $\zeta \in H_0^1(\Omega) \cap H_\mu^2(\Omega)$ satisfy (4.2.12). In view of (4.2.19), ζ_{k-1} is the DG approximation of ζ on the k-th level, and $P_k^{k-1}\zeta_{k-1}$ is the DG approximation of ζ on the $(k-1)$-st level as in the proof of Lemma 4.10.

It follows from Theorem 2.29, (4.1.5), (4.1.19) and (4.2.19) that

$$\begin{aligned}
\|(Id_{k-1} - P_k^{k-1}I_{k-1}^k)\zeta_{k-1}\|_{0,k-1} &= \|\zeta_{k-1} - P_k^{k-1}\zeta_{k-1}\|_{0,k-1} \\
&\le C\|\zeta_{k-1} - P_k^{k-1}\zeta_{k-1}\|_{L_{2,-\mu}(\Omega)} \\
&\le C\big[\|\zeta_{k-1} - \zeta\|_{L_{2,-\mu}(\Omega)} + \|\zeta - P_k^{k-1}\zeta_{k-1}\|_{L_{2,-\mu}(\Omega)}\big] \\
&\le Ch_k^2\|\phi\|_{L_{2,\mu}(\Omega)} \\
&\le Ch_k^2\|\zeta_{k-1}\|_{2,k} \\
&\le Ch_k\|\zeta_{k-1}\|_{1,k} \le Ch_k\|\zeta_{k-1}\|_{1,k-1}.
\end{aligned}$$

□

We have verified the assumptions (4.2.2)–(4.2.5) for the additive theory. Therefore we can apply the results in [31] to obtain the following convergence theorems for the V-cycle and F-cycle algorithms.

Theorem 4.12. *The output $MG_V(k, g, z_0, m, m)$ of the V-cycle algorithm (Algorithm* 2.35*) applied to* (2.5.12) *satisfies the following estimate*:

$$\|z - MG_V(k, g, z_0, m, m)\|_{1,k} \leq \frac{C}{m}\|z - z_0\|_{1,k},$$

where the positive constant C is independent of the grid level k, provided that the number of smoothing steps m is greater than a positive integer m_* that is also independent of k.

Theorem 4.13. *The output $MG_F(k, g, z_0, m, m)$ of the F-cycle algorithm (Algorithm* 2.36*) applied to* (2.5.12) *satisfies the following estimate*:

$$\|z - MG_F(k, g, z_0, m, m)\|_{1,k} \leq \frac{C}{m}\|z - z_0\|_{1,k},$$

where the positive constant C is independent of the grid level k, provided that the number of smoothing steps m is greater than a positive integer m_* that is also independent of k.

Theorem 4.12 and 4.13 illustrate that both the V-cycle and F-cycle algorithms are contractions with contraction number independent of grid level, provided the number of smoothing steps is sufficiently large. Furthermore, the contraction numbers decrease at the rate of $1/m$ for both algorithms with m smoothing steps. Results of numerical experiments will be reported in the next section.

4.3 Numerical Results

In this section we report the contraction numbers of the W-cycle, F-cycle and V-cycle algorithms for the DG methods (2.5.1) on the L-shaped domain $(-1, 1)^2 \setminus ([0, 1] \times [-1, 0])$ with graded meshes (cf. Figure 2.2). The triangulations $\mathcal{T}_1, \ldots, \mathcal{T}_7$ are generated by the refinement procedure described in Section 2.3, where the grading parameter at the reentrant corner is taken to be 2/3.

We use $\eta = 1$ and $\lambda = 1/35$ for the method of Brezzi et al. and tabulate the contraction numbers in Tables 4.3–4.3. We find that the W-cycle (resp. F-cycle and V-cycle) algorithm is a contraction for $m \geq 2$ (resp. $m \geq 3$ and $m \geq 5$).

TABLE 4.1. Contraction numbers of the W-cycle algorithm on the L-shaped domain for the method of Brezzi et al. ($\eta = 1$)

	$k=1$	$k=2$	$k=3$	$k=4$	$k=5$	$k=6$	$k=7$
$m=2$	0.69	0.75	0.76	0.79	0.78	0.79	0.79
$m=3$	0.53	0.65	0.72	0.72	0.74	0.74	0.75
$m=4$	0.44	0.60	0.66	0.68	0.69	0.71	0.71
$m=5$	0.39	0.55	0.61	0.64	0.65	0.66	0.67
$m=6$	0.33	0.50	0.56	0.61	0.62	0.63	0.64
$m=7$	0.30	0.47	0.54	0.57	0.59	0.60	0.60
$m=8$	0.26	0.34	0.51	0.55	0.57	0.57	0.58
$m=9$	0.22	0.41	0.48	0.52	0.53	0.54	0.54

TABLE 4.2. Contraction numbers of the F-cycle algorithm on the L-shaped domain for the method of Brezzi et al. ($\eta = 1$)

	$k=1$	$k=2$	$k=3$	$k=4$	$k=5$	$k=6$	$k=7$
$m=3$	0.53	0.65	0.72	0.72	0.74	0.74	0.75
$m=4$	0.44	0.60	0.66	0.68	0.70	0.71	0.71
$m=5$	0.39	0.55	0.61	0.64	0.65	0.66	0.67
$m=6$	0.33	0.50	0.56	0.61	0.62	0.63	0.64
$m=7$	0.30	0.47	0.54	0.57	0.60	0.60	0.60
$m=8$	0.26	0.44	0.51	0.55	0.57	0.58	0.58
$m=9$	0.22	0.41	0.48	0.52	0.53	0.54	0.54
$m=10$	0.20	0.39	0.44	0.47	0.52	0.52	0.53

For the LDG method, we use $\eta = 1$ and $\lambda = 1/20$. The results are reported in Tables 4.3–4.3. In this case the W-cycle (resp. F-cycle and V-cycle) algorithm is a contraction for $m = 3$ (resp. $m \geq 4$ and $m \geq 5$).

We take $\eta = 4$ and $\lambda = 1/80$ for the method of Bassi et al. The contraction numbers are tabulated in Tables 4.3–4.3. We found that the W-cycle (resp. F-cycle and V-cycle) algorithm is a contraction for $m \geq 1$ (resp. $m \geq 3$ and $m \geq 4$).

TABLE 4.3. Contraction numbers of the V-cycle algorithm on the L-shaped domain for the method of Brezzi et al. ($\eta = 1$)

	$k=1$	$k=2$	$k=3$	$k=4$	$k=5$	$k=6$	$k=7$
$m=5$	0.39	0.58	0.65	0.69	0.69	0.73	0.90
$m=6$	0.33	0.54	0.60	0.62	0.68	0.68	0.70
$m=7$	0.30	0.50	0.56	0.52	0.62	0.65	0.66
$m=8$	0.26	0.47	0.53	0.57	0.61	0.63	0.63
$m=9$	0.22	0.44	0.48	0.56	0.57	0.60	0.61
$m=10$	0.20	0.42	0.46	0.53	0.57	0.58	0.59
$m=11$	0.19	0.40	0.44	0.49	0.54	0.57	0.57
$m=12$	0.17	0.38	0.43	0.46	0.50	0.54	0.55

TABLE 4.4. Contraction numbers of the W-cycle algorithm on the L-shaped domain for the LDG method ($\eta = 1$)

	$k=1$	$k=2$	$k=3$	$k=4$	$k=5$	$k=6$	$k=7$
$m=3$	0.99	0.88	0.65	0.63	0.63	0.63	0.64
$m=4$	0.65	0.43	0.51	0.55	0.57	0.56	0.57
$m=5$	0.43	0.38	0.45	0.49	0.50	0.51	0.52
$m=6$	0.28	0.33	0.41	0.44	0.46	0.47	0.47
$m=7$	0.18	0.29	0.37	0.39	0.42	0.43	0.44
$m=8$	0.13	0.26	0.33	0.37	0.39	0.39	0.40
$m=9$	0.11	0.24	0.30	0.32	0.36	0.37	0.38
$m=10$	0.09	0.22	0.29	0.32	0.35	0.36	0.36

For the SIPG method, we use $\eta = 10$ and $\lambda = 1/40$. The contraction numbers are tabulated in Tables 4.10–4.3. The W-cycle (resp. F-cycle and V-cycle) algorithm is a contraction for $m \geq 2$ (resp. $m \geq 4$ and $m \geq 6$).

Remark 4.14. *For all four DG methods, the W-cycle algorithm and the F-cycle algorithm have similar contraction numbers when they are both contractions.*

Finally, the asymptotic behaviors of the contraction numbers of the W-cycle and V-cycle algorithms for all four DG methods with respect to the number of smoothing steps for $k = 6$ are depicted in Figure 4.1–4.2. The log-log graphs confirm that the contraction number decreases at the rate of m^{-1}, as predicted by Theorems 4.6 and 4.12.

TABLE 4.5. Contraction numbers of the F-cycle algorithm on the L-shaped domain for the LDG method ($\eta = 1$)

	$k=1$	$k=2$	$k=3$	$k=4$	$k=5$	$k=6$	$k=7$
$m=4$	0.65	0.43	0.51	0.54	0.57	0.57	0.58
$m=5$	0.43	0.38	0.45	0.49	0.50	0.52	0.52
$m=6$	0.28	0.33	0.41	0.44	0.45	0.47	0.47
$m=7$	0.18	0.29	0.37	0.39	0.42	0.43	0.44
$m=8$	0.13	0.26	0.33	0.37	0.39	0.39	0.40
$m=9$	0.11	0.24	0.30	0.32	0.36	0.37	0.38
$m=10$	0.09	0.22	0.29	0.32	0.35	0.36	0.36
$m=11$	0.07	0.20	0.22	0.31	0.33	0.34	0.34

TABLE 4.6. Contraction numbers of the V-cycle algorithm on the L-shaped domain for the LDG method ($\eta = 1$)

	$k=1$	$k=2$	$k=3$	$k=4$	$k=5$	$k=6$	$k=7$
$m=5$	0.43	0.45	0.53	0.64	0.72	0.77	0.81
$m=6$	0.28	0.35	0.36	0.42	0.48	0.48	0.50
$m=7$	0.18	0.31	0.38	0.41	0.48	0.48	0.49
$m=8$	0.13	0.28	0.34	0.39	0.41	0.45	0.46
$m=9$	0.11	0.25	0.30	0.35	0.39	0.43	0.43
$m=10$	0.09	0.23	0.28	0.35	0.38	0.40	0.41
$m=11$	0.07	0.21	0.28	0.33	0.37	0.38	0.39
$m=12$	0.06	0.20	0.25	0.32	0.36	0.36	0.38

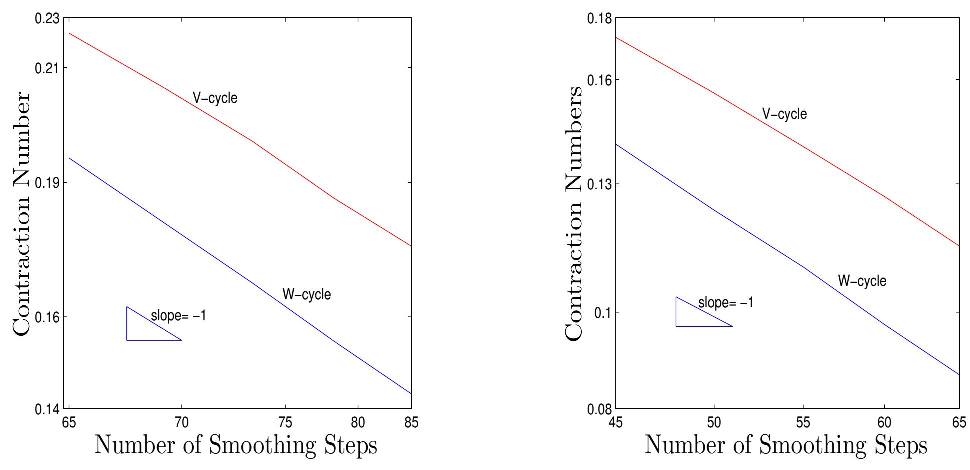

FIGURE 4.1. Asymptotic behaviors of the contraction numbers with respect to the number of smoothing steps for the method of Brezzi et al. (left, $\eta = 1$) and for the LDG method (right, $\eta = 1$)

TABLE 4.7. Contraction numbers of the W-cycle algorithm on the L-shaped domain for the method of Bassi et al. ($\eta = 4$)

	$k=1$	$k=2$	$k=3$	$k=4$	$k=5$	$k=6$	$k=7$
$m=1$	0.81	0.89	0.91	0.91	0.91	0.91	0.91
$m=2$	0.79	0.85	0.86	0.87	0.87	0.87	0.87
$m=3$	0.72	0.80	0.83	0.83	0.84	0.83	0.83
$m=4$	0.65	0.75	0.81	0.80	0.81	0.80	0.81
$m=5$	0.61	0.71	0.76	0.78	0.78	0.79	0.79
$m=6$	0.55	0.70	0.74	0.78	0.77	0.77	0.78
$m=7$	0.51	0.67	0.72	0.75	0.76	0.77	0.77
$m=8$	0.49	0.66	0.71	0.72	0.74	0.75	0.75

TABLE 4.8. Contraction numbers of the F-cycle algorithm on the L-shaped domain for the method of Bassi et al. ($\eta = 4$)

	$k=1$	$k=2$	$k=3$	$k=4$	$k=5$	$k=6$	$k=7$
$m=3$	0.72	0.82	0.83	0.83	0.83	0.83	0.84
$m=4$	0.65	0.78	0.81	0.80	0.81	0.80	0.81
$m=5$	0.61	0.76	0.76	0.78	0.78	0.79	0.79
$m=6$	0.55	0.71	0.74	0.78	0.77	0.77	0.78
$m=7$	0.51	0.69	0.72	0.75	0.76	0.77	0.77
$m=8$	0.49	0.68	0.71	0.72	0.74	0.75	0.75
$m=9$	0.45	0.65	0.68	0.71	0.72	0.74	0.74
$m=10$	0.41	0.63	0.68	0.68	0.71	0.72	0.72

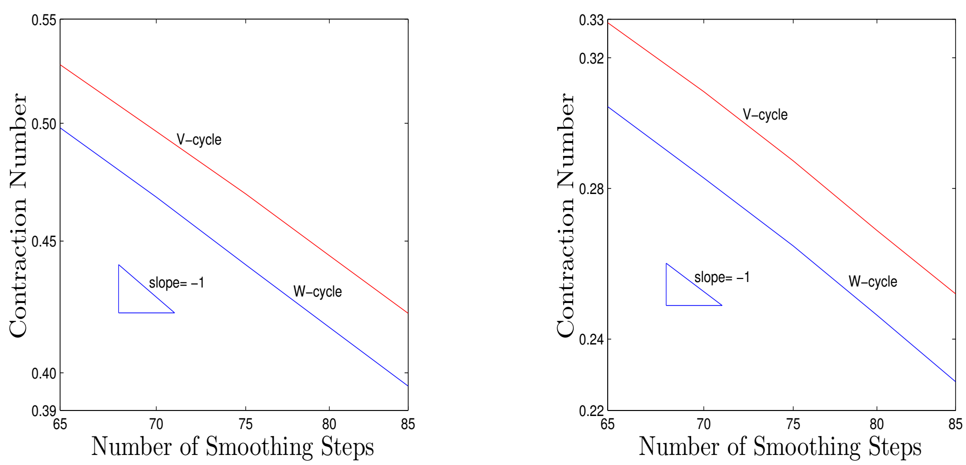

FIGURE 4.2. Asymptotic behaviors of the contraction numbers with respect to the number of smoothing steps for the method of Bassi et al. (left, $\eta = 4$) and for the SIP method (right, $\eta = 10$)

TABLE 4.9. Contraction numbers of the V-cycle algorithm on the L-shaped domain for the method of Bassi et al. ($\eta = 4$)

	$k=1$	$k=2$	$k=3$	$k=4$	$k=5$	$k=6$	$k=7$
$m=4$	0.65	0.76	0.83	0.80	0.82	0.93	0.99
$m=5$	0.61	0.73	0.77	0.80	0.81	0.81	0.82
$m=6$	0.55	0.73	0.74	0.78	0.80	0.81	0.80
$m=7$	0.51	0.70	0.73	0.76	0.79	0.80	0.80
$m=8$	0.49	0.69	0.71	0.76	0.78	0.78	0.78
$m=9$	0.45	0.67	0.69	0.73	0.75	0.77	0.77
$m=10$	0.41	0.65	0.69	0.71	0.75	0.75	0.76
$m=11$	0.39	0.64	0.67	0.69	0.70	0.73	0.74

TABLE 4.10. Contraction numbers of the W-cycle algorithm on the L-shaped domain for the SIP method ($\eta = 10$)

	$k=1$	$k=2$	$k=3$	$k=4$	$k=5$	$k=6$	$k=7$
$m=2$	0.82	0.77	0.80	0.79	0.79	0.80	0.79
$m=3$	0.61	0.71	0.71	0.73	0.75	0.75	0.76
$m=4$	0.47	0.61	0.68	0.72	0.72	0.73	0.73
$m=5$	0.44	0.59	0.66	0.68	0.70	0.70	0.71
$m=6$	0.39	0.54	0.61	0.66	0.67	0.69	0.69
$m=7$	0.35	0.52	0.59	0.65	0.66	0.67	0.67
$m=8$	0.31	0.48	0.59	0.64	0.65	0.66	0.66
$m=9$	0.28	0.47	0.58	0.62	0.64	0.65	0.65

TABLE 4.11. Contraction numbers of the F-cycle algorithm on the L-shaped domain for the SIP method ($\eta = 10$)

	$k=1$	$k=2$	$k=3$	$k=4$	$k=5$	$k=6$	$k=7$
$m=4$	0.47	0.61	0.68	0.72	0.72	0.73	0.73
$m=5$	0.44	0.59	0.66	0.68	0.70	0.70	0.71
$m=6$	0.39	0.54	0.61	0.66	0.67	0.69	0.69
$m=7$	0.35	0.52	0.59	0.65	0.66	0.68	0.68
$m=8$	0.31	0.48	0.59	0.64	0.65	0.66	0.66
$m=9$	0.28	0.47	0.58	0.62	0.64	0.65	0.65
$m=10$	0.25	0.45	0.56	0.62	0.63	0.64	0.64
$m=11$	0.24	0.43	0.53	0.58	0.60	0.62	0.63

TABLE 4.12. Contraction numbers of the V-cycle algorithm on the L-shaped domain for the SIP method ($\eta = 10$)

	$k = 1$	$k = 2$	$k = 3$	$k = 4$	$k = 5$	$k = 6$	$k = 7$
$m = 6$	0.39	0.56	0.60	0.69	0.71	0.73	0.77
$m = 7$	0.35	0.53	0.57	0.69	0.71	0.72	0.73
$m = 8$	0.31	0.49	0.62	0.67	0.69	0.70	0.71
$m = 9$	0.28	0.47	0.60	0.64	0.67	0.69	0.70
$m = 10$	0.25	0.45	0.56	0.64	0.67	0.68	0.69
$m = 11$	0.24	0.44	0.55	0.64	0.66	0.67	0.68
$m = 12$	0.22	0.42	0.54	0.61	0.64	0.67	0.67
$m = 13$	0.20	0.41	0.51	0.60	0.64	0.66	0.66

Chapter 5

Hodge Decomposition and Maxwell's Equations

In this chapter we propose a new numerical approach for the two-dimensional Maxwell's equation (1.2.8) that is based on the Hodge decomposition. The resulting discrete problems will be solved by multigrid methods in Chapter 6.

5.1 Hodge Decomposition

Let $\Omega \subset \mathbb{R}^2$ be a bounded polygonal domain and $\boldsymbol{f} \in [L_2(\Omega)]^2$. Consider the problem of finding $\boldsymbol{u} \in H_0(\text{curl};\Omega) \cap H(\text{div}^0;\Omega)$ such that

$$(\nabla \times \boldsymbol{u}, \nabla \times \boldsymbol{v}) + \alpha(\boldsymbol{u}, \boldsymbol{v}) = (\boldsymbol{f}, \boldsymbol{v}) \qquad \forall \boldsymbol{v} \in H_0(\text{curl};\Omega) \cap H(\text{div}^0;\Omega). \quad (5.1.1)$$

We assume that (5.1.1) is uniquely solvable, i.e., $-\alpha$ is not a Maxwell eigenvalue. In particular, we assume $\alpha \neq 0$ when Ω is not simply connected.

Let $\xi = \nabla \times \boldsymbol{u} \in H^1(\Omega)$. Then ξ satisfies the equation (cf. (2.2.16))

$$\nabla \times \xi + \alpha \boldsymbol{u} = Q\boldsymbol{f}, \quad (5.1.2)$$

where $Q : [L^2(\Omega)]^2 \longrightarrow H(\text{div}^0;\Omega)$ is the orthogonal projection. Note that, for any $\psi \in H^1(\Omega)$, we have (cf. [68, Theorem 3.1]) $\nabla \times \psi \in H(\text{div}^0;\Omega)$, where

$$\nabla \times \psi = \begin{bmatrix} \frac{\partial \psi}{\partial x_2} \\ -\frac{\partial \psi}{\partial x_1} \end{bmatrix}.$$

Hence ξ is determined by

$$\begin{aligned}(\nabla \times \xi, \nabla \times \psi) + \alpha(\xi, \psi) =& (\nabla \times \xi, \nabla \times \psi) + \alpha(\boldsymbol{u}, \nabla \times \psi) \quad (5.1.3)\\ =& (Q\boldsymbol{f}, \nabla \times \psi) = (\boldsymbol{f}, \nabla \times \psi) \qquad \forall \psi \in H^1(\Omega)\end{aligned}$$

when $\alpha \neq 0$, and by (5.1.3) together with the constraint

$$(\xi, 1) = \int_\Omega \xi \, dx = \int_\Omega \nabla \times \boldsymbol{u} \, dx = \int_{\partial\Omega} \boldsymbol{n} \times \boldsymbol{u} \, ds = 0 \tag{5.1.4}$$

when Ω is simply connected and $\alpha = 0$. The problem (5.1.3) is uniquely solvable (cf. [33, Lemma 3.2]).

In the derivation of (5.1.3) we used the following fact (cf. [68, Theorems 2.11 and 2.12]):

$$\boldsymbol{v} \in H_0(\mathrm{curl}; \Omega), \text{ if and only if } (\nabla \times \boldsymbol{v}, \psi) = (\boldsymbol{v}, \nabla \times \psi) \quad \forall \psi \in H^1(\Omega). \tag{5.1.5}$$

For any $\boldsymbol{u} \in H_0(\mathrm{curl}; \Omega) \cap H(\mathrm{div}^0; \Omega)$, there is a unique decomposition:

$$\boldsymbol{u} = \nabla \times \phi + \sum_{j=1}^{m} c_j \nabla \varphi_j, \tag{5.1.6}$$

where $\phi \in H^1(\Omega)$ satisfies

$$\frac{\partial \phi}{\partial n} = 0 \qquad \text{on } \partial\Omega, \tag{5.1.7}$$

and the constraint

$$(\phi, 1) = \int_\Omega \phi \, dx = 0. \tag{5.1.8}$$

The non-negative integer m is the Betti number for Ω ($m = 0$ if Ω is simply connected), and the functions $\varphi_1, \ldots, \varphi_m$ are defined as follows.

Suppose $\partial\Omega$ has $m+1$ components. We denote the outer boundary of Ω by Γ_0, and the m components of the inner boundary by $\Gamma_1, \ldots, \Gamma_m$. Then the functions φ_j are determined by

$$(\nabla \varphi_j, \nabla v) = 0 \qquad \forall\, v \in H_0^1(\Omega), \tag{5.1.9a}$$

$$\varphi_j\big|_{\Gamma_0} = 0, \tag{5.1.9b}$$

$$\varphi_j\big|_{\Gamma_i} = \delta_{ji} = \begin{cases} 1 & j = i \\ 0 & j \neq i \end{cases} \quad \text{for } 1 \leq i \leq m. \tag{5.1.9c}$$

We refer to (5.1.6) as the Hodge decomposition of $\boldsymbol{u} \in H_0(\text{curl};\Omega) \cap H(\text{div}^0;\Omega)$. Detailed justifications of (5.1.6) can be found in [33, Section 2].

The following lemma is crucial for the derivation of the new numerical approach. The proof is identical with the proof of Lemma 2.4 in [33].

Lemma 5.1. *Let $\psi \in \mathcal{H}_\Omega$, which is the space of harmonic functions spanned by the functions $\varphi_1, \dots, \varphi_m$ defined by* (5.1.9). *Then we have*

$$(\nabla \times \eta, \nabla\psi) = 0 \qquad \forall\, \eta \in H^1(\Omega). \tag{5.1.10}$$

Note that (5.1.5) and (5.1.10) imply $\nabla\mathcal{H}_\Omega \subset H_0(\text{curl};\Omega) \cap H(\text{div}^0;\Omega)$. We can use (5.1.5), (5.1.6) and Lemma 5.1 to show that ϕ in (5.1.6) satisfies

$$\begin{aligned}(\nabla \times \phi, \nabla \times \psi) =& \Big(\nabla \times \phi + \sum_{j=1}^{m} c_j \nabla\varphi_j, \nabla \times \psi\Big) \\ =& (\boldsymbol{u}, \nabla \times \psi) = (\nabla \times \boldsymbol{u}, \psi) = (\xi, \psi) \qquad \forall\, \psi \in H^1(\Omega).\end{aligned} \tag{5.1.11}$$

Note that $\alpha \neq 0$ when $m \geq 1$ since 0 is a Maxwell eigenvalue for domains that are not simply connected. In this case we can take $\boldsymbol{v} = \nabla\varphi_i$ in (5.1.1) and arrive at the equation

$$\alpha\Big(\nabla \times \phi + \sum_{j=1}^{m} c_j \nabla\varphi_j, \nabla\varphi_i\Big) = (\boldsymbol{f}, \nabla\varphi_i),$$

which together with Lemma 5.1 implies

$$\sum_{j=1}^{m} (\nabla\varphi_j, \nabla\varphi_i) c_j = \frac{1}{\alpha}(\boldsymbol{f}, \nabla\varphi_i) \qquad \text{for} \quad 1 \leq i \leq m. \tag{5.1.12}$$

Remark 5.2. *The bilinear form $(\varphi, \varrho) \to (\nabla\varphi, \nabla\varrho)$ is symmetric positive-definite on $\mathcal{H}_\Omega$, because $(\nabla\varphi, \nabla\varphi) = 0$ implies $\varphi = 0$ since φ vanishes on the outer boundary Γ_0 of Ω. Hence the system* (5.1.12) *is symmetric positive-definite.*

We can therefore solve (5.1.1) by the following procedure.

(1) Compute a numerical approximation $\tilde{\xi}$ of ξ by solving (5.1.3) when $\alpha \neq 0$ and by solving (5.1.3) with constraint (5.1.4) when Ω is simply connected and $\alpha = 0$.

(2) Compute a numerical approximation $\tilde{\phi}$ of ϕ by solving (5.1.11) under the constraint (5.1.8), where ξ is replaced by $\tilde{\xi}$.

(3) Compute numerical approximations $\tilde{\varphi}_1, \ldots, \tilde{\varphi}_m$ of $\varphi_1, \ldots, \varphi_m$ by solving (5.1.9).

(4) Compute numerical approximations $\tilde{c}_1, \ldots, \tilde{c}_m$ of $c_1, \ldots, c_m$ by solving (5.1.12), where $\varphi_1, \ldots, \varphi_m$ are replaced by $\tilde{\varphi}_1, \ldots, \tilde{\varphi}_m$

(5) The numerical approximation $\tilde{\boldsymbol{u}}$ of $\boldsymbol{u}$ is given by

$$\tilde{\boldsymbol{u}} = \nabla \times \tilde{\phi} + \sum_{j=1}^{m} \tilde{c}_j \nabla \tilde{\varphi}_j.$$

Remark 5.3. *The equations* (5.1.3) *and* (5.1.11) *can be rewritten as*

$$\begin{aligned} (\nabla\xi, \nabla\psi) + \alpha(\xi, \psi) &= (\boldsymbol{f}, \nabla \times \psi) \qquad && \forall\, \psi \in H^1(\Omega), \\ (\nabla\phi, \nabla\psi) &= (\xi, \psi) && \forall\, \psi \in H^1(\Omega). \end{aligned}$$

Hence the boundary value problems for ξ and ϕ are Neumann problems for the Laplace operator.

Since the boundary value problems in Steps (1)–(3) are standard second order scalar elliptic boundary value problems, they can be solved by many methods. We will demonstrate this numerical approach by a P_1 finite element method in the following section.

5.2 A P_1 Finite Element Method

Let $\mathcal{T}_h$ be a simplicial triangulation of Ω with mesh size h and $V_h \subset H^1(\Omega)$ be the P_1 finite element space associated with $\mathcal{T}_h$.

For $\alpha \neq 0$, the P_1 finite element method for (5.1.3) is to find $\xi_h \in V_h$ such that

$$(\nabla \times \xi_h, \nabla \times v) + \alpha(\xi_h, v) = (\boldsymbol{f}, \nabla \times v) \qquad \forall\, v \in V_h, \tag{5.2.1}$$

For $\alpha > 0$, the problem (5.2.1) is symmetric positive-definite and hence well-posed. It is also well-posed for $\alpha < 0$ provided $-\alpha$ is not a Maxwell eigenvalue and h is sufficiently small (cf. Theorem 5.5 below).

Note that (5.2.1) implies

$$(\xi_h, 1) = 0. \tag{5.2.2}$$

When Ω is simply connected and $\alpha = 0$, $\xi_h \in V_h$ is defined by (5.2.1) together with the constraint (5.2.2). This is a well-posed problem because of the Poincaré-Friedrichs inequality (cf. (2.1.5a)).

The P_1 finite element method for (5.1.11) is to find $\phi_h \in V_h$ such that

$$(\nabla \times \phi_h, \nabla \times v) = (\xi_h, v) \qquad \forall\, v \in V_h, \tag{5.2.3a}$$

$$(\phi_h, 1) = 0. \tag{5.2.3b}$$

The problem (5.2.3) is well-posed because of (2.1.5a) and (5.2.2).

In the case where $m \geq 1$, the P_1 finite element approximation $\varphi_{j,h} \in V_h$ for the harmonic function φ_j in the Hodge decomposition (5.1.6) is determined by

$$(\nabla \varphi_{j,h}, \nabla v) = 0 \qquad \forall\, v \in V_h \cap H_0^1(\Omega), \tag{5.2.4a}$$

$$\varphi_{j,h}\big|_{\Gamma_0} = 0, \tag{5.2.4b}$$

$$\varphi_{j,h}\big|_{\Gamma_i} = \delta_{ji} = \begin{cases} 1 & j = i \\ 0 & j \neq i \end{cases} \quad \text{for } 1 \leq i \leq m. \tag{5.2.4c}$$

We then compute $c_{1,h}, \ldots, c_{m,h}$ by solving the symmetric positive-definite system

$$\sum_{j=1}^{m} (\nabla \varphi_{j,h}, \nabla \varphi_{i,h}) c_{j,h} = \frac{1}{\alpha}(\boldsymbol{f}, \nabla \varphi_{i,h}) \quad \text{for } 1 \leq i \leq m. \tag{5.2.5}$$

Note that we assume $\alpha \neq 0$ when Ω is not simply connected.

Finally we define the piecewise constant approximation $\boldsymbol{u}_h$ of $\boldsymbol{u}$ by

$$\boldsymbol{u}_h = \nabla \times \phi_h + \sum_{j=1}^{m} c_{j,h} \nabla \varphi_{j,h}. \tag{5.2.6}$$

5.3 Error Analysis

In this section we present the error analysis for the P_1 finite element method introduced in Section 5.2. A properly graded triangulation $\mathcal{T}_h$ is used to recover optimal convergence rates on a general polygonal domain $\Omega \subset \mathbb{R}^2$. The error analysis based on uniform meshes can be found in [33].

Let $\omega_1, \ldots, \omega_L$ be the interior angles at the corners $c_1, \ldots, c_L$ of Ω and $\boldsymbol{f} \in [L_2(\Omega)]^2$. The triangulation $\mathcal{T}_h$ that is used in the rest of this section satisfies the property (2.3.1), where the grading parameters $\mu_1, \ldots, \mu_L$ are chosen according to (2.2.32).

We begin by comparing ξ_h and $\xi = \nabla \times \boldsymbol{u}$ under the $\| \cdot \|_{2,-\mu}$ norm, which is defined by (2.4.46).

Theorem 5.4. *For $\alpha > 0$ (general Ω) and $\alpha = 0$ (simply connected Ω), we have*

$$\|\xi - \xi_h\|_{L_{2,-\mu}(\Omega)} \leq Ch\|\boldsymbol{f}\|_{L_2(\Omega)}. \tag{5.3.1}$$

Proof. We will prove (5.3.1) by a duality argument.

Let $\zeta \in H^1(\Omega)$ be determined by

$$(\nabla \times \zeta, \nabla \times v) + \alpha(\zeta, v) = (\phi_\mu^{-2}(\xi - \xi_h), v) \qquad \forall\, v \in H^1(\Omega). \tag{5.3.2}$$

Note that (5.1.4) and (5.2.2) imply

$$(\xi - \xi_h, 1) = 0. \tag{5.3.3}$$

Let $\Pi_h : C(\bar{\Omega}) \longrightarrow V_h$ be the nodal interpolation operator for the P_1 finite element. We will first prove that

$$|\zeta - \Pi_h \zeta|_{H^1(\Omega)} \leq Ch\|\xi - \xi_h\|_{L_{2,-\mu}(\Omega)}. \tag{5.3.4}$$

Let $\mathcal{T}_{h,\ell}$ be the collection of triangles in $\mathcal{T}_h$ that touch a corner c_ℓ of Ω. Then we have

$$|\zeta - \Pi_h\zeta|^2_{H^1(\Omega)} = \sum_{T\in\mathcal{T}_h''} |\zeta - \Pi_h\zeta|^2_{H^1(T)} + \sum_{T\in\mathcal{T}_h'} |\zeta - \Pi_h\zeta|^2_{H^1(T)}, \tag{5.3.5}$$

where $\mathcal{T}_h' = \bigcup_{\omega_\ell>\pi} \mathcal{T}_{h,\ell}$ and $\mathcal{T}_h'' = \mathcal{T}_h \setminus \mathcal{T}_h'$.

For the triangles away from the reentrant corners, we derive from (2.2.33), (2.2.34), (2.2.37), (2.3.1), (2.3.2) and a standard interpolation error estimate [51, 43] that

$$\begin{aligned}
\sum_{T\in\mathcal{T}_h''} |\zeta - \Pi_h\zeta|^2_{H^1(T)} &\le C \sum_{T\in\mathcal{T}_h''} h_T^2 |\zeta|^2_{H^2(T)} \\
&\le C \sum_{T\in\mathcal{T}_h''} h^2 [\Phi_\mu(T)]^2 \sum_{i,j=1}^{2} \|\partial^2\zeta/\partial x_i \partial x_j\|^2_{L_2(T)} \\
&\le Ch^2 \sum_{i,j=1}^{2} \sum_{T\in\mathcal{T}_h''} \|\phi_\mu^2 (\partial^2\zeta/\partial x_i \partial x_j)\|^2_{L_2(T)} \\
&\le Ch^2 \|\phi_\mu^{-2}(\xi - \xi_h)\|^2_{L_{2,\mu}(\Omega)} \\
&\le Ch^2 \|\xi - \xi_h\|^2_{L_{2,-\mu}(\Omega)}.
\end{aligned} \tag{5.3.6}$$

For the triangles that touch a reentrant corner, we can apply an interpolation error estimate for fractional order Sobolev spaces [65] together with (2.2.38) and (2.3.5) to obtain

$$\begin{aligned}
\sum_{T\in\mathcal{T}_h'} |\zeta - \Pi_h\zeta|^2_{H^1(T)} \le& C \sum_{\omega_\ell>\pi} \sum_{T\in\mathcal{T}_{h,\ell}} h_T^{2\mu_\ell} |\zeta|^2_{H^{1+\mu_\ell}(T)} \\
\le& Ch^2 \sum_{\omega_\ell>\pi} |\zeta|^2_{H^{1+\mu_\ell}(\mathcal{N}_{\ell,\delta})} \\
\le& Ch^2 \|\phi_\mu^{-2}(\xi - \xi_h)\|^2_{L_{2,\mu}(\Omega)} \\
\le& Ch^2 \|\xi - \xi_h\|^2_{L_{2,-\mu}(\Omega)},
\end{aligned} \tag{5.3.7}$$

where $\mathcal{N}_{\ell,\delta} = \{x \in \Omega : |x - c_\ell| < \delta\}$ is the neighborhood around the corner c_ℓ for $1 \le \ell \le L$. Without loss of generality we may assume $h < \delta$.

Hence the estimate (5.3.4) is a direct consequence of (5.3.5), (5.3.6) and (5.3.7). Similar arguments yield

$$\|\zeta - \Pi_h\zeta\|_{L_2(\Omega)} + h|\zeta - \Pi_h\zeta|_{H^1(\Omega)} \le Ch^2\|\xi - \xi_h\|_{L_{2,-\mu}(\Omega)}. \tag{5.3.8}$$

It follows from (5.3.2), the Galerkin orthogonality (cf. (5.1.3) and (5.2.1))

$$\big(\nabla \times (\xi - \xi_h), \nabla \times v\big) + \alpha(\xi - \xi_h, v) = 0 \qquad \forall\, v \in V_h, \tag{5.3.9}$$

and (5.3.8) that

$$\begin{aligned}
\|\xi - \xi_h\|^2_{L_{2,-\mu}(\Omega)} &= \big(\nabla \times \zeta, \nabla \times (\xi - \xi_h)\big) + \alpha(\zeta, \xi - \xi_h) \\
&= \big(\nabla \times (\zeta - \Pi_h\zeta), \nabla \times (\xi - \xi_h)\big) + \alpha(\zeta - \Pi_h\zeta, \xi - \xi_h) \\
&\le C\big(\|\zeta - \Pi_h\zeta\|_{L_2(\Omega)} + \|\nabla \times (\zeta - \Pi_h\zeta)\|_{L_2(\Omega)}\big) \\
&\qquad \times \big(\|\xi - \xi_h\|_{L_2(\Omega)} + \|\nabla \times (\xi - \xi_h)\|_{L_2(\Omega)}\big) \\
&\le Ch\|\xi - \xi_h\|_{L_{2,-\mu}(\Omega)}\big(\|\xi - \xi_h\|_{L_2(\Omega)} + \|\nabla \times (\xi - \xi_h)\|_{L_2(\Omega)}\big),
\end{aligned}$$

which together with (2.1.5a) and (5.3.3) implies

$$\|\xi - \xi_h\|_{L_{2,-\mu}(\Omega)} \le Ch|\xi - \xi_h|_{H^1(\Omega)}. \tag{5.3.10}$$

Now we estimate $|\xi - \xi_h|_{H^1(\Omega)}$. Let $v \in V_h$ satisfy $(v, 1) = 0$. It follows from (2.1.5a), (5.3.3) and (5.3.9) that

$$\begin{aligned}
|\xi - \xi_h|^2_{H^1(\Omega)} + \alpha\|\xi - \xi_h\|^2_{L_2(\Omega)} &= \big(\nabla \times (\xi - \xi_h), \nabla \times (\xi - v)\big) + \alpha(\xi - \xi_h, \xi - v) \\
&\le C|\xi - \xi_h|_{H^1(\Omega)}|\xi - v|_{H^1(\Omega)},
\end{aligned}$$

which implies

$$|\xi - \xi_h|_{H^1(\Omega)} \le C|\xi - v|_{H^1(\Omega)} \qquad \forall\, v \in V_h. \tag{5.3.11}$$

It follows from (5.3.10) and (5.3.11) that

$$\|\xi - \xi_h\|_{L_{2,-\mu}(\Omega)} \le Ch \inf_{v \in V_h} |\xi - v|_{H^1(\Omega)}. \tag{5.3.12}$$

Under the assumption that $\boldsymbol{f} \in [L_2(\Omega)]^2$, we have the following stability estimate from the well-posedness of the continuous problem:

$$\|\xi\|_{H^1(\Omega)} \le C\|\boldsymbol{f}\|_{L_2(\Omega)}. \tag{5.3.13}$$

Therefore the estimate (5.3.1) follows from (5.3.12) and (5.3.13) □

Theorem 5.5. *The discrete problem* (5.2.1) *is well-posed for* $\alpha < 0$*, provided* $-\alpha$ *is not a Maxwell eigenvalue and* h *is sufficiently small. Under these conditions the estimate* (5.3.1) *remains valid.*

Proof. We follow the approach of Schatz (cf. [89]). Assuming that (5.2.1) has a solution $\xi_h \in V_h$. we can apply the same duality argument in the proof of Theorem 5.4 to obtain the estimate (5.3.10).

Let $v \in V_h$ satisfy $(v, 1) = 0$. It follows from (2.1.5a), (5.1.4), (5.2.2), (5.3.9) and (5.3.10) that

$$\begin{aligned}
|\xi - \xi_h|^2_{H^1(\Omega)} &= \big(\nabla \times (\xi - \xi_h), \nabla \times (\xi - v)\big) + \alpha(\xi - \xi_h, \xi - v) - \alpha\|\xi - \xi_h\|^2_{L_2(\Omega)} \\
&\le C\|\nabla \times (\xi - \xi_h)\|_{L_2(\Omega)}\|\nabla \times (\xi - v)\|_{L_2(\Omega)} + |\alpha|\|\xi - \xi_h\|^2_{L_{2,-\mu}(\Omega)} \\
&\le C\Big(|\xi - \xi_h|_{H^1(\Omega)}|\xi - v|_{H^1(\Omega)} + h^2|\xi - \xi_h|^2_{H^1(\Omega)}\Big).
\end{aligned}$$

Hence, for h sufficiently small,

$$|\xi - \xi_h|_{H^1(\Omega)} \le C|\xi - v|_{H^1(\Omega)} \qquad \forall\, v \in V_h,$$

which again implies (5.3.11).

In the special case where $\boldsymbol{f} = \mathbf{0}$, $\xi = 0$ and $v = 0$, we deduce from (5.2.2) and (5.3.11) that the only solution of the homogeneous discrete problem is trivial. Hence the discrete problem (5.2.1) is well-posed for h sufficient small, and then the estimate (5.3.1) follows from (5.3.10), (5.3.11) and (5.3.13). □

Corollary 5.6. *Under the assumptions in Theorem* 5.4 *and Theorem* 5.5*, we have*

$$\|\xi - \xi_h\|_{L_2(\Omega)} \leq Ch\|\boldsymbol{f}\|_{L_2(\Omega)}. \tag{5.3.14}$$

Remark 5.7. *If* $\boldsymbol{f}$ *is a piecewise smooth vector field, then it follows from* (5.3.10) *and Remark* 6.3 *in* [33] *that*

$$\|\xi - \xi_h\|_{L_2(\Omega)} \leq C_\varepsilon h^{(3/2)-\varepsilon}. \tag{5.3.15}$$

Next we compare ϕ_h and ϕ.

Lemma 5.8. *We have*

$$|\phi - \phi_h|_{H^1(\Omega)} \leq Ch\|\boldsymbol{f}\|_{L_2(\Omega)}. \tag{5.3.16}$$

Proof. Since $(\xi, 1) = 0$, there exits a unique $\tilde{\phi}_h$ such that

$$(\nabla \times \tilde{\phi}_h, \nabla \times v) = (\xi, v) \qquad \forall\, v \in V_h, \tag{5.3.17a}$$

$$(\tilde{\phi}_h, 1) = 0. \tag{5.3.17b}$$

Combine (5.2.3) and (5.3.17), we have

$$\big(\nabla \times (\tilde{\phi}_h - \phi_h), \nabla \times v\big) = (\xi - \xi_h, v) \qquad \forall\, v \in V_h, \tag{5.3.18}$$

and $(\tilde{\phi}_h - \phi_h, 1) = 0$. Then from (2.1.5a), (5.3.14) and (5.3.18), we arrive at

$$\begin{aligned} |\tilde{\phi}_h - \phi_h|^2_{H^1(\Omega)} &= \|\nabla \times (\tilde{\phi}_h - \phi_h)\|^2_{L_2(\Omega)} \\ &= (\xi - \xi_h, \tilde{\phi}_h - \phi_h) \\ &\leq \|\xi - \xi_h\|_{L_2(\Omega)}\|\tilde{\phi}_h - \phi_h\|_{L_2(\Omega)} \\ &\leq Ch\|\boldsymbol{f}\|_{L_2(\Omega)}|\tilde{\phi}_h - \phi_h|_{H^1(\Omega)}, \end{aligned} \tag{5.3.19}$$

which implies

$$|\tilde{\phi}_h - \phi_h|_{H^1(\Omega)} \leq Ch\|\boldsymbol{f}\|_{L_2(\Omega)}. \tag{5.3.20}$$

By subtracting (5.3.17a) from (5.1.11), we obtain the Galerkin relation

$$(\nabla \times (\phi - \tilde{\phi}_h), \nabla \times v) = 0 \qquad \forall\, v \in V_h, \tag{5.3.21}$$

which together with the arguments in Theorem 5.4 (for $\alpha = 0$) implies

$$|\phi - \tilde{\phi}_h|_{H^1(\Omega)} = \inf_{v \in V_h} |\phi - v|_{H^1(\Omega)} \leq Ch\|\xi\|_{L_2(\Omega)}. \tag{5.3.22}$$

Therefore the estimate (5.3.16) follows from (5.3.13), (5.3.20) and (5.3.22). □

We then turn to compare $\varphi_{j,h}$ and φ_j.

Lemma 5.9. *We have, for* $1 \leq j \leq m$,

$$|\varphi_j - \varphi_{j,h}|_{H^1(\Omega)} \leq Ch. \tag{5.3.23}$$

Proof. In view of (5.1.9) and (5.2.4), the Galerkin relation

$$\big(\nabla(\varphi_j - \varphi_{j,h}), \nabla v\big) = 0 \qquad \forall\, v \in V_h \cap H_0^1(\Omega),$$

implies that

$$|\varphi_j - \varphi_{j,h}|_{H^1(\Omega)} = \inf_{\substack{v \in V_h \\ v|_{\partial\Omega} = \varphi_j|_{\partial\Omega}}} |\varphi_j - v|_{H^1(\Omega)} \leq |\varphi_j - \Pi_h \varphi_j|_{H^1(\Omega)}. \tag{5.3.24}$$

Combining (5.3.24), the interpolation error estimate for Dirichlet problem (cf. [33, Section 5]) and similar arguments in the proof of Theorem 5.4 implies (5.3.23). □

Next we compare $c_{j,h}$ and c_j. First we observe that (5.3.23) implies

$$\big|(\boldsymbol{f}, \nabla\varphi_j) - (\boldsymbol{f}, \nabla\varphi_{j,h})\big| \leq Ch\|\boldsymbol{f}\|_{L_2(\Omega)} \qquad \text{for} \quad 1 \leq j \leq m. \tag{5.3.25}$$

Furthermore, since $\varphi_i - \varphi_{i,h} \in H_0^1(\Omega)$ for $1 \leq i \leq m$, (5.1.9a) implies

$$(\nabla\varphi_i, \nabla\varphi_j) - (\nabla\varphi_{i,h}, \nabla\varphi_{j,h}) = (\nabla(\varphi_i - \varphi_{i,h}), \nabla(\varphi_{j,h} - \varphi_j)) \qquad \text{for} \quad 1 \leq i, j \leq m,$$

and hence, in view of (5.3.23),

$$\big|(\nabla\varphi_i, \nabla\varphi_j) - (\nabla\varphi_{i,h}, \nabla\varphi_{j,h})\big| \leq Ch^2 \qquad \text{for} \quad 1 \leq i, j \leq m. \tag{5.3.26}$$

Lemma 5.10. *For h sufficiently small, we have*

$$|c_j - c_{j,h}| \le Ch\|\boldsymbol{f}\|_{L_2(\Omega)} \qquad \text{for} \quad 1 \le j \le m. \tag{5.3.27}$$

Proof. We can write (5.1.12) and (5.2.5) as

$$\mathbf{A}\mathbf{c} = \mathbf{b} \quad \text{and} \quad \mathbf{A}_h\mathbf{c}_h = \mathbf{b}_h,$$

where $\mathbf{c} \in \mathbb{R}^m$ (resp. $\mathbf{c}_h \in \mathbb{R}^m$) is the vector whose j-th component is c_j (resp. $c_{j,h}$), $\mathbf{A} \in \mathbb{R}^{m\times m}$ (resp. $\mathbf{A}_h \in \mathbb{R}^{m\times m}$) is the matrix whose (i,j)-th component is $(\nabla\varphi_j, \nabla\varphi_i)$ (resp. $(\nabla\varphi_{j,h}, \nabla\varphi_{i,h})$), and $\mathbf{b} \in \mathbb{R}^m$ (resp. $\mathbf{b}_h \in \mathbb{R}^m$) is the vector whose j-th component is $\alpha^{-1}(\boldsymbol{f}, \nabla\varphi_j)$ (resp. $\alpha^{-1}(\boldsymbol{f}, \nabla\varphi_{j,h})$).

Note that

$$\|\mathbf{b}\|_\infty \le |\alpha|^{-1}\big(\max_{1\le j\le m} \|\nabla\varphi_j\|_{L_2(\Omega)}\big)\|\boldsymbol{f}\|_{L_2(\Omega)} \le C\|\boldsymbol{f}\|_{L_2(\Omega)}, \tag{5.3.28}$$

and the estimates (5.3.25)–(5.3.26) are translated into

$$\|\mathbf{b} - \mathbf{b}_h\|_\infty \le Ch\|\boldsymbol{f}\|_{L_2(\Omega)} \quad \text{and} \quad \|\mathbf{A} - \mathbf{A}_h\|_\infty \le Ch^2. \tag{5.3.29}$$

The estimate (5.3.27) follows from the identity

$$\mathbf{c} - \mathbf{c}_h = \mathbf{A}^{-1}\mathbf{b} - \mathbf{A}_h^{-1}\mathbf{b}_h = \mathbf{A}^{-1}(\mathbf{b} - \mathbf{b}_h) + \mathbf{A}^{-1}(\mathbf{A}_h - \mathbf{A})\mathbf{A}_h^{-1}\big((\mathbf{b}_h - \mathbf{b}) + \mathbf{b}\big)$$

and (5.3.28)–(5.3.29). ∎

Remark 5.11. *In view of Remark* 6.8 *in* [33]*, in the case where $\boldsymbol{f}$ is piecewise smooth, the estimate* (5.3.27) *can be improved to*

$$|c_j - c_{j,h}| \le C_\epsilon h^{(3/2)-\epsilon} \qquad \text{for any } \epsilon \text{ and} \quad 1 \le j \le m. \tag{5.3.30}$$

Finally, we can compare $\boldsymbol{u}_h$ and $\boldsymbol{u}$ by putting all the estimates together.

Theorem 5.12. *For h sufficiently small, we have*

$$\|\boldsymbol{u} - \boldsymbol{u}_h\|_{L_2(\Omega)} \le Ch\|\boldsymbol{f}\|_{L_2(\Omega)}. \tag{5.3.31}$$

Proof. First we observe that the solutions $c_1, \ldots, c_m$ of (5.1.12) satisfy

$$|c_j| \le C\|\boldsymbol{f}\|_{L_2(\Omega)} \qquad \text{for} \quad 1 \le j \le m. \tag{5.3.32}$$

Secondly we have, from (5.1.6) and (5.2.6),

$$\begin{aligned}
\|\boldsymbol{u} - \boldsymbol{u}_h\|_{L_2(\Omega)} &\le |\phi - \phi_h|_{H^1(\Omega)} + \sum_{j=1}^{m} |c_j\varphi_j - c_{j,h}\varphi_{j,h}|_{H^1(\Omega)} \\
&\le |\phi - \phi_h|_{H^1(\Omega)} + \sum_{j=1}^{m} \big(|c_j - c_{j,h}|\,|\varphi_j|_{H^1(\Omega)} + |c_{j,h}|\,|\varphi_j - \varphi_{j,h}|_{H^1(\Omega)}\big) \\
&\le |\phi - \phi_h|_{H^1(\Omega)} + \sum_{j=1}^{m} |c_j - c_{j,h}|\big(|\varphi_j|_{H^1(\Omega)} + |\varphi_j - \varphi_{j,h}|_{H^1(\Omega)}\big) \\
&\quad + \sum_{j=1}^{m} |c_j|\,|\varphi_j - \varphi_{j,h}|_{H^1(\Omega)}.
\end{aligned} \tag{5.3.33}$$

The estimate (5.3.31) follows from (5.3.16), (5.3.23), (5.3.27), (5.3.32) and (5.3.33).

□

Chapter 6

Multigrid Methods for Maxwell's Equations

In this chapter we first introduce multigrid methods for the nonconforming finite element methods, which were developed in Chapter 3 for solving the CCGD problem (1.2.9). We report the numerical results on a square domain with uniform meshes. Then we study multigrid methods for the P_1 finite element method introduced in Chapter 5 for solving the two-dimensional Maxwell's equation (5.1.1). Numerical results on graded meshes are reported.

6.1 Multigrid Methods for Nonconforming Finite Element Methods

Let $\mathcal{T}_k$ be a family of uniform triangulations on the unit square, h_k be the mesh size of $\mathcal{T}_k$. Let V_k be the space of weakly continuous P_1 vector fields associated with $\mathcal{T}_k$ for $k \geq 0$. More precisely, let $\mathcal{E}_k$ (resp. $\mathcal{E}_k^b$ and $\mathcal{E}_k^i$) be the set of the edges (resp. boundary edges and interior edges) of $\mathcal{T}_k$. Then

$$\begin{aligned} V_k = \{\boldsymbol{v} \in [L_2(\Omega)]^2 : \boldsymbol{v}_T = \boldsymbol{v}\big|_T \in [P_1(T)]^2 \quad \forall\, T \in \mathcal{T}_k, \\ \boldsymbol{v} \text{ is continuous at the midpoint of any } e \in \mathcal{E}_k, \\ \boldsymbol{n} \times \boldsymbol{v} \text{ vanishes at the midpoint of any } e \in \mathcal{E}_k^b\}. \end{aligned}$$

Let $a_k(\cdot,\cdot)$ be the analog of $a_h(\cdot,\cdot)$, which is defined by (3.2.15). The k-th level nonconforming finite element method for (1.2.9) is:
Find $\boldsymbol{u}_k \in V_k$ such that

$$a_k(\boldsymbol{u}_k, \boldsymbol{v}) = (\boldsymbol{f}, \boldsymbol{v}) \qquad \forall\, \boldsymbol{v} \in V_k. \tag{6.1.1}$$

Note that the edge weight $\Phi_\mu(e)$ in the definition of $a_k(\cdot,\cdot)$ equals 1 for all $e \in \mathcal{E}_k$ on the square domain.

We can rewrite (6.1.1) as

$$A_k \boldsymbol{u}_k = \boldsymbol{f}_k, \tag{6.1.2}$$

where $A_k : V_k \longrightarrow V_k'$ and $\boldsymbol{f}_k \in V_k'$ are defined by

$$\langle A_k \boldsymbol{w}, \boldsymbol{v} \rangle = a_k(\boldsymbol{w}, \boldsymbol{v}) \qquad \forall\, \boldsymbol{v}, \boldsymbol{w} \in V_k, \tag{6.1.3}$$

$$\langle \boldsymbol{f}_k, \boldsymbol{v} \rangle = (\boldsymbol{f}, \boldsymbol{v}) \qquad \forall\, \boldsymbol{v} \in V_k. \tag{6.1.4}$$

Here $\langle \cdot, \cdot \rangle$ is the canonical bilinear form on $V_k' \times V_k$.

We consider the W-cycle multigrid algorithm (Algorithm 2.32) for the equation

$$A_k \boldsymbol{z} = \boldsymbol{g}, \tag{6.1.5}$$

where $\boldsymbol{g} \in V_k'$.

The operator B_k used in the smoothing steps is taken to be $h_k^2 Id_k$, where Id_k is the identity operator on V_k.

We first define the coarse-to-fine intergrid transfer operator $I_{k-1}^k : V_{k-1} \longrightarrow V_k$ by averaging. More precisely, let m_e be a midpoint of an interior edge e in $\mathcal{T}_k$, then we define

$$(I_{k-1}^k \boldsymbol{v})(m_e) = \frac{1}{2}\big(\boldsymbol{v}_1(m_e) + \boldsymbol{v}_2(m_e)\big),$$

where $\boldsymbol{v}_i = \boldsymbol{v}\big|_{T_i}$ for $i = 1, 2$ and T_1, T_2 are the triangles in $\mathcal{T}_{k-1}$ that share e as a common edge. If $e \in \partial\Omega$, then we define

$$(I_{k-1}^k \boldsymbol{v})(m_e) = 0.$$

Recall that the error propagation operator $E_k : V_k \longrightarrow V_k$ for the k-th level W-cycle algorithm has the following recursive relation:

$$E_k = R_k^{m_2}(Id_k - I_{k-1}^k P_k^{k-1} + I_{k-1}^k E_{k-1}^2 P_k^{k-1}) R_k^{m_1},$$

where $R_k : V_k \longrightarrow V_k$ is defined by (2.5.19), and $P_k^{k-1} : V_{k-1} \longrightarrow V_k$ is the transpose of I_{k-1}^k with respect to the variational forms, i.e.,

$$a_{k-1}(P_k^{k-1}\boldsymbol{w}, \boldsymbol{v}) = a_k(\boldsymbol{w}, I_{k-1}^k \boldsymbol{v}) \qquad \forall\, \boldsymbol{v} \in V_{k-1},\, \boldsymbol{w} \in V_k.$$

Let the mesh-dependent norms $\|\boldsymbol{v}\|_{1,k}$ be defined by

$$\|\boldsymbol{v}\|_{1,k}^2 = \langle A_k \boldsymbol{v}, \boldsymbol{v}\rangle = a_k(\boldsymbol{v}, \boldsymbol{v}) \qquad \forall\, \boldsymbol{v} \in V_k,\ k \geq 1. \tag{6.1.6}$$

The contraction numbers of the W-cycle algorithm with respect to the norm $\|\cdot\|_{1,k}$ are tabulated in Table 6.1. We take $\gamma = 1$ and $\alpha = 1$ in the definition of $a_k(\cdot,\cdot)$. We use $\lambda = 1/20$ as the damping factor in (2.5.13) such that the condition (2.5.14) is satisfied. We find that the W-cycle algorithm is a contraction for $m \geq 7$.

TABLE 6.1. Contraction numbers of the W-cycle algorithm on the square domain $(0,1)^2$ for the nonconforming finite element method with I_{k-1}^k being averaging

	$k=1$	$k=2$	$k=3$	$k=4$	$k=5$	$k=6$	$k=7$
$m=7$	0.82	0.71	0.94	0.81	0.85	0.85	0.83
$m=8$	0.74	0.69	0.86	0.74	0.79	0.79	0.76
$m=9$	0.67	0.67	0.78	0.71	0.71	0.71	0.71
$m=10$	0.61	0.68	0.73	0.68	0.71	0.70	0.71
$m=11$	0.56	0.70	0.71	0.70	0.71	0.70	0.71
$m=12$	0.52	0.70	0.69	0.70	0.70	0.70	0.70
$m=13$	0.48	0.69	0.68	0.79	0.69	0.69	0.70

Next, we choose the coarse-to-fine intergrid transfer operator $I_{k-1}^k : V_{k-1} \longrightarrow V_k$ as follows. For any $\boldsymbol{v} \in V_{k-1}$, we define $(I_{k-1}^k \boldsymbol{v})(m_e)$ by averaging if e is a part of an edge in $\mathcal{E}_{k-1}$. Otherwise, for any $T \in \mathcal{T}_k$, the value of $(I_{k-1}^k \boldsymbol{v})(m_e)$ is determined by the following conditions:

$$\nabla \times (I_{k-1}^k \boldsymbol{v}) = \nabla \times \boldsymbol{v} \qquad \text{on } T, \tag{6.1.7a}$$

$$\nabla \cdot (I_{k-1}^k \boldsymbol{v}) = \nabla \cdot \boldsymbol{v} \qquad \text{on } T. \tag{6.1.7b}$$

The contraction numbers of the W-cycle algorithm with such choice of I_{k-1}^k are tabulated in Table 6.2. We take $\gamma = 1$, $\alpha = 1$ and $\lambda = 1/20$. The W-cycle algorithm is a contraction for $m \geq 6$ in this case.

TABLE 6.2. Contraction numbers of the W-cycle algorithm on the square domain $(0, 1)^2$ for the nonconforming finite element method

	$k=1$	$k=2$	$k=3$	$k=4$	$k=5$	$k=6$	$k=7$
$m=6$	0.90	0.87	0.97	0.98	0.92	0.93	0.93
$m=7$	0.86	0.81	0.91	0.85	0.82	0.82	0.83
$m=8$	0.83	0.80	0.81	0.74	0.70	0.70	0.69
$m=9$	0.78	0.58	0.58	0.62	0.60	0.60	0.60
$m=10$	0.72	0.53	0.55	0.56	0.56	0.56	0.53
$m=11$	0.68	0.50	0.51	0.49	0.50	0.50	0.49
$m=12$	0.65	0.46	0.47	0.46	0.46	0.45	0.46

Finally, we consider multigrid methods for the discontinuous finite element method, which was introduced in Section 3.3.

Let $\tilde{V}_k$ be the space of discontinuous P_1 vector fields, i.e.,

$$\tilde{V}_k = \{\boldsymbol{v} \in [L_2(\Omega)]^2 : \boldsymbol{v}_T = \boldsymbol{v}\big|_T \in [P_1(T)]^2 \quad \forall T \in \mathcal{T}_k\}.$$

Let $\tilde{a}_k(\cdot,\cdot)$ be the analog of $\tilde{a}_h(\cdot,\cdot)$, which is defined by (3.3.2). The k-th level discontinuous finite element method for (1.2.9) is:

Find $\boldsymbol{u}_k \in \tilde{V}_k$ such that

$$\tilde{a}_k(\boldsymbol{u}_k, \boldsymbol{v}) = (\boldsymbol{f}, \boldsymbol{v}) \qquad \forall\, \boldsymbol{v} \in \tilde{V}_k. \tag{6.1.8}$$

We can rewrite (6.1.8) as

$$A_k \boldsymbol{u}_k = \boldsymbol{f}_k, \tag{6.1.9}$$

where $A_k : \tilde{V}_k \longrightarrow \tilde{V}_k'$ and $\boldsymbol{f}_k \in \tilde{V}_k'$ are defined by

$$\langle A_k \boldsymbol{w}, \boldsymbol{v}\rangle = \tilde{a}_k(\boldsymbol{w}, \boldsymbol{v}) \qquad \forall\, \boldsymbol{v}, \boldsymbol{w} \in \tilde{V}_k, \tag{6.1.10}$$

$$\langle \boldsymbol{f}_k, \boldsymbol{v}\rangle = (\boldsymbol{f}, \boldsymbol{v}) \qquad \forall\, \boldsymbol{v} \in \tilde{V}_k. \tag{6.1.11}$$

Here $\langle \cdot, \cdot \rangle$ is the canonical bilinear form on $\tilde{V}_k' \times \tilde{V}_k$.

We consider the W-cycle multigrid algorithm (Algorithm 2.32) for the equation $A_k \boldsymbol{z} = \boldsymbol{g}$, where $\boldsymbol{g} \in \tilde{V}_k'$.

Let the coarse-to-fine intergrid transfer operator $I_{k-1}^k : \tilde{V}_{k-1} \longrightarrow \tilde{V}_k$ satisfy (6.1.7) such that $I_{k-1}^k \boldsymbol{v}$ is continuous at the midpoints of interior edges. Let the operator $B_k : \tilde{V}_k \longrightarrow \tilde{V}_k'$ be defined by

$$\begin{aligned}\langle B_k \boldsymbol{w}, \boldsymbol{v} \rangle =& h_k^2 (\boldsymbol{w}, \boldsymbol{v}) + \sum_{e \in \mathcal{E}_k} \frac{1}{|e|} \int_e (\Pi_e^0 [\![\boldsymbol{n} \times \boldsymbol{w}]\!])\, (\Pi_e^0 [\![\boldsymbol{n} \times \boldsymbol{v}]\!]) ds \\ &+ \sum_{e \in \mathcal{E}_k^i} \frac{1}{|e|} \int_e (\Pi_e^0 [\![\boldsymbol{n} \cdot \boldsymbol{w}]\!])(\Pi_e^0 [\![\boldsymbol{n} \cdot \boldsymbol{v}]\!]) ds \qquad \forall\, \boldsymbol{v}, \boldsymbol{w} \in \tilde{V}_k,\end{aligned}$$

where $|e|$ denotes the length of the edge e, and Π_e^0 is the orthogonal projection from $L_2(e)$ to the space of constant functions on e.

Let the mesh-dependent norms $|\!|\!| \boldsymbol{v} |\!|\!|_{1,k}$ be defined by

$$|\!|\!| \boldsymbol{v} |\!|\!|_{1,k}^2 = \langle A_k \boldsymbol{v}, \boldsymbol{v} \rangle = \tilde{a}_k(\boldsymbol{v}, \boldsymbol{v}) \qquad \forall\, \boldsymbol{v} \in \tilde{V}_k,\ k \geq 1. \tag{6.1.12}$$

The contraction numbers of the W-cycle algorithm with respect to the norm $|\!|\!| \cdot |\!|\!|_{1,k}$ are tabulated in Table 6.3. We take $\gamma = 1$ and $\alpha = 1$ in the definition of $\tilde{a}_k(\cdot, \cdot)$ and the damping factor $\lambda = 1/10$.

TABLE 6.3. Contraction numbers of the W-cycle algorithm on the square domain $(0,1)^2$ for the discontinuous finite element method

	$k=1$	$k=2$	$k=3$	$k=4$	$k=5$	$k=6$	$k=7$
$m=9$	0.99	0.61	0.52	0.52	0.52	0.52	0.52
$m=10$	0.91	0.54	0.48	0.48	0.49	0.49	0.49
$m=11$	0.81	0.54	0.45	0.45	0.45	0.45	0.45
$m=12$	0.76	0.54	0.42	0.42	0.42	0.42	0.42
$m=13$	0.72	0.65	0.52	0.39	0.39	0.39	0.39
$m=14$	0.59	0.50	0.36	0.36	0.36	0.37	0.34
$m=15$	0.50	0.46	0.33	0.32	0.32	0.32	0.32

The convergence analysis of multigrid methods for the discrete problems (6.1.1) and (6.1.8) is currently under investigation. Graded meshes must be used on non-convex domains in order to achieve the uniform convergence of multigrid algorithms.

6.2 Multigrid Methods for the P_1 Finite Element Method

In this section we consider the multigrid methods for the P_1 finite element method, which was proposed in Chapter 5 for solving the two-dimensional Maxwell's equation (5.1.1).

Let $\mathcal{T}_0, \mathcal{T}_1, \ldots$ be a sequence of triangulations generated by the refinement procedure that was described in Section 2.3, h_k be the mesh size of $\mathcal{T}_k$, V_k be the corresponding P_1 finite element space associated with $\mathcal{T}_k$ for $k \geq 0$. We define

$$a(w,v) = (\nabla \times w, \nabla \times v) + \alpha(w,v) \qquad \forall\, v, w \in H^1(\Omega). \tag{6.2.1}$$

The k-th level P_1 finite element method for (5.1.3) ($\alpha \neq 0$) is:

Find $\xi_k \in V_k$ such that

$$A_k \xi_k = f_k, \tag{6.2.2}$$

where $A_k : V_k \longrightarrow V_k'$ and $f_k \in V_k'$ are defined by

$$\begin{aligned} \langle A_k w, v \rangle &= a(w,v) \qquad && \forall\, v, w \in V_k, \\ \langle f_k, v \rangle &= (\boldsymbol{f}, \nabla \times v) \qquad && \forall\, v \in V_k. \end{aligned}$$

Here $\langle \cdot, \cdot \rangle$ is the canonical bilinear form on $V_k' \times V_k$.

We consider the W-cycle multigrid algorithm (Algorithm 2.32) for the equation

$$A_k z = g, \tag{6.2.3}$$

where $g \in V_k'$.

The error propagation operator $E_k : V_k \longrightarrow V_k$ for the k-th level W-cycle algorithm has the following recursive relation (cf. Lemma 2.33):

$$E_k = R_k^{m_2}(Id_k - I_{k-1}^k P_k^{k-1} + I_{k-1}^k E_{k-1}^2 P_k^{k-1}) R_k^{m_1}.$$

Here the coarse-to-fine intergrid transfer operator $I_{k-1}^k : V_{k-1} \longrightarrow V_k$ is taken to be the natural injection and the operator $P_k^{k-1} : V_k \longrightarrow V_{k-1}$ is the transpose of I_{k-1}^k with respect to the variational forms, i.e.,

$$a(P_k^{k-1}w, v) = a(w, I_{k-1}^k v) \qquad \forall\, v \in V_{k-1},\, w \in V_k. \tag{6.2.4}$$

The operator $B_k : V_k \longrightarrow V_k'$ in the definition of R_k (cf. (2.5.19)) is defined by

$$\langle B_k w, v\rangle = h_k^2 \sum_{T\in\mathcal{T}_k} \sum_{p\in\mathcal{N}_T} w(p)v(p) \qquad \forall\, v, w \in V_k, \tag{6.2.5}$$

where $\mathcal{N}_T$ is the set of the vertices of the triangle T.

In the application of k-th level iteration to (6.2.2), we use the following full multigrid algorithm, where we apply W-cycle algorithm r times at each level.

Algorithm 6.1. *Full Multigrid Algorithm for* (6.2.2).
For $k = 0$, $\widehat{\xi}_0 = A_0^{-1} f_0$.
For $k \geq 1$, *the solution* $\widehat{\xi}_k$ *is obtained recursively from*

$$\begin{aligned} \xi_0^k &= I_{k-1}^k \widehat{\xi}_{k-1}, \\ \xi_\ell^k &= MG_W(k, f_k, \xi_{\ell-1}^k, m_1, m_2), \quad 1 \leq \ell \leq r, \\ \widehat{\xi}_k &= \xi_r^k. \end{aligned}$$

In the case where $m \geq 1$, we can apply the full multigrid algorithm to obtain an approximate solution $\widehat{\varphi}_{j,k}$ $(1 \leq j \leq m)$ of the k-th level discrete problem (5.2.4) for the Dirichlet boundary value problem (5.1.9).

When Ω is not simply connected, for each level k, we compute $\widehat{c}_{1,k}, \ldots, \widehat{c}_{m,k}$ by solving

$$\sum_{j=1}^{m} (\nabla\widehat{\varphi}_{j,k}, \nabla\widehat{\varphi}_{i,k})\widehat{c}_{j,k} = \frac{1}{\alpha}(\boldsymbol{f}, \nabla\widehat{\varphi}_{i,k}) \quad \text{for } 1 \leq i \leq m. \tag{6.2.6}$$

In the rest of this section we introduce the multigrid methods for solving (5.1.3) $(\alpha = 0)$ and (5.1.11), which are singular Neumann problems.

Let $\widehat{V}_k = \{v \in V_k : (v, 1) = 0\}$. The k-th level P_1 finite element method for (5.1.3) ($\alpha = 0$) is as follows:

Find $\xi_k \in \widehat{V}_k$ such that

$$\tilde{A}_k \xi_k = f_k, \tag{6.2.7}$$

where $\tilde{A}_k : \widehat{V}_k \longrightarrow \widehat{V}_k'$ and $f_k \in \widehat{V}_k'$ are defined by

$$\begin{aligned} \langle \tilde{A}_k w, v\rangle &= (\nabla \times w, \nabla \times v) \qquad && \forall\, v, w \in \widehat{V}_k, \\ \langle f_k, v\rangle &= (\boldsymbol{f}, \nabla \times v) && \forall\, v \in \widehat{V}_k. \end{aligned}$$

Here $\langle \cdot, \cdot\rangle$ is the canonical bilinear form on $\widehat{V}_k' \times \widehat{V}_k$. We can apply Algorithm 6.1 to obtain an approximate solution $\widehat{\xi_k}$ of (6.2.7).

In practice, we consider the following k-th level P_1 finite element method for (5.1.11):

Find $\phi_k \in \widehat{V}_k$ such that

$$\tilde{A}_k \phi_k = g_k, \tag{6.2.8}$$

where $g_k \in \widehat{V}_k'$ is defined by

$$\langle g_k, v\rangle = (\widehat{\xi_k}, v) \qquad \forall\, v \in \widehat{V}_k.$$

Here $\widehat{\xi_k}$ is the approximate solution of (6.2.2) ($\alpha \neq 0$) or (6.2.7) ($\alpha = 0$) obtained by the Algorithm 6.1.

We now apply the following full multigrid algorithm to solve (6.2.8):

Algorithm 6.2. *Full Multigrid Algorithm for* (6.2.8).

For $k = 0$, $\widehat{\phi}_0 \in \widehat{V}_0$ *is determined by* $\tilde{A}_0 \widehat{\phi}_0 = g_0$.

For $k \geq 1$, the approximation solution $\widehat{\phi}_k$ is obtained recursively from

$$\begin{aligned}
\phi_0^k &= I_{k-1}^k \widehat{\phi}_{k-1}, \\
\phi_\ell^k &= MG_W(k, g_k, \phi_{\ell-1}^k, m_1, m_2), \quad 1 \leq \ell \leq r, \\
\widehat{\phi}_k &= \phi_r^k.
\end{aligned}$$

Finally, we define the approximation $\widehat{\boldsymbol{u}}_k$ of $\boldsymbol{u}$ for each level k by

$$\widehat{\boldsymbol{u}}_k = \nabla \times \widehat{\phi}_k + \sum_{j=1}^{m} \widehat{c}_{j,k} \nabla \widehat{\varphi}_{j,k}. \tag{6.2.9}$$

The convergence analysis of multigrid methods introduced in this section is currently under investigation.

In the rest of this section we report the numerical results for the P_1 finite element method. The numerical solutions presented in Tables 6.4– 6.8 are obtained by full multigrid methods, where r is taken to be 2, and the smoothing steps m is taken to be 5.

The first set of experiments is performed on the unit square $(0,1)^2$ with uniform meshes. First we take the exact solution to be

$$\boldsymbol{u} = \begin{bmatrix} \sin(\pi x_2) \\ \\ \sin(\pi x_1) \end{bmatrix} \tag{6.2.10}$$

and solve (5.1.1) for $\alpha = -1$, $0\,\text{and}\,1$ with $\boldsymbol{f} = \nabla \times (\nabla \times \boldsymbol{u}) - \alpha \boldsymbol{u} \in H(\text{div}^0; \Omega)$. The results are tabulated in Table 6.4.

We then take the right-hand side function to be

$$\boldsymbol{f} = \begin{cases} \begin{bmatrix} 1 \\ 0 \end{bmatrix} & \text{if } x_1 \leq x_2, \\ \begin{bmatrix} 0 \\ 2 \end{bmatrix} & \text{if } x_1 > x_2. \end{cases} \tag{6.2.11}$$

TABLE 6.4. Results for (5.1.1) on the square domain $(0,1)^2$ with uniform meshes and the exact solution given by (6.2.10)

h_k	$\frac{\|\nabla\times\boldsymbol{u}-\widehat{\xi}_k\|_{L_2}}{\|\boldsymbol{f}\|_{L_2}}$	Order	h_k	$\frac{\|\boldsymbol{u}-\widehat{\boldsymbol{u}}_k\|_{L_2}}{\|\boldsymbol{f}\|_{L_2}}$	Order
		$\alpha=-1$			
1/16	4.07E−04	1.98	1/16	6.38E−03	0.99
1/32	1.01E−05	2.00	1/32	3.19E−03	1.00
1/64	2.53E−05	2.00	1/64	1.60E−03	1.00
1/128	6.31E−06	2.00	1/128	7.99E−04	1.00
1/256	1.58E−06	2.00	1/265	3.99E−04	1.00
		$\alpha=0$			
1/16	3.68E−04	1.98	1/16	5.73E−03	0.99
1/32	9.13E−05	2.00	1/32	2.87E−03	1.00
1/64	2.27E−05	2.00	1/64	1.43E−03	1.00
1/128	5.68E−06	2.00	1/128	7.18E−04	1.00
1/256	1.42E−06	2.00	1/265	3.59E−04	1.00
		$\alpha=1$			
1/16	3.41E−04	2.00	1/16	5.20E−03	0.99
1/32	8.44E−05	2.01	1/32	2.60E−03	1.00
1/64	2.10E−05	2.01	1/64	1.30E−03	1.00
1/128	5.24E−06	2.00	1/128	6.52E−04	1.00
1/256	1.31E−06	2.00	1/265	3.26E−04	1.00

Since the exact solution is not known, we estimate the errors by the differences of the numerical solutions between two consecutive levels. The results are tabulated in Table 6.5 for $\alpha=-1$, 0 and 1.

In the second set of experiments, we examine the convergence behavior of our numerical schemes on the L-shaped domain $(-1,1)^2\setminus[0,1]^2$. The exact solution is taken to be

$$\boldsymbol{u}=\nabla\times\Big(r^{2/3}\cos\Big(\frac{2}{3}\theta-\frac{\pi}{3}\Big)\phi(x)\Big),\qquad (6.2.12)$$

where (r,θ) are the polar coordinates at the origin and $\phi(x)=(1-x_1^2)^2(1-x_2^2)^2$.

We check the performance of the numerical scheme on graded meshes. The grading parameter is taken to be 2/3 at the reentrant corner $(0,0)$ (cf. Figure 6.1). The results are tabulated in Table 6.6 for $\alpha=-1$, 0 and 1.

The goal of the third set of experiments is to exam the convergence behavior of the numerical schemes on a doubly connected domain

$$\Omega=(0,4)^2\setminus[1,3]^2.$$

TABLE 6.5. Results for (5.1.1) on the square domain $(0,1)^2$ with uniform meshes and right-hand side function given by (6.2.11)

h_k	$\frac{\|\nabla\times\boldsymbol{u}-\widehat{\xi}_k\|_{L_2}}{\|\boldsymbol{f}\|_{L_2}}$	Order	h	$\frac{\|\boldsymbol{u}-\widehat{\boldsymbol{u}}_k\|_{L_2}}{\|\boldsymbol{f}\|_{L_2}}$	Order
		$\alpha=-1$			
1/8	2.92E−03	1.42	1/8	7.30E−03	0.93
1/16	1.06E−03	1.47	1/16	3.70E−03	0.98
1/32	3.76E−04	1.49	1/32	1.86E−03	0.99
1/64	1.34E−04	1.49	1/64	9.31E−04	1.00
1/128	4.73E−05	1.50	1/128	4.65E−04	1.00
		$\alpha=0$			
1/8	2.82E−03	1.40	1/8	6.61E−03	0.93
1/16	1.04E−03	1.45	1/16	3.35E−03	0.98
1/32	3.72E−04	1.47	1/32	1.68E−03	0.99
1/64	1.34E−04	1.49	1/64	8.43E−04	1.00
1/128	4.73E−05	1.49	1/128	4.22E−04	1.00
		$\alpha=1$			
1/8	2.73E−03	1.39	1/8	6.05E−03	0.92
1/16	1.02E−03	1.43	1/16	3.07E−03	0.98
1/32	3.69E−04	1.46	1/32	1.54E−03	0.99
1/64	1.32E−04	1.48	1/64	7.72E−04	1.00
1/128	4.71E−05	1.49	1/128	3.86E−04	1.00

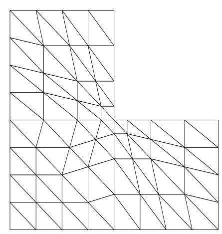

FIGURE 6.1. Graded meshes on the L-shaped domain

The solution $\boldsymbol{u}$ of (5.1.1) can be written as

$$\boldsymbol{u} = \nabla\times\phi + c\nabla\varphi, \tag{6.2.13}$$

where c is a constant number and the harmonic function φ satisfies the following boundary conditions:

$$\varphi\big|_{\Gamma_0} = 0 \quad \text{and} \quad \varphi\big|_{\Gamma_1} = 1.$$

Here Γ_0 (resp. Γ_1) is the boundary of $(0,4)^2$ (resp. $(1,3)^2$).

First we take the exact solution to be

$$\boldsymbol{u} = \begin{bmatrix} x_2(1-x_2)(3-x_2)(4-x_2) \\ \\ x_1(1-x_1)(3-x_1)(4-x_1) \end{bmatrix} \tag{6.2.14}$$

TABLE 6.6. Results for (5.1.1) on the L-shaped domain and the exact solution given by (6.2.12)

h_k	$\frac{\|\nabla\times\boldsymbol{u}-\widehat{\xi}_k\|_{L_2}}{\|\boldsymbol{f}\|_{L_2}}$	Order	h	$\frac{\|\boldsymbol{u}-\widehat{\boldsymbol{u}}_k\|_{L_2}}{\|\boldsymbol{f}\|_{L_2}}$	Order
$\alpha=-1$					
1/16	4.95E−03	1.86	1/16	7.34E−03	1.55
1/32	1.37E−03	1.88	1/32	2.97E−03	1.30
1/64	3.63E−04	1.89	1/64	1.38E−03	1.11
1/128	9.75E−05	1.90	1/128	6.77E−04	1.02
1/256	2.60E−05	1.90	1/256	3.40E−04	0.99
$\alpha=0$					
1/16	2.03E−03	1.84	1/16	5.21E−03	1.13
1/32	5.55E−04	1.87	1/32	2.55E−03	1.02
1/64	1.50E−04	1.88	1/64	1.28E−03	0.99
1/128	4.04E−05	1.89	1/128	6.49E−04	0.98
1/256	1.08E−05	1.90	1/256	3.29E−04	0.98
$\alpha=1$					
1/16	1.43E−03	1.85	1/16	4.88E−03	1.03
1/32	3.87E−04	1.89	1/32	2.45E−03	0.99
1/64	1.03E−04	1.91	1/64	1.24E−03	0.98
1/128	2.74E−05	1.91	1/128	6.29E−04	0.98
1/256	7.25E−06	1.92	1/256	3.19E−04	0.98

and check the convergence behavior of the numerical schemes on Ω with graded meshes. The grading parameter is taken to be 2/3 at the reentrant corners $(1,1)$, $(1,3)$, $(3,1)$ and $(3,3)$ (cf. Figure 6.2). The numerical results are tabulated in

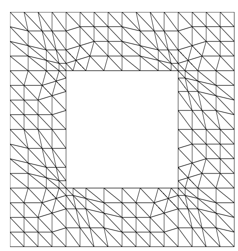

FIGURE 6.2. Graded meshes on the doubly connected domain

Table 6.7 for $\alpha=-1$ and 1.

Note that in this case $\boldsymbol{u}$ is the curl of a quintic polynomial and hence $c=0$ in (6.2.13). It is observed that $\widehat{c}_k=0$ up to machine error.

TABLE 6.7. Results for (5.1.1) on the doubly connected domain and the exact solution given by (6.2.14)

h_k	$\frac{\lVert\nabla\times\boldsymbol{u}-\widehat{\xi}_k\rVert_{L_2}}{\lVert\boldsymbol{f}\rVert_{L_2}}$	Order	$\lvert\widehat{c}_k\rvert$	$\frac{\lVert\boldsymbol{u}-\widehat{\boldsymbol{u}}_k\rVert_{L_2}}{\lVert\boldsymbol{f}\rVert_{L_2}}$	Order
$\alpha=-1$					
1/8	4.59E−03	1.99	1.78E−16	1.22E−02	1.05
1/16	1.15E−03	2.00	1.22E−16	6.06E−03	1.01
1/32	2.86E−04	2.00	2.53E−16	3.03E−03	1.01
1/64	7.16E−05	2.00	5.57E−17	1.51E−03	1.00
1/128	1.79E−05	2.00	7.32E−17	7.57E−04	1.00
$\alpha=1$					
1/8	2.10E−03	1.99	8.65E−16	1.02E−02	0.99
1/16	5.27E−04	2.00	9.43E−16	5.13E−03	0.99
1/32	1.32E−04	2.00	7.81E−16	2.57E−03	1.00
1/64	3.29E−05	2.00	1.34E−17	1.29E−03	1.00
1/128	8.22E−06	2.00	2.57E−17	6.43E−04	1.00

We then take the right-hand side function to be

$$\boldsymbol{f}=\begin{cases}\begin{bmatrix}1+x_1\\0\end{bmatrix} & \text{if } x_1\le x_2 \text{ and } 3\le x_1\le 4,\\[2ex] \begin{bmatrix}0\\1+x_2\end{bmatrix} & \text{otherwise.}\end{cases}\tag{6.2.15}$$

The results are reported in Table 6.8 for $\alpha=-1$ and 1.

TABLE 6.8. Results for (5.1.1) on the doubly connected domain and right-hand side function given by (6.2.15)

h_k	$\frac{\lVert\nabla\times\boldsymbol{u}-\widehat{\xi}_k\rVert_{L_2}}{\lVert\boldsymbol{f}\rVert_{L_2}}$	Order	$\widehat{c}_k$	Order	$\frac{\lVert\boldsymbol{u}-\widehat{\boldsymbol{u}}_k\rVert_{L_2}}{\lVert\boldsymbol{f}\rVert_{L_2}}$	Order
$\alpha=-1$						
1/4	7.18E−01	0.91	0.764157	0.91	8.36E−01	0.86
1/8	1.95E−01	1.88	0.765826	1.58	3.01E−01	1.48
1/16	4.01E−02	2.28	0.766367	1.62	1.24E−01	1.28
1/32	1.03E−02	1.97	0.766528	1.75	6.07E−02	1.03
1/64	2.79E−03	1.88	0.766570	1.79	3.09E−02	0.98
$\alpha=1$						
1/4	7.33E−03	1.69	-0.764157	0.91	9.03E−02	0.83
1/8	2.22E−03	1.72	-0.765826	1.58	4.97E−02	0.86
1/16	6.60E−04	1.75	-0.766367	1.62	2.71E−02	0.87
1/32	1.99E−04	1.70	-0.766528	1.75	1.48E−02	0.87
1/64	6.63E−05	1.58	-0.766570	1.79	7.98E−03	0.89

Chapter 7
Conclusions

In this dissertation we have investigated nonconforming finite element methods for two-dimensional Maxwell's equations and their solutions by multigrid algorithms. We have also studied multigrid methods for discontinuous Galerkin methods on graded meshes for the Poisson problem.

We show that the elliptic curl-curl and grad-div problem appearing in electromagnetics can be solved by two types of nonconforming finite element methods on graded meshes. The first method is based on a discretization using Crouzeix-Raviart weakly continuous vector fields. Optimal convergence rates in both the energy norm and the L_2 norm are achieved on general polygonal domains, provided that two consistency terms involving the jumps of the vector fields are included in the discretization and properly graded meshes are used. The second method uses discontinuous P_1 vector fields and two additional over-penalized terms are added to the scheme. Similar convergence results are established on nonconforming meshes. We also report numerical results for multigrid algorithms applied to the resulting discrete problems on the unit square. The convergence analysis of multigrid methods for the discretized curl-curl and grad-div problem is currently under investigation.

Since there are many similarities between nonconforming finite element methods for Maxwell's equations on graded meshes and discontinuous Galerkin (DG) methods for the Poisson problem on graded meshes, we also investigate multigrid algorithms for discontinuous Galerkin methods. We consider a class of symmetric discontinuous Galerkin methods for a model Poisson problem on graded meshes.

The elliptic regularity results in terms of weighted Sobolev norms are used in the analysis. Optimal order error estimates are derived in both the energy norm and the L_2 norm. Then we establish the uniform convergence of W-cycle, V-cycle and F-cycle multigrid algorithms for the resulting discrete problems on non-convex domains, where the model problem has singularities. We show that the convergence of the multigrid algorithms on non-convex domains with properly graded meshes is identical to the convergence of multigrid methods on convex domains with quasi-uniform meshes.

Then we propose a new numerical approach for two-dimensional Maxwell's equations that is based on the Hodge decomposition for divergence-free vector fields. In this approach, an approximate solution for Maxwell's equations can be obtained by solving standard second order scalar elliptic boundary value problems. We demonstrate its performance using P_1 finite element methods. We can recover $O(h)$ convergence on non-convex domains, provided that graded meshes are used. Finally we study multigrid methods for Maxwell's equations based on the new approach. All the theoretical results obtained in this dissertation are confirmed by numerical results.

References

[1] R.A. Adams and J.J.F. Fournier. *Sobolev Spaces (Second Edition).* Academic Press, Amsterdam, 2003.

[2] Th. Apel. *Anisotropic Finite Elements.* Teubner, Stuttgart, 1999.

[3] Th. Apel, A.-M. Sändig, and J.R. Whiteman. Graded mesh refinement and error estimates for finite element solutions of elliptic boundary value problems in non-smooth domains. *Math. Methods Appl. Sci.*, 19:63–85, 1996.

[4] D.N. Arnold. An interior penalty finite element method with discontinuous elements. *SIAM J. Numer. Anal.*, 19:742–760, 1982.

[5] D.N. Arnold, F. Brezzi, B. Cockburn, and L.D. Marini. Unified analysis of discontinuous Galerkin methods for elliptic problems. *SIAM J. Numer. Anal.*, 39:1749–1779, 2001/02.

[6] D.N. Arnold, F. Brezzi, and L.D. Marini. A family of discontinuous Galerkin finite elements for the Reissner-Mindlin plate. *J. Sci. Comput.*, 22/23:25–45, 2005.

[7] F. Assous, P. Ciarlet Jr., E. Garcia, and J. Segré. Time-dependent Maxwell's equations with charges in singular geometries. *Comput. Methods Appl. Mech. Engrg.*, 196:665–681, 2006.

[8] F. Assous, P. Ciarlet, Jr., S. Labrunie, and S. Lohrengel. The singular complement method. In N. Debit, M. Garbey, R. Hoppe, D. Keyes, Y. Kuznetsov, and J. Périaux, editors, *Domain Decomposition Methods in Science and Engineering*, pages 161–189. CIMNE, Barcelona, 2002.

[9] F. Assous, P. Ciarlet, Jr., S. Labrunie, and J. Segré. Numerical solution to the time-dependent Maxwell equations in axisymmetric singular domains: the singular complement method. *J. Comput. Phys.*, 191:147–176, 2003.

[10] F. Assous, P. Ciarlet, Jr., and E. Sonnendrücker. Resolution of the Maxwell equation in a domain with reentrant corners. *M2AN Math. Model. Numer. Anal.*, 32:359–389, 1998.

[11] I. Babuška. Finite element method for domains with corners. *Computing*, 6:264–273, 1970.

[12] I. Babuška, R.B. Kellogg, and J. Pitkäranta. Direct and inverse error estimates for finite elements with mesh refinements. *Numer. Math.*, 33:447–471, 1979.

[13] I. Babuška, and J. Osborn. Eigenvalue problems. In P.G. Ciarlet and J.L. Lions, editors, *Handbook of Numerical Analysis, Vol. II*, pages 641–787, 1991.

[14] C. Băcuţă, V. Nistor, and L.T. Zikatanov. Improving the rate of convergence of 'high order finite elements' on polygons and domains with cusps. *Numer. Math.*, 100:165–184, 2005.

[15] G. Baker. Finite element methods for elliptic equations using nonconforming elements. *Math. Comp.*, 31:45–89, 1977.

[16] G.A. Baker, W.N. Jureidini, and O.A. Karakashian. Piecewise solenoidal vector fields and the Stokes problem. *SIAM J. Numer. Anal.*, 27:1466–1485, 1990.

[17] R.E. Bank and T.F. Dupont. An optimal order process for solving finite element equations. *Math. Comp.*, 36:35–51, 1981.

[18] F. Bassi, S. Rebay, G. Mariotti, S. Pedinotti, and M. Savini. A higher order accurate discontinuous finite element method for inviscid and viscous turbomachinery flows. Proceedings of 2nd European Conference on Turbomachinery, Fluid Dynamics and Thermodynamics, In R. Decuypere and G. Dilbelius, editors, Technologisch Instituut, Antewerpen, Belgium, pages 99–108, 1997.

[19] K.J. Bathe, C. Nitikitpaiboon, and X. Wang. A mixed displacement-based finite element formulation for acoustic fluid-structure interaction. *Comput. Struct.*, 56:225–237, 1995.

[20] A. Bermúdez and R. Rodríguez. Finite element computation of the vibration modes of a fluid-solid system. *Comput. Methods Appl. Mech. Engrg.*, 119:355–370, 1994.

[21] M. Birman and M. Solomyak. L^2-theory of the Maxwell operator in arbitrary domains. *Russ. Math. Surv.*, 42:75–96, 1987.

[22] D. Boffi and L. Gastaldi. On the "$-$grad div $+\, s$ curl rot" operator. *Computational fluid and solid mechanics, Vol. 1, 2* (*Cambridge, MA, 2001*), pages 1526–1529. Elsevier, Amsterdam, 2001.

[23] A.-S. Bonnet-Ben Dhia, C. Hazard, and S. Lohrengel. A singular field method for the solution of Maxwell's equations in polyhedral domains. *SIAM J. Appl. Math.*, 59:2028–2044, 1999.

[24] A. Bossavit. Discretization of electromagnetic problems: the "generalized finite differences" approach. In P.G. Ciarlet, W.H.A. Schilders, and E.J.W. Ter Maten, editors, *Handbook of Numerical Analysis, Vol. XIII*, pages 105–197. North-Holland, Amsterdam, 2005.

[25] J.H. Bramble, D.Y. Kwak and J.E. Pasciak. Uniform convergence of multigrid V-cycle iterations for indefinitee and nonsymmetric problems. *SIAM J. Numer. Anal.*, 31:1746–1763, 1994.

[26] J.H. Bramble, J.E. Pasciak and J. Xu. The analysis of multigrid algorithms for nonsymmetric and indefinite elliptic problems. *Math. Comp.*, 51:389-414, 1988.

[27] J.H. Bramble and X. Zhang. The analysis of multigrid methods. In P.G. Ciarlet and J.L. Lions, editors, *Handbook of Numerical Analysis, Vol. VII*, pages 173–415. North-Holland, Amsterdam, 2000.

[28] J.J. Brannick, H. Li, and L.T. Zikatanov. Uniform convergence of the multigrid V-cycle on graded meshes for corner singularities. *Numer. Linear Algebra Appl.*, 15:291–306, 2008.

[29] S.C. Brenner. An optimal-order multigrid method for P_1 nonconforming finite elements. *Math. Comp.*, 52:1–15, 1989.

[30] S.C. Brenner. Convergence of multigrid V-cycle algorithm for second order boundary value problems without full elliptic regularit. *Math. Comp.*, 71:507–525, 2002.

[31] S.C. Brenner. Convergence of nonconforming V-cycle and F-cycle multigrid algorithms for second order elliptic boundary value problems. *Math. Comp.*, 73:1041–1066, 2004.

[32] S.C. Brenner and C. Carstensen. Finite element methods. In E. Stein, R. de Borst, and T.J.R. Hughes, editors, *Encyclopedia of Computational Mechanics*, pages 73–118. Wiley, Weinheim, 2004.

[33] S.C. Brenner, J. Cui, Z. Nan, and L.-Y. Sung. Hodge decomposition and Maxwell's equations. submitted, 2010.

[34] S.C. Brenner, J. Cui, T. Gudi, and L.-Y. Sung. Multigrid algorithms for symmetric discontinuous Galerkin methods on graded meshes. submitted, 2009.

[35] S.C. Brenner, J.Cui, and L.-Y. Sung. An interior penalty method for a two dimensional curl-curl minus grad-div problem. *ANZIAM J*, 50:947–975, 2008.

[36] S.C. Brenner, J.Cui, and L.-Y. Sung. Multigrid methods for the symmetric interior penalty method on graded meshes. *Numer. Linear Algebra Appl.*, 16:481–501, 2009.

[37] S.C. Brenner, J.Cui, F. Li, and L.-Y. Sung. A nonconforming finite element method for a two-dimensional curl-curl and grad-div problem. *Numer. Math.*, 109:509–533, 2008

[38] S.C. Brenner, F. Li, and L.-Y. Sung. A nonconforming penalty method for a two dimensional curl-curl problem. *Math. Models Methods Appl. Math.*, 19:651-668, 2009

[39] S.C. Brenner, F. Li, and L.-Y. Sung. A locally divergence-free interior penalty method for two dimensional curl-curl problems. *SIAM J. Numer. Anal.*, 46:1190–1211, 2008.

[40] S.C. Brenner, F. Li, and L.-Y. Sung. A locally divergence-free nonconforming finite element method for the time-harmonic Maxwell equations. *Math. Comp.*, 76:573–595, 2007.

[41] S.C. Brenner, F. Li, and L.-Y. Sung. Nonconforming Maxwell eigensolvers. *J. Sci. Comput.*, 40:51–85, 2009.

[42] S.C. Brenner and L. Owens. A W-cycle algorithm for a weakly over-penalized interior penalty method. *Comput. Methods Appl. Mech. Engrg.*, 196:3823–3832, 2007.

[43] S.C. Brenner and L.R. Scott. *The Mathematical Theory of Finite Element Methods (Third Edition)*. Springer-Verlag, New York, 2008.

[44] S.C. Brenner and L.-Y. Sung. C^0 interior penalty methods for fourth order elliptic boundary value problems on polygonal domains. *J. Sci. Comput.*, 22/23:83–118, 2005.

[45] S.C. Brenner and L.-Y. Sung. Multigrid algorithms for C^0 interior penalty methods. *SIAM J. Numer. Anal.*, 44:199–223, 2006.

[46] S.C. Brenner and L.-Y. Sung. A quadratic nonconforming element for $H(\mathrm{curl};\Omega) \cap H(\mathrm{div};\Omega)$. *Appl. Math. Lett.*, 22:892–896, 2009.

[47] S.C. Brenner and J. Zhao. Convergence of multigrid algorithms for interior penalty methods. *Appl. Numer. Anal. Comput. Math.*, 2:3–18, 2004.

[48] F. Brezzi, G. Manzini, D. Marini, P. Pietra, and A. Russo. Discontinuous Galerkin approximations for elliptic problems *Numer. Methods Partial Differential equaitons,* 16:365-378, 2002.

[49] P. Castillo, B. Cockburn, I. Perugia and D. Schötzau. An *a priori* error analysis of the local discontinuous Galerkin method for elliptic problems. *SIAM J. Numer. Anal.*, 38:1676–1706, 2000.

[50] P. Ciarlet, Jr. Augmented formulations for solving Maxwell equations. *Comput. Methods Appl. Mech. Engrg.*, 194:559–586, 2005.

[51] P. Ciarlet, Jr. *The Finite Element Methods for Elliptic Problems.*, North-Holland, Amsterdam, 1978.

[52] B. Cockburn and C.-W. Shu. The local discontinuous Galerkin method for time-dependent convection-diffusion systems. *SIAM J. Numer. Anal.*, 35:2440–2463, 1998.

[53] J.L. Coulomb. Finite element three dimensional magnetic field computation. *IEEE Trans, Magenetics.*, 17:3241-3246, 1981.

[54] M. Costabel. A remark on the regularity of solutions of Maxwell's equations on Lipschitz domains. *Math. Methods Appl. Sci.*, 12:36–368, 1990.

[55] M. Costabel. A coercive bilinear form for Maxwell's equations. *J. Math. Anal. Appl.*, 157:527–541, 1991.

[56] M. Costabel and M. Dauge. Maxwell and Lamé eigenvalues on polyhedra. *Math. Methods Appl. Sci.*, 22:243–258, 1999.

[57] M. Costabel and M. Dauge. Singularities of electromagnetic fields in polyhedral domains. *Arch. Ration. Mech. Anal.*, 151:221–276, 2000.

[58] M. Costabel and M. Dauge. Weighted regularization of Maxwell equations in polyhedral domains. *Numer. Math.*, 93:239–277, 2002.

[59] M. Costabel, M. Dauge, and C. Schwab. Exponential convergence of hp-FEM for Maxwell equations with weighted regularization in polygonal domains. *Math. Models Methods Appl. Sci.*, 15:575–622, 2005.

[60] M. Crouzeix and P.-A. Raviart. Conforming and nonconforming finite element methods for solving the stationary Stokes equations I. *RAIRO Anal. Numér.*, 7:33–75, 1973.

[61] M. Dauge. *Elliptic Boundary Value Problems on Corner Domains,* Lecture Notes in Mathematics 1341. Springer-Verlag, Berlin-Heidelberg, 1988.

[62] L. Demkowicz. Finite element methods for Maxwell equations. In E. Stein, R. de Borst, and T.J.R. Hughes, editors, *Encyclopedia of Computational Mechanics*, pages 723–737. Wiley, Weinheim, 2004.

[63] V.A. Dobrev, R.D. Lazarov, P.S. Vassilevski, and L.T. Zikatanov. Two-level preconditioning of discontinuous Galerkin approximations of second-order elliptic equations. *Numer. Linear Algebra Appl.*, 13:753–770, 2006.

[64] J. Douglas, Jr. and T. Dupont. Interior penalty procedures for elliptic and parabolic Galerkin methods. *Computing Methods in Applied Sciences (Second Internat. Sympos., Versailles, 1975),* Lecture Notes in Phys., 58:207-216. Springer, Berlin, 1976.

[65] T. Dupont and R. Scott. Polynomial approximation of functions in Sobolev spaces. *Math. Comp.*, 34:441–463, 1980.

[66] G. Engel, K. Garikipati, T.J.R. Hughes, M.G. Larson, L. Mazzei, and R.L. Taylor. Continuous/discontinuous finite element approximations of fourth order elliptic problems in structural and continuum mechanics with applications to thin beams and plates, and strain gradient elasticity. *Comput. Methods Appl. Mech. Engrg.*, 191:3669–3750, 2002.

[67] L. Evans. *Partial Differential Equations.* American Mathematical Society, Providence, 1998.

[68] V. Girault and P.-A. Raviart. *Finite Element Methods for Navier-Stokes Equations. Theory and Algorithms.* Springer-Verlag, Berlin, 1986.

[69] J. Gopalakrishnan and G. Kanschat. A multilevel discontinuous Galerkin method. *Numer. Math.*, 95:527–550, 2003.

[70] P. Grisvard. *Elliptic Problems in Non Smooth Domains.* Pitman, Boston, 1985.

[71] W. Hackbusch. *Multi-grid Methods and Applications.* Springer-Verlag, Berlin-Heidelberg-New York-Tokyo, 1985.

[72] M.A. Hamdi, Y. Ousset, and G. Verchery. A displacement method for the analysis of vibrations of coupled fluid-structure systems. *Internat. J. Numer. Methods Engrg.*, 13:139–150, 1978.

[73] P. Hansbo and M.G. Larson. Discontinuous Galerkin methods for incompressible and nearly incompressible elasticity by Nitsche's method. *Comput. Methods Appl. Mech. Engrg.*, 191:1895–1908, 2002.

[74] C. Hazard and S. Lohrengel. A singular field method for Maxwell's equations: Numerical aspects for 2D magnetostatics. *SIAM J. Numer. Anal.*, 40:1021–1040, 2002.

[75] R. Hiptmair. Finite elements in computational electromagnetism. *Acta Numer.*, 11:237–339, 2002.

[76] V. Kondratiev. Boundary value problems for elliptic equations in domains with conical or angular points. *Trans. Moscow Math. Soc.*, pages 227–313, 1967.

[77] R. Leis. Zur Theorie elektromagnetischer Schwingungen in anisotopen inhomgenen Medien. *Math. Z.*, 106:213–224, 1968.

[78] Q. Lin and J. Lin. *Finite Element Methods: Accuracy and Improvement.* Science Press, Beijing, 2006.

[79] S.F. McCormick (editor). *Multigrid Methods*, volume 3 of *Frontiers in Applied Mathematics.* SIAM, Philadelphia, 1987.

[80] P. Monk. *Finite Element Methods for Maxwell's Equations.* Oxford University Press, New York, 2003.

[81] S.A. Nazarov and B.A. Plamenevsky. *Elliptic Problems in Domains with Piecewise Smooth Boundaries.* de Gruyter, Berlin-New York, 1994.

[82] J. Nečas. *Les Méthodes Directes en Théorie des Équations Elliptiques.* Masson, Paris, 1967.

[83] J.-C. Nédélec. Mixed finite elements in $\mathbf{R}^3$. *Numer. Math.*, 35:315–341, 1980.

[84] J.-C. Nédélec. A new family of mixed finite elements in $\mathbf{R}^3$. *Numer. Math.*, 50:57–81, 1986.

[85] P. Neittaanmäki and R Picard. Error estimates for the finite element approximation to a Maxwell-type boundary value problem. *Numer. Funct. Anal. Optimiz*, 2:267-285, 1980.

[86] M. H. van Raalte and P. W. Hemker. Two-level multigrid analysis for the convection-diffusion equation discretized by a discontinuous Galerkin method. *Numer. Linear Algebra Appl.*, 12:563–584, 2005.

[87] B.M.A Rahman and J.B. Davies. Finite element analysis of optical and microwave waveguide problems. *IEEE Trans. Microwave Theory Tech.*, 32:20–28, 1984.

[88] B. Rivière, M.F. Wheeler, and V. Girault. A priori error estimates for finite element methods based on discontinuous approximation spaces for elliptic problems. *SIAM J. Numer. Anal.*, 39:902–931, 2001.

[89] A. Schatz. An observation concerning Ritz-Galerkin methods with indefinite bilinear forms. *Math. Comp.*, 28:959–962, 1974.

[90] E.M. Stein. *Singular Integrals and Differentiability Properties of Functions.* Princeton University Press, Princeton, 1970.

[91] U. Trottenberg, C. Oosterlee, and A. Schüller. *Multigrid.* Academic Press, San Diego, 2001.

[92] L.B. Wahlbin. *Superconvergence in Galerkin Finite Element Methods,* Lecture Notes in Mathematics 1605. Springer-Verlag, Berlin, 1995.

[93] C. Weber. A local compactness theorem for Maxwell's equations. *Math. Methods Appl. Sci.*, 2:12–25, 1980.

[94] T. Weiland. On the unique numerical solution of Maxwellian eigenvalue prolems in three dimensions. *Part. Accel.*, 17:277–242, 1985.

[95] M.F. Wheeler. An elliptic collocation-finite-element method with interior penalties. *SIAM J. Numer. Anal.*, 15:152–161, 1978.

[96] T.P. Wihler. Locking-free adaptive discontinuous Galerkin FEM for linear elasticity problems. *Math. Comp.*, 75:1087–1102, 2006.

[97] K.J. Witsch. A remark on a compactness result in electromagnetic theory. *Math. Methods Appl. Sci.*, 16:123–129, 1993.

[98] K. Yosida. *Functional Analysis.* Classics in Mathemactics. Springer-Verlag, Berlin, 1995.

[99] H. Yserentant. The convergence of multilevel methods for solving finite-element equations in the presence of singularities. *Math. Comp.*, 47:399–409, 1986.

[100] J. Zhao. Convergence of the nonconforming V-cycle and F-cycle methods for the biharmonic problem using the Morley element. *ETNA,* 17:112-132, 2004.

Vita

Jintao Cui was born in June 1981, in Shandong Province, P.R. China. He earned his Bachelor of Science degree from the Department of Applied Mathematics, Dalian University of Technology, in June 2004. In August 2004 he went to the University of South Carolina to pursue his graduate studies in mathematics. After two years he transferred to the Louisiana State University to continue his studies and research. He is currently a candidate for the degree of Doctor of Philosophy in mathematics, which will be awarded in August 2010.

The following is a list of publications and preprints resulting from this dissertation:

- S.C. Brenner, J. Cui, Z. Nan, and L.-Y. Sung. *Hodge Decomposition and Maxwell's Equations*, submitted, 2010
- S.C. Brenner, J. Cui, T. Gudi, and L.-Y. Sung. *Multigrid Algorithms for Symmetric Discontinuous Galerkin Methods on Graded Meshes*, submitted, 2009
- S.C. Brenner, J. Cui, and L.-Y. Sung. *Multigrid Methods for the Symmetric Interior Penalty Method on Graded Meshes,* Numer. Linear Algebra Appl., 16:481–501, 2009
- S.C. Brenner, J. Cui, and L.-Y. Sung. *An Interior Penalty Method for a Two-Dimensional Curl-Curl Minus Grad-Div Problem*, ANZIAM J. 50:947–975, 2008
- S.C. Brenner, J. Cui, F. Li, and L.-Y. Sung. *A Nonconforming Finite Element Method for a Two-Dimensional Curl-Curl and Grad-Div Problem*, Numer. Math. 109:509–533, 2008